

ON THE INTERACTION OF ACTINOMYCIN AND DNA

Thesis by  
Richard Walter Hyman

In Partial Fulfillment of the Requirements  
For the Degree of  
Doctor of Philosophy

California Institute of Technology  
Pasadena, California  
1970

(Submitted December , 1969)

THEY ALSO SERVE WHO ONLY STAND AND WAIT

-- J. Milton

(in restaurants,  
but not on tennis courts)

-- N. Davidson

ACKNOWLEDGMENTS

I want to express my appreciation to

Ron Davis, for listening;

Grace and Mike Dahmus, for giving;

the National Institutes of Health, for providing;

and

Norman Davidson,

for being Norman Davidson.

## ABSTRACT

Experiments have been accomplished that (a) further define the nature of the strong, G-containing DNA binding sites for actinomycin D (AMD), and (b) quantitate the in vitro inhibition of E. coli RNA polymerase activity by T7 DNA-bound AMD.

Twenty-five to forty percent of the G's of crab dAT are disallowed as strong AMD binding sites. The G's are measured to be randomly distributed, and, therefore, this datum cannot be explained on the basis of steric interference alone. Poly dAC:TG binds as much AMD and as strongly as any natural DNA, so the hypothesis that the unique strong AMD binding sites are G and a neighboring purine is incorrect. The datum can be explained on the basis of both steric interference and the fact that TGA is a disallowed sequence for strong AMD binding.

Using carefully defined in vitro conditions, there is one RNA synthesized per T7 DNA by E. coli RNA polymerase. The rate of the RNA polymerase-catalyzed reaction conforms to the equation

$$\frac{1}{\text{rate}} = \frac{1}{k_A(\text{ATP})} + \frac{1}{k_G(\text{GTP})} + \frac{1}{k_C(\text{CTP})} + \frac{1}{k_U(\text{UTP})}$$

T7 DNA-bound AMD has only modest effects on initiation and termination of the polymerase-catalyzed reaction, but a large inhibitory effect on propagation. In the presence of bound AMD,  $k_G$  and  $k_C$  are decreased, whereas  $k_A$  and  $k_U$  are unaffected. These facts are

interpreted to mean that on the microscopic level, on the average, the rates of incorporation of ATP and UTP are the same in the absence or presence of bound AMD, but that the rates of incorporation of GTP and CTP are decreased in the presence of AMD.

## TABLE OF CONTENTS

CHAPTER	TITLE	PAGE
	ON THE INTERACTION OF ACTINOMYCIN AND DNA	
1	The Binding of Actinomycin to Crab dAT: The Nature of the DNA Binding Site	1
2	On the Nature of the Actinomycin D-DNA Binding Site	7
3	The Kinetics of the In Vitro Inhibition of Transcription by Actinomycin	58
	PROPOSITIONS	108

CHAPTER 1

The Binding of Actinomycin to Crab dAT:

The Nature of the DNA Binding Site

Richard W. Hyman and Norman Davidson

The following paper appeared in Biochemical and Biophysical Research Communications, 26, 116 (1967), and is reprinted here with the express written permission of Academic Press, Inc., New York.

THE BINDING OF ACTINOMYCIN TO CRAB dAT;  
THE NATURE OF THE DNA BINDING SITE

Richard W. Hyman and Norman Davidson

Gates and Crellin Laboratories of Chemistry\* and  
Norman W. Church Laboratory of Chemical Biology  
California Institute of Technology  
Pasadena, California 91109

Received November 29, 1966

The present communication deals with the nature of the binding site on DNA for actinomycin D (AMD). We find that with the component of Cancer antenarrius crab DNA known as crab dAT, for which the ratio of GC to AT base pairs is 1:28, the strong binding saturates at one actinomycin per 56 base pairs. This result most probably excludes the hypothesis that a GpG sequence on one strand is required for strong binding. Several alternate hypotheses, which are consistent with the results, are examined.

The strong binding sites for AMD appear to occur only in native two-stranded DNA (Goldberg, Rabinowitz, and Reich, 1962; Cavaliere and Nemchin, 1964; Gellert, Smith, Neville, and Felsenfeld, 1965). Since synthetic dAT does not bind at all (Goldberg, et al., 1962; Gellert, et al., 1965; Kahan, Kahan, and Hurwitz, 1963) a GC base pair must be present in these sites. Studies with nucleosides suggest that G rather than C is the critical residue for binding (Kersten, 1961). However, in a number of DNA's with a GC content varying from 75 to 25%, the number of AMD binding sites is fairly constant at about 1 per 7 base pairs (Gellert, et al., 1965). Thus, either there is some further requirement for the sequence around a G in order for binding to occur, or repulsive

---

\* Contribution No. 3452

interactions (either directly steric or indirectly by local distortion of the DNA structure) between neighboring actinomycins limit the amount of binding. Hamilton, Fuller, and Reich (1963) estimate that the direct steric effect of the cyclic peptide chains of actinomycin would extend for about three base pairs.

Crab dAT is mainly an alternating AT copolymer, with about 3% of GC base pairs. A method for the preparation of this material in its fully native form, without disruption of the GC base pairs, has been developed in this Laboratory (Davidson, Widholm, Nandi, Jensen, Olivera, and Wang, 1965). In this DNA, GC base pairs are sufficiently rare so that steric interactions are less likely to be important; furthermore, the sequence GpG occurs in a very low frequency. It therefore seemed of interest to investigate the binding of actinomycin to native crab dAT.

#### Experimental

Cancer antenarrius DNA was prepared essentially by the method of Smith (1963) except that all steps were carried out in the cold. The component called crab dAT was separated by the mercury-cesium sulfate buoyant density method of Davidson, et al. (1965). This DNA is an alternating copolymer with 3.5% GC base pairs (Widholm, 1965); its properties are generally very similar to those of the better known Cancer borealis dAT (2.7% GC). Actinomycin D was a gift from Merck, Sharp, and Dohme.

Equilibrium binding studies were made by sedimenting the DNA-AMD complex and measuring the concentration of free AMD remaining in the supernatant solution. Three ml of solution containing known amounts (spectrally determined) of DNA and AMD were placed in a carefully washed SW39 polyallomer tube and covered with two ml of mineral oil. The bottom ml also contained 20% sucrose. Salt concentrations were  $10^{-3}$  M phosphate,  $10^{-2}$  M NaCl, pH 7. The rotor was spun at 42,000 rpm for six hours at 20°C thereby pelleting the AMD-DNA complex. The

polyallomer tubes were dripped from the side, one ml from the bottom, and two ml of supernatant solution collected. The free AMD concentration was then measured by spectrophotometry, using 1 and 5 cm path lengths. Actinomycin readily adsorbs to glass surfaces and was handled with polypropylene tubes and pipets.

#### Results and Discussion

Plots of the binding of actinomycin to native calf thymus DNA and crab dAT are shown in Fig. 1. The vertical coordinate,  $\bar{r}$ , is the ratio of

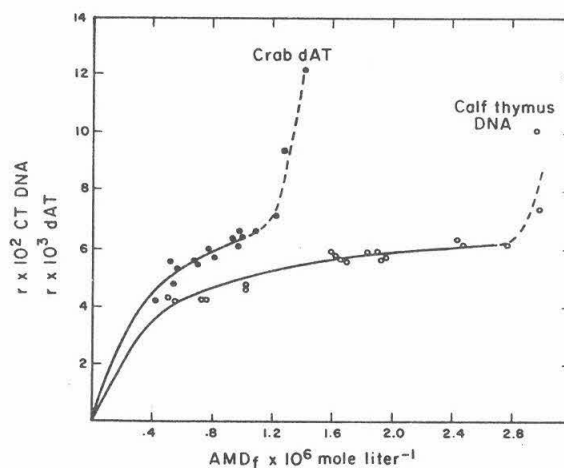


Fig. 1

bound AMD to total nucleotides; the horizontal coordinate is the concentration of free AMD. The curves indicate a strong binding reaction at low free actinomycin concentration followed by further uptake of AMD at a higher free AMD concentration. A least-squares analysis of a Scatchard plot of these data in the strong binding region gives  $K = 2.3 (\pm .5) \times 10^6$  mole<sup>-1</sup> liter, and one site per 14 ( $\pm 1$ ) nucleotides, for calf thymus DNA. These values agree well with those reported by Gellert, *et al.* (1965).

For crab dAT, the intrinsic binding constant is  $2.5 (\pm .5) \times 10^6$

mole<sup>-1</sup> liter, and there is one site per 112 ( $\pm 4$ ) nucleotides, or one per 56 base pairs. Since the binding constant is of the same order of magnitude as for calf thymus and other typical DNA's, the binding site on crab dAT appears to be a typical strong binding site. There is approximately one such binding site for every two GC base pairs in crab dAT.

The nearest neighbor frequencies for Cancer borealis dAT (2.7% GC) have been determined by Schwartz, Trautner, and Kornberg (1962). These data are: ApA = 0.0127, TpT = 0.0126; CpA = 0.0100, TpG = 0.0089; GpA = 0.0042, TpC = 0.0015; CpT = 0.0004, ApG = 0.0018; GpT = 0.0081; ApC = 0.0069; GpG = 0.0009, CpC = 0.0009; TpA = 0.504; ApT = 0.429; CpG = 0.0007; GpC = 0.0015. From these data, 0.939 of the G residues are followed by non-G; 0.927 of the G residues are preceded by a non-G residue. If there is no correlation between the probability of a base preceding a G and the probability of a base following a G, 0.87 of the G residues do not have a G residue on either side as a nearest neighbor. If these data for Cancer borealis dAT apply to Cancer antennarius dAT, and if all the binding sites involve a G residue, the data exclude the possibility that adjacent G's on the same strand are needed to define a strong binding site.

Professor Don Crothers has pointed out the following argument to us. The nearest neighbor frequencies for Cancer borealis show that 0.64 of the G's are followed by a pyrimidine and 0.74 of the G's are preceded by a pyrimidine. Thus, assuming no correlation between the nucleotides preceding and following the G,  $1 - (0.64 \cdot 0.74) = 0.52$  of the G's have a purine as a nearest neighbor. Thus, the assumption that a binding site consists of a G plus an adjacent purine is consistent with the observation of one site per two G's.

Apart from the nearest neighbor frequencies, nothing is known about the distribution of GC base pairs along the chain. If the distribution is random, and if  $p$  = frequency of occurrence of an AT base pair, the

probability that a sequence following a given GC pair consists of  $(\underline{n} - 1)$  AT pairs followed by a GC pair is  $p^{n-1}(1 - p)$ . The average length of such a sequence is  $\langle \underline{n} \rangle = 1/(1 - p)$ . The value of  $\underline{n}$  such that half the sequences are equal to or shorter than  $\underline{n}$  is  $\ln 2/(1 - p)$ . Thus, if  $\langle \underline{n} \rangle = 28$ , half the sequences are longer than 19 base pairs. It seems unlikely that a steric interaction between actinomycins would extend this large distance.

Therefore, if every GC base pair is intrinsically a binding site, the observation that only 1/2 of them are available for strong binding implies that the GC base pairs are not distributed at random along the crab dAT chain but there is sufficient bunching to decrease the fractional number of sites to 1/2. Alternatively, there is an additional sequence requirement around a G; for example, the one suggested by Crothers that the G must have a neighboring purine.

We are grateful to Dr. J. Widholm for advice and instruction on the preparation of crab dAT. This research has been supported by Grant GM-10991 from the U. S. P. H. S. One of us (R. W. H.) is an N. I. H. Trainee under Grant GM 1262.

#### References

- Cavalieri, L. and Nemchin, R. (1964). *Biochim. Biophys. Acta*, 87, 641.  
 Davidson, N., Widholm, J., Nandi, U.S., Jensen, R., Olivera, B.M., and Wang, J.C. (1965). *Proc. Natl. Acad. Sci., U.S.*, 53, 111.  
 Gellert, M., Smith, C.E., Neville, D., and Felsenfeld, G. (1965). *J. Mol. Biol.*, 11, 445.  
 Goldberg, I.H., Rabinowitz, M., and Reich, E. (1962). *Proc. Natl. Acad. Sci., U.S.*, 48, 2094.  
 Hamilton, L.D., Fuller, W., and Reich, E. (1963). *Nature*, 198, 538.  
 Hurwitz, J., Furth, J.J., Malamy, M., and Alexander, M. (1962). *Proc. Natl. Acad. Sci., U.S.*, 49, 1222.  
 Kahan, E., Kahan, F.M., and Hurwitz, J. (1963). *J. Biol. Chem.*, 238, 2491.  
 Kersten, W. (1961). *Biochim. Biophys. Acta*, 47, 610.  
 Schwartz, M.N., Trautner, T.A., and Kornberg, A. (1962). *J. Biol. Chem.*, 237, 1961.  
 Smith, M. (1963). *Biochem. Biophys. Res. Comm.*, 10, 67.  
 Widholm, J. (1965). Ph. D. Thesis, California Institute of Technology.

## CHAPTER 2

On the Nature of the Actinomycin D-DNA Binding Site

Richard W. Hyman and Norman Davidson

The following paper has been prepared  
for submission to Biochimica et Biophysica Acta.

**SUMMARY**

1. 25 to 40% of the guanines of crab dAT are disallowed as strong actinomycin D (AMD) binding sites.

2. The GC base pairs of crab dAT are shown to be (most probably) randomly distributed. Therefore, steric interference alone is not responsible for restricting the number of binding sites.

3. Poly dAC:TG binds as much DNA and as strongly as any irregular DNA. Therefore, guanine and a neighboring purine is not the unique binding site.

4. The data can be explained on the basis of steric interference combined with the recent report by Wells (1) that TGA is a non-binding sequence.

## INTRODUCTION

Strong binding sites for actinomycin D (AMD) occur only in native, two-stranded DNA (2-4). A GC base pair, and most probably the guanine residue, is implicated as part or all of the binding site (2, 4-6). DNA's varying in GC content from 25-75% all have a saturation level for strong binding of about one site for every seven base pairs. This fact suggests either that a steric interaction prevents binding of actinomycin molecules to GC pairs which are closer to each other than about seven base pairs, or that only certain nucleotide sequence around a G are binding sites. In a previous paper (7), we studied this question by measuring the saturation level of AMD binding for crab dAT which contains 97% AT base pairs, mainly as an alternating copolymer, and 3.0% GC base pairs. If the distribution of GC base pairs is random, most of them are more than seven nucleotide pairs apart. The steric hypothesis then predicts a binding of one AMD per GC base pair for crab dAT; that is, one binding site for every 33 nucleotide pairs. We actually observed one site for every 56 ( $\pm 2$ ) base pairs, and now using a different method, 42 ( $\pm 4$ ) base pairs. This datum could be interpreted if only G's surrounded by certain specific sequences were binding sites, or if G's within a specific sequence were not binding sites. We specifically considered the possibility that only a G adjacent to another purine was a binding site. An alternate explanation is that the saturation level of binding is due to steric interactions and that GC base pairs in crab dAT are not randomly distributed.

In the present communication we examine and eliminate the possibility that only G's next to purine are binding sites, by observing that poly dAC:TG, a DNA in which guanine has only pyrimidines as neighbors, can bind AMD.

We have also attempted to answer the question of possible clustering of G residues. The principle of this experiment is as follows: crab dAT is transcribed by RNA polymerase to give RNA, faithfully and indiscriminately. This RNA, called crab rAU, is treated with RNase T<sub>1</sub> which is known to cleave RNA at every G, leaving a 5'-terminal Gp. The size distribution of the molecules in the digest gives the distribution of G's along the DNA chain of crab dAT. We find that the G's are not clustered, but are distributed at random.

## MATERIALS

Actinomycin D was a gift from Merck Sharpe & Dohme. Crab dAT was prepared from Cancer antennarius as previously described (8). Calf thymus DNA, from the Worthington Biochemical Corporation, was used without further purification. Poly dAC:TG was a generous gift from M. Chamberlin. Labeled and unlabeled nucleoside triphosphates were from Schwarz BioResearch. Phosphoenolpyruvate (PEP) and pyruvate kinase (type II from rabbit skeletal muscle) were purchased from the Sigma Chemical Company. Yeast high-molecular-weight RNA, sperimidine, yeast transfer RNA, and pronase (B grade) were from Calbiochem. The pronase (~ 2 mg/ml) was autodigested at 37°C for an hour before use to remove any traces of nuclease. Electrophoretically purified and RNase-free DNase was purchased from the Worthington Biochemical Corporation. The DNase was assayed for RNase contamination in the conventional manner at an overload concentration of 1 mg/ml. No acid-soluble  $A_{260}$  above background could be measured after two hours' incubation at 37°C. The DNase was stored at -20°C.

Phenol was redistilled under nitrogen shortly before use, and equilibrated with sterile sodium citrate buffer, pH 6. A few drops of mercapto-ethanol were added, and the phenol was stored under nitrogen at 4°C in the dark. Bentonite was prepared by M. Dahmus according to the method of H. Fraenkel-Conrat (9). For the handling of any RNA, especially crab rAU, all solutions were in sterile double-distilled

water. All glassware and centrifuge tubes were washed in 5 M NaCl and 5% sodium dodecyl sulfate (SDS), rinsed thoroughly in distilled water, and autoclaved.

RNA polymerase was fraction IV of Chamberlin and Berg (10) and was prepared by G. K. Dahmus, working in the laboratory of J. Bonner. We are grateful to her for her skill and generosity. The RNA polymerase used had an absolute dependence on exogenous DNA and was free of nuclease contamination by the following criteria. (These assays were performed in cooperation with R. W. Davis.) To assay for DNase, the polymerase was incubated in the appropriate salt and temperature conditions for 15 minutes and for two hours with  $\phi$ X 174 DNA (90% single-stranded circles). At the end of the incubation period, the DNA was mounted for electron microscopic examination by the basic protein-film technique in the presence of formamide to stretch out the single-stranded DNA (11, 12). The numbers of circles and linears were easily scored. In the RNA polymerase preparation used, there was no increase in the percent of linears compared to the appropriate control incubations without polymerase. The RNase assay was performed analogously except that 23 S ribosomal RNA from E. coli was used instead of  $\phi$ X 174 DNA. The mounting of the RNA for electron microscopic examination was also done in the presence of formamide, which spreads the RNA so that it is easily visualized. 23 S ribosomal RNA possesses the property that its most RNase-sensitive place is almost exactly in the center of the molecule, so that while

measurements of the length of RNA are as yet somewhat inexact, one can readily distinguish between whole and half molecules. In the RNA polymerase used, no RNase activity above a control containing no polymerase was observed. These two assays are especially useful, since they consume only a very small amount of material, and since they are more sensitive than the conventional measurement of acid-soluble material. The RNA polymerase had an activity of 2520 units per  $A_{280}$  unit, where one unit is defined as one m  $\mu$ mole of total nucleoside-triphosphates incorporation in 15 minutes on 6  $\mu$ g of crab dAT using the incubation conditions of So et al. (13). For the enzyme preparation, we take  $E_{280}^{1\%} = 10$  (ref. 14). The polymerase was stored under liquid nitrogen.

Sucrose gradients were made with sucrose M. A. (density gradient grade, RNase-free) from Mann Research Laboratories, Inc.

RNase  $T_1$  from Calbiochem was assayed for specificity by comparing its action on yeast high molecular weight RNA and poly rAU (1:1) random copolymer from Schwarz BioResearch for 15 minutes and for six hours by the Takahashi procedure, but in 0.01 M sodium citrate buffer, pH 6, and at 34°C. The data of Table 1 demonstrate that RNase  $T_1$  has a specificity for yeast RNA at very least a hundred-fold over poly rAU. In fact, the soluble  $A_{260}$  measured for poly rAU is within the experimental limits of being zero.

TABLE I

ASSAY FOR SPECIFICITY OF RNASE T<sub>1</sub>

RNase T<sub>1</sub> was tested on each RNA at 34° C in 0.01 M sodium citrate buffer, pH 6. Each tube contained 1.0 ml of 1 mg/ml of RNA or poly rAU. The reaction was stopped by the addition of 0.1 ml of 0.75% uranyl acetate in 25% perchloric acid. After sitting on ice for one-half hour, the tubes were clinically centrifuged. 0.2 ml of the supernatant was added to 5.0 ml of distilled water, and the A<sub>260</sub> read.

	A <sub>260</sub>	
	15 min	6 hr
poly rAU	0.002	0.003
yeast RNA	0.246	0.320

## METHODS

The binding curve of AMD to poly dAC:TG was determined by a spectrophotometric procedure as described by Gellert *et al.* (4). The detailed conditions are described in the legend to Figure 2.

The conditions for DNA-directed RNA synthesis described below are basically the high ionic strength medium (0.1 M Tris; 0.2 M KCl, 0.012 M MgCl<sub>2</sub>) described by So *et al.* (13). These salt concentrations were selected in preference to the low ionic strength (0.04 M Tris, 0.004 M MgCl<sub>2</sub>, 0.001 M MnCl<sub>2</sub>) medium of Chamberlin and Berg (10) for several reasons: (a) Nonspecific poly A synthesis is suppressed in the high ionic strength medium (13; D. McConnell, personal communication); (b) It is the common experience that net synthesis stops after less than an hour of incubation at low ionic strength, but continues for several hours at high ionic strength; (c) As is shown in Table 2, there is considerable selectivity for AT-rich templates at low ionic strength, and none at high ionic strength.

The large-scale synthesis of crab rAU from crab dAT as a template was carried out in a final volume of 5 ml in a solvent consisting of: 0.1 M Tris (pH 7.5 at 34°C), 0.012 M MgCl<sub>2</sub>, 0.2 M KCl, 0.0012 M spermidine, each nucleoside triphosphate at  $2 \times 10^{-3}$  M, 0.01 M mercaptoethanol, 20 µg/ml pyruvate kinase,  $2.3 \times 10^{-3}$  M phosphoenolpyruvate, crab dAT at a concentration of 0.20 A<sub>260</sub> units/ml, 60 units/ml of RNA polymerase, <sup>14</sup>C-UTP and <sup>3</sup>H-CTP at specific activities of 0.25 and 25 c/mole, respectively. After incubation for

TABLE II  
COMPARISON OF RNA SYNTHESIS  
AT LOW AND HIGH IONIC STRENGTH

Template	Nucleotide Incorporation <sup>a</sup>	
	Low salt m $\mu$ moles	High salt m $\mu$ moles
crab main component DNA, 42% GC	0.06	2.6
crab dAT, 3% GC	1.7	2.7

<sup>a</sup> Each 0.25 ml reaction mixture contained 6  $\mu$ g of template, and 6  $\mu$ g of polymerase; incubation was at 37°C for 15 minutes.

1.5 hours at 34°C, 1.0 ml of yeast RNA (1 mg/ml) followed by 0.5 ml of bentonite (30 mg/ml) were added at room temperature. After vigorous shaking, the bentonite was removed by centrifugation. DNase solution (200  $\mu$ l, 1.7 mg/ml) pronase (200  $\mu$ l, 1.0 mg/ml), and SDS (1.0 ml, 10%) were added in that order, with a 20 minute incubation time for each reagent. An equal volume of phenol was added, the mixture was shaken vigorously, and the upper aqueous phase removed after a low-speed spin. This step was repeated until no denatured protein appeared at the interface. After several ether extractions to remove the phenol, the aqueous solution was adjusted to be 0.1 M in NaCl, and 2 vols. of cold 95% ethanol were added. After standing at -20°C for two hours, the RNA precipitate was collected as follows. A film of precipitate had formed on the sides of the 20 ml test tube. The liquid was decanted and centrifuged at 15,000 rpm for 10 min; the resulting precipitate, dissolved in 2 ml of sterile 0.01 M citrate buffer, pH 6, was labeled crab rAU "A". The film of RNA was also dissolved in 2 ml of buffer and labeled crab rAU "B". Each sample of RNA was dialyzed against 0.1 M sodium chloride, 0.01 M sodium citrate, pH 6, and then against 0.01 M sodium citrate, pH 6.

The product is primarily rAU, which is capable of self-renaturation and, therefore, likely to form both intra-strand and inter-strand duplexes. In order to estimate the molecular weight of the product from its sedimentation coefficient, the sedimentation velocity measurements were made in a dimethylsulfoxide (DMSO) based solvent

to disrupt secondary structure (15). The quantity of 5.0 ml of concentrated buffer and 5.0 or 20.0 gm of sucrose were made up to 100 ml with DMSO to give 5.0% and 20% W/V sucrose solutions in about 95% DMSO, respectively, 0.01 M Na<sub>3</sub> citrate. These solutions were used for the preformed gradient for sedimentation analysis. Yeast transfer RNA was sedimented in a separate tube as standard.

We can assign to each fraction of the sucrose gradient an  $S_{20,w}$  value from its position relative to the standard yeast tRNA and the meniscus (16). We then use an equation of the form

$$S_{20,w} = kM^m$$

to relate sedimentation coefficient and molecular weight. Theoretically, for a non-free-draining ideal random coil,  $m = 0.5$ . Experimentally,  $m$  is about 0.4 (refs. 15, 17). Boedtker's equation (17),  $S_{20,w} = 0.05 M^{0.40}$ , is for RNA after treatment with formaldehyde which completely disrupts secondary structure and for sedimentation of the unstructured RNA through a denaturing solvent. She has calibrated her equation for small RNA's, including yeast transfer RNA ( $S_{20,w, CH_2O} = 2.94$ ). These data then are closely applicable to our experimental conditions and will be used in our analysis. We, therefore, convert  $S_{20,w}$  to molecular weight and then molecular weight to degree of polymerization "n", using the equation

$$\log n = 2.50 \log S_{20,w, CH_2O} + 0.70. \quad (1)$$

For each fraction of the gradient of the final RNase T<sub>1</sub> digest of crab rAU, then, we can assign an "n", a degree of polymerization, and we can calculate the percent of the total of each isotope in the fraction. The latter is the weight fraction, W(n). The mole fraction is

$$X(n) = \left( \frac{W(n)}{n} \right) / \sum \frac{W(n)}{n} \quad (2)$$

The curve X(n) versus n can then be constructed, and integrated and normalized graphically.

RNase T<sub>1</sub> digestions were carried out in sodium citrate buffer pH6 at 24° C. It is essential for the present experiment that digestion be complete and that the crab rAU be cleaved at every G.

In a preliminary test on the digestion of tRNA (Figure 1), there was no change in the sedimentation pattern of the digest between the third and fourth additions of enzyme when fractions of 0.5 enzyme units were added per A<sub>260</sub> unit of RNA at six-hour intervals. The ratio of T<sub>1</sub> units/A<sub>260</sub> = 2.0 (Figure 1c) is taken as the minimum necessary for total digestion.

The amount of RNase T<sub>1</sub> digestion needed for cleavage of all the guanines was actually established in the final experiment. The sample of crab rAU was digested with enzyme, and an aliquot was subjected to preparative zone centrifugation. The remainder of the sample was treated with more enzyme, and another zone sedimentation analysis performed. This cycle was continued until the sedimentation

Figure 1. The sequential degradation of yeast tRNA by RNase T<sub>1</sub> followed by sucrose gradient centrifugation. Each period of digestion was 6 hours at 34° C. The cumulative ratios of RNase T<sub>1</sub> units to RNA A<sub>260</sub> units are: (a) 1.0, (b) 1.5, (c) 2.0, (d) 2.5. Sedimentation is from right to left, at 20° C for (a) 23 hours at 35 Krpm, (b) 19 hours at 41 Krpm, (c) 19 hours at 43 Krpm, and (d) 19 hours at 43 Krpm. The pattern of (d) is essentially identical to that of (c).

One unit of enzyme is the amount necessary to produce one A<sub>260</sub> unit of acid-soluble material after 15 minutes' incubation under the conditions of buffer and temperature employed.

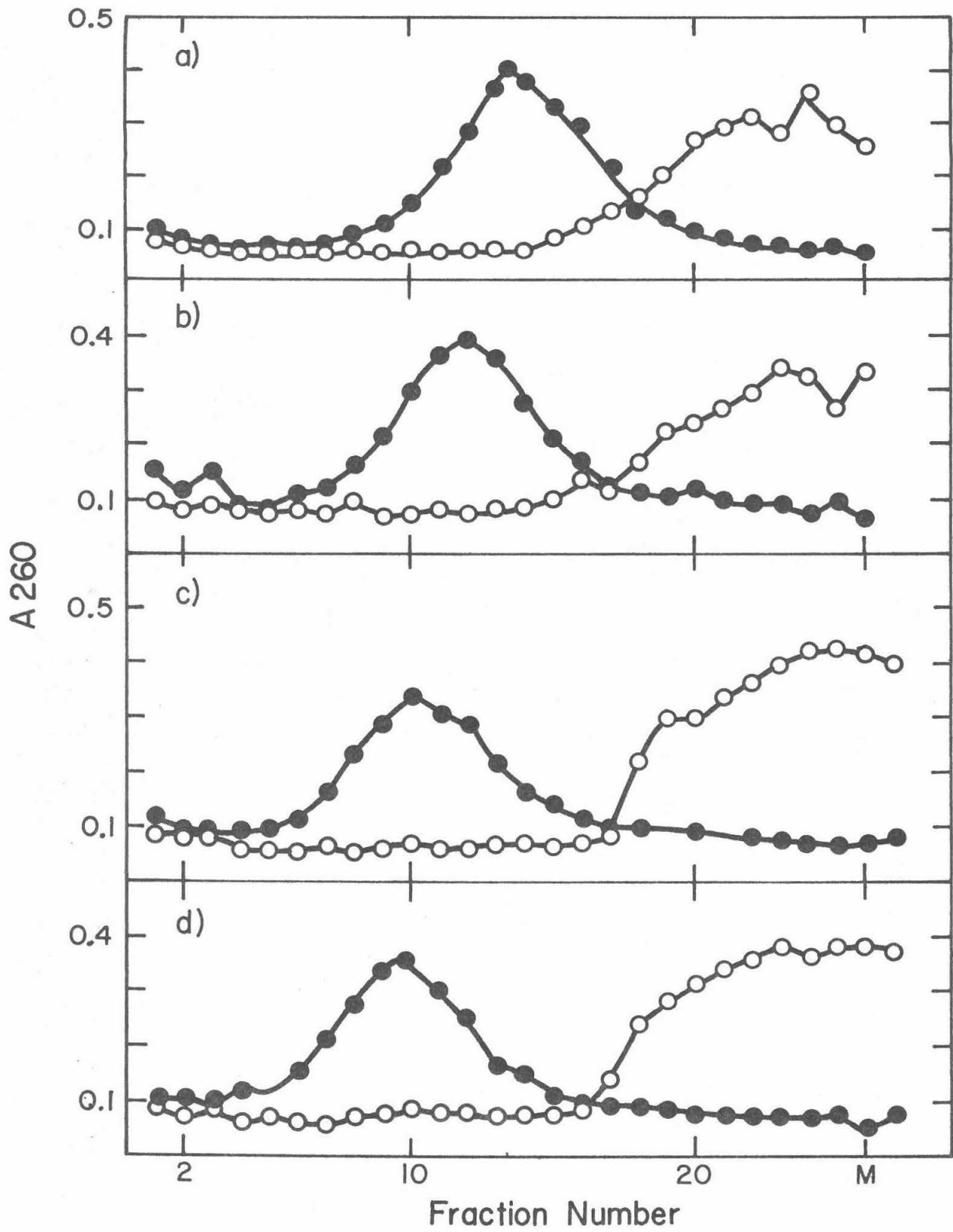


FIG 1

pattern ceased changing with further addition of enzyme; this required 16 enzyme units per  $A_{260}$  unit of RNA.

## RESULTS

### Binding of AMD by poly dAC:TG

Because of the limited quantities of the polynucleotide available, the binding of AMD to poly dAC:TG was measured spectrophotometrically. As a check on the method, the binding of AMD by calf thymus DNA, which we had previously measured by a sedimentation method, was measured as was the binding of AMD to crab dAT.

The reaction to be studied is



Let  $D_o$ ,  $D_b$ , and  $D_f (= D_o - D_b)$  be the total, bound, and free AMD concentrations, respectively. Let  $P_o$  be the total DNA concentration in units of moles of nucleotides per liter, and  $\alpha$  the number of strong binding sites per nucleotide ( $\alpha < 1$ ). Then, the binding constant  $K$  is given by

$$K = \frac{D_b}{D_f(\alpha P_o - D_b)} \quad (4)$$

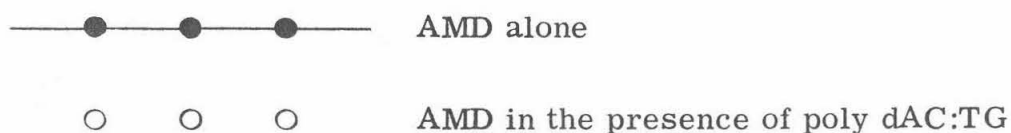
The spectral titration is based on the fact that at  $425 \text{ m}\mu$  the absorbance of bound AMD is 40% less than the absorbance of free AMD. The experiment consists of adding equal aliquots of AMD to buffer and to a DNA solution and measuring the absorbance difference,  $\Delta A$ . Such a titration is shown in Figure 2.

Let  $\Delta A_{\text{max}}$  be the maximum absorbance difference at high

Figure 2. The spectral titration of poly dAC: TG by AMD.

$$P_0 = 1.92 \times 10^{-5} \text{ M}$$

$$(\text{AMD})_{\text{stock}} = 1.4 \times 10^{-5} \text{ M}$$



A 5 cm microcell (with total volume 5 ml, but giving reproducible values with only 2 ml) was firmly held in place by an adaptor in the sample compartment of a Cary 14 spectrophotometer. The DNA phosphate concentration was usually about  $2 \times 10^{-5}$  M. Aliquots of a concentrated AMD solution ( $A_{440} \approx 0.25$ ;  $1 \times 10^{-5}$  M) were added with the aid of either a 50  $\mu$ l or a 100  $\mu$ l Hamilton syringe fitted with thin polyethylene tubing. After addition, the solution was stirred with a teflon rod for several minutes, and the  $A_{425}$  was measured.  $\epsilon_{425} = 23,500$  for free AMD. These titrations were done at room temperature, 25°C, in 0.01 M NaCl, 0.001 M sodium phosphate buffer, pH 7.0.

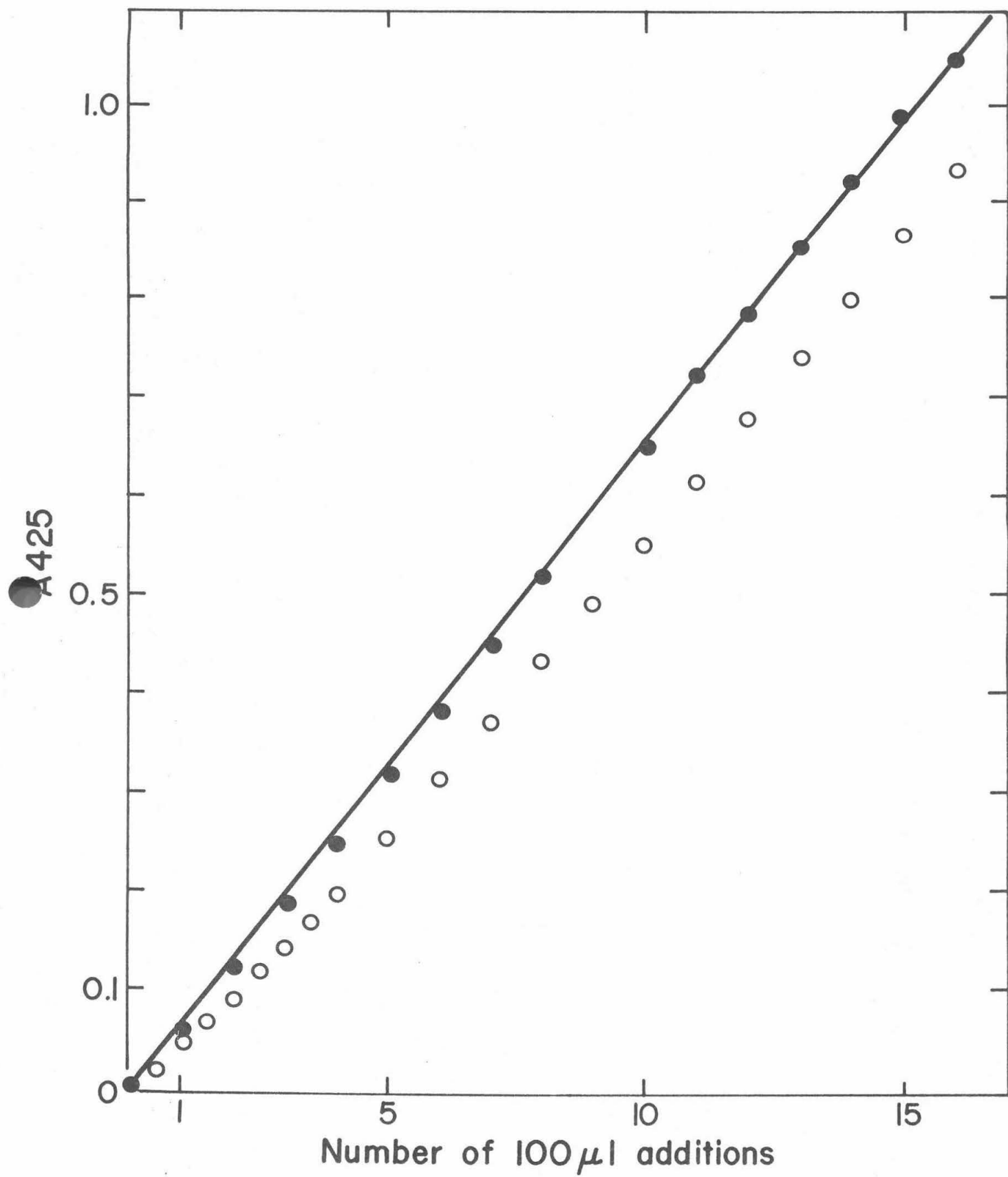


FIG 2

AMD concentration where all  $\alpha P_0$  binding sites are occupied and  $\Delta A$  the absorbance difference at an AMD concentration  $D_0$ . Then

$$\frac{\Delta A}{\Delta A_{\max}} = \frac{D_b}{\alpha P_0} \quad (5)$$

It follows from Equation (4) that

$$\frac{1}{\Delta A_{\max} - \Delta A} = K \frac{D_0}{\Delta A} - \frac{K \alpha P_0}{\Delta A_{\max}} \quad (6)$$

Furthermore,

$$D_0 = \frac{A_{425}}{\epsilon_{425} L} \quad (7)$$

where  $L$  is the path length of the cell,  $A_{425}$  is the absorbance of the AMD solution in buffer, and  $\epsilon_f$  is the molar extinction coefficient of free AMD at 425  $m\mu$  ( $\epsilon_{425} = 23,000$ ). An appropriate plot (Figure 3) of the experimental data is, therefore, suggested by the equation

$$\frac{1}{\Delta A_{\max} - \Delta A} = \frac{K}{\epsilon_f L} \frac{A_{425}}{\Delta A} - \frac{K \alpha P_0}{\Delta A_{\max}} \quad (8)$$

The results of several such titrations and of other binding measurements are presented in Table 3. It may be seen that the micro-

Figure 3. The data of Figure 2, the spectral titration of poly dAC:TG by AMD, plotted according to Equation (8).  $\Delta A_{\max} = 0.1159$ ;  $\epsilon_{425} = 23,500$ ;  $L = 5$  cm.

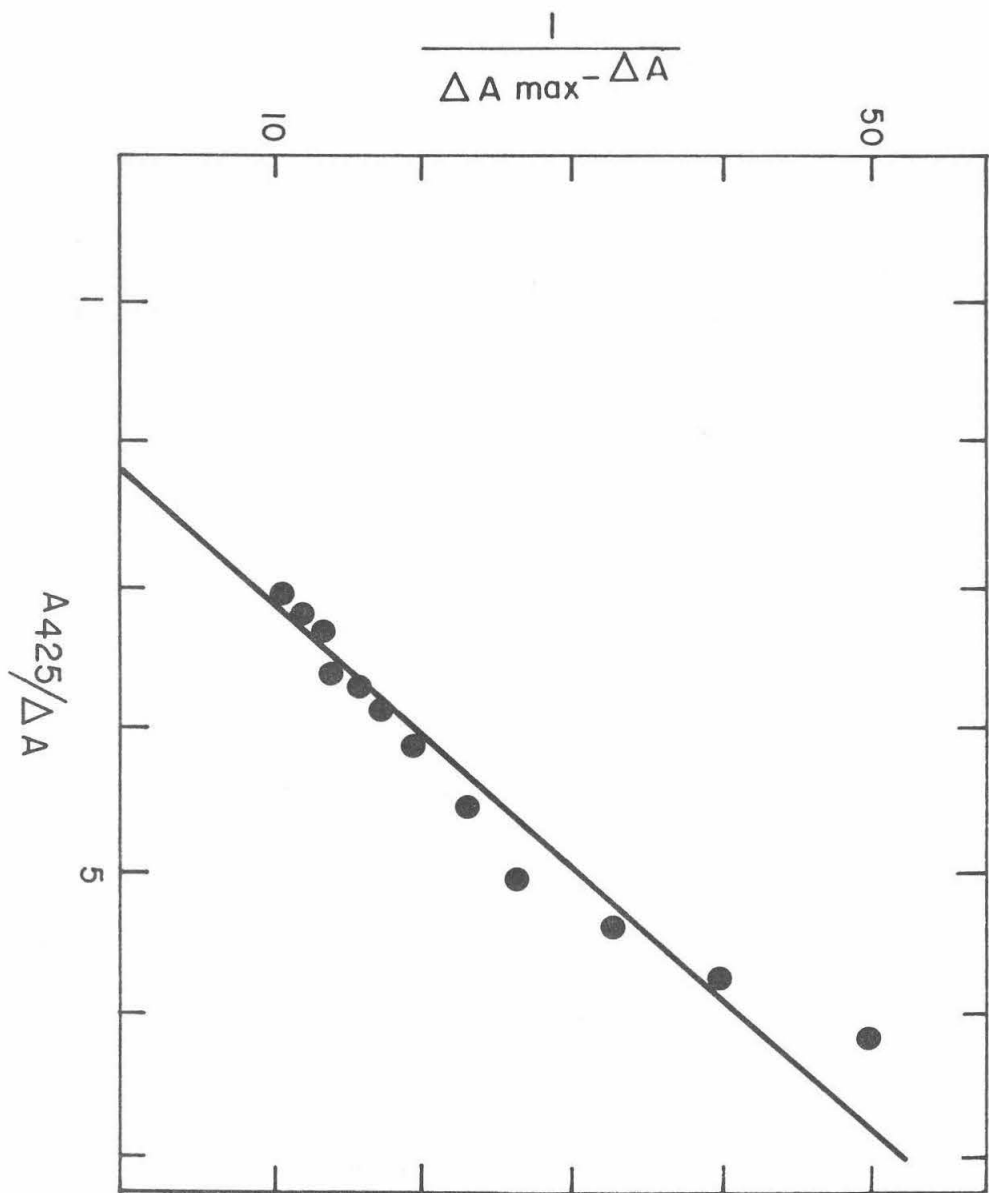


FIG 3

TABLE III  
BINDING PARAMETERS FOR AMD

DNA	Method	$K \times 10^{-6}$ $M^{-1}$	$1/2\alpha$ base pairs per site	Reference
CT DNA 42% G+C	spectral	6	8	Gellert <u>et al.</u> (4)
	equilibrium dialysis	4	9	Gellert <u>et al.</u> (4)
	ultracent	$2.3 \pm 0.5$	$7 \pm 1$	Hyman and Davidson (7)
	spectral	2.3	9	Müller and Crothers (18)
	10 cm spectral	$2.9 \pm 0.3$	$7 \pm 1$	this work
	5 cm micro spectral	$3.0 \pm 0.4$	$6 \pm 1$	this work
crab dAT 3.0% G+C	ultracent	$2.5 \pm 0.5$	$56 \pm 2$	Hyman and Davidson (7)
	5 cm micro spectral	$1.2 \pm 0.2$	$45 \pm 4$	this work
poly dAC:TG 50% G+C	5 cm micro spectral	$1.3 \pm 0.2$	$5 \pm 1$	this work
	equilibrium dialysis	1.3	12	Wells and Larson (19)

spectrophotometric titrations gave results for  $K$  and for  $\alpha$  in agreement with those from other methods. These measurements are reproducible to 15%. The main source of experimental error appears to be the retention of a small amount of AMD within the delivery tube so that less AMD is actually added than is calculated to be added. This error would result in the calculation of a value for  $1/2\alpha$  smaller than the true value.

The binding constant per site for poly dAC:TG is identical to that measured independently and coincidentally by Wells and Larson (19) using equilibrium dialysis, and is about the same as for a typical DNA. We measure one binding site for every 5 base pairs, which is the same as for an irregular DNA. Wells and Larson's (19) value of 12 base pairs per site is significantly larger than ours. Since they detect no strong binding sites for crab dAT by their method, we believe their values for saturation binding (base pairs per site) to be consistently high. Furthermore, since AMD binding does not cause long-term distortions of the DNA helix (20), AMD binding of repeating sequence polymers should be an "all or none" phenomenon (subject only to close range steric interference). If one guanine is a site, then since all the guanines are within identical nucleotide sequences, they should all be sites, subject only to steric limitations:  $1/2\alpha = 6$  base pairs/site. Poly dAC:TG behaves as an "all" phenomenon: therefore,  $1/2\alpha = 5 \pm 1$  base pairs/site is the correct saturation value.

The new datum for crab dAT and our best measurement of the

G + C content of crab dAT, 3.0% (see later), allow us to better estimate the fraction of guanines that are not strong binding sites for AMD. One site for every guanine corresponds to a  $1/2\alpha = 33$  base pairs/site. Using two different experimental techniques, we measure  $1/2\alpha$  for crab dAT to be  $56 \pm 2$  and  $45 \pm 4$ . These data indicate that 25 to 40% of the guanines of crab dAT are not strong AMD binding sites.

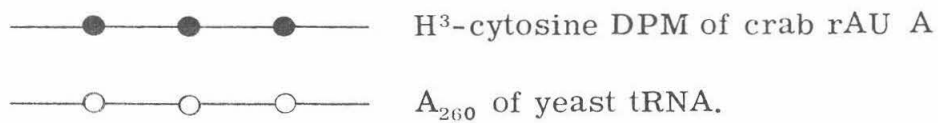
#### The crab rAU experiment

Both samples of crab rAU A and B have an overall u/c ratio of 31.5. With the exception of the very small material (which makes an insignificant contribution to the total mass), each size group of crab rAU also has an u/c ratio of 31.5 (Figure 6). This ratio corresponds to a template 97% AT and 3.0% GC, which represents the best measurements to date of the base composition of Cancer antennarius dAT.

The necessity of determining molecular weight in a disruptive solvent like DMSO is demonstrated in Figures 4 and 5, which show the sedimentation behavior of crab rAU A on a normal sucrose gradient and on a gradient in DMSO. In an ordinary sucrose gradient, crab rAU A shows a very large polydispersity; whereas, in a gradient containing DMSO crab rAU A shows a broad but well-defined peak. Clearly, the use of DMSO is a necessity for measuring the true molecular weight of an RNA like crab rAU.

As suspected, crab rAU B has a larger average size than crab rAU A, and therefore, crab rAU B is a better starting material for

Figure 4. Crab rAU A sedimented on a normal sucrose gradient against yeast tRNA as a marker. Sedimentation is from right to left: 4.5 hours, 45 Krpm, 20° C.



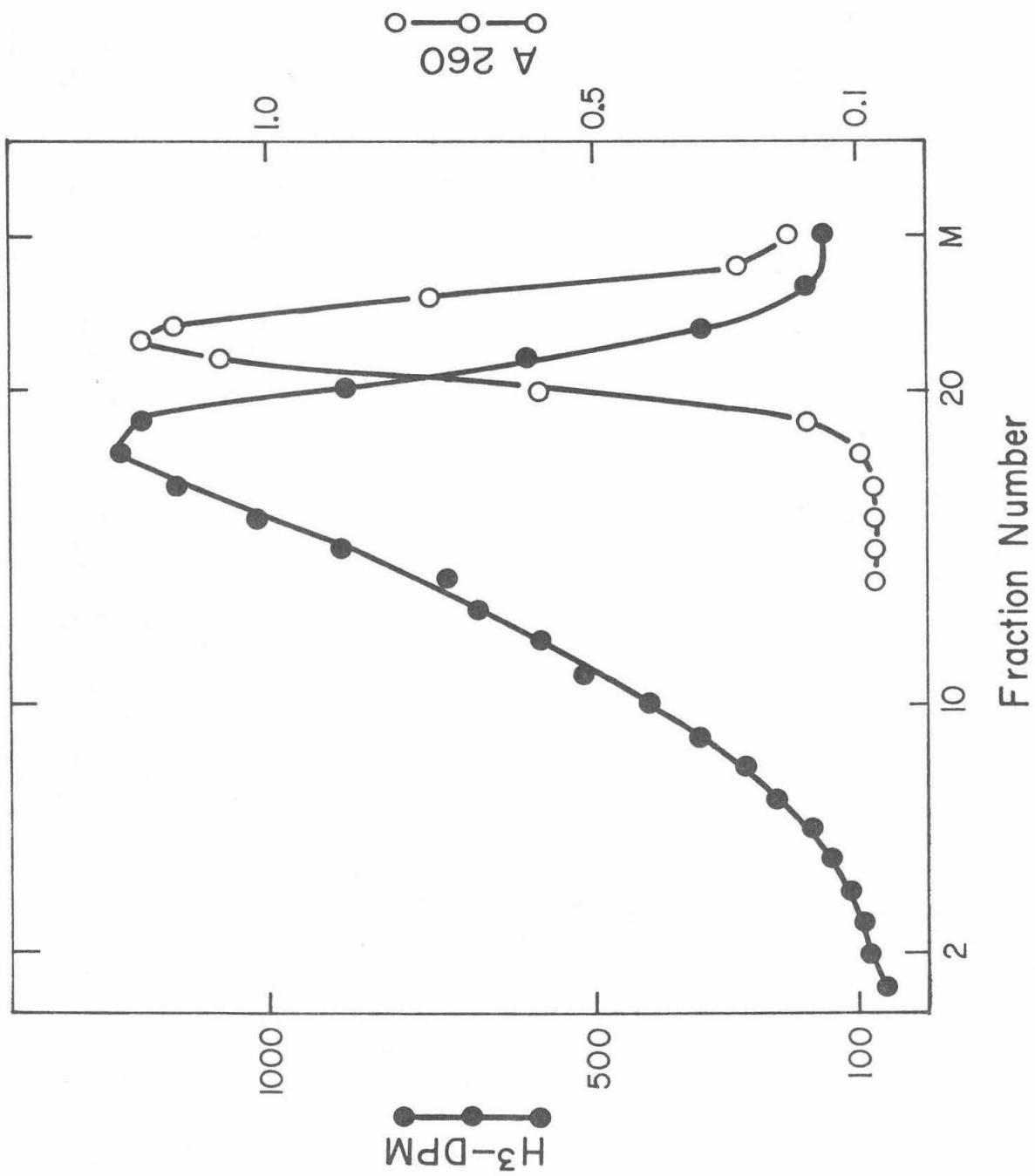
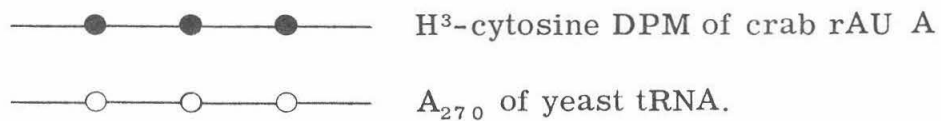


FIG 4

Figure 5. Crab rAU A sedimented on a 5 ml, 5 - 20 w/v% sucrose gradient, 5 v/v% water, 0.01 M citrate pH 5.5, 95 v/v% DMSO against yeast tRNA for 22.5 hours at 42 Krpm and 20°C.



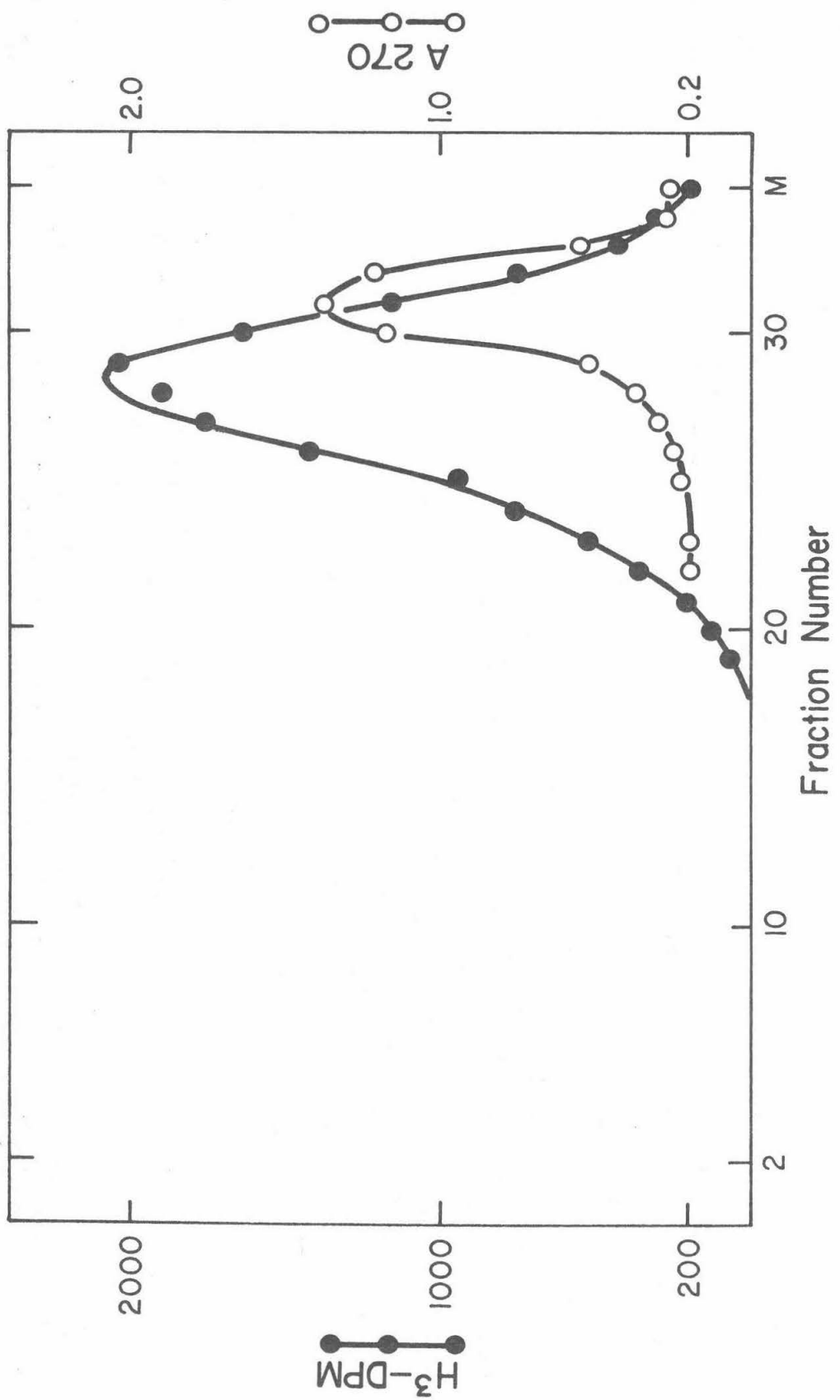


FIG 5

the RNase  $T_1$  digestion. The sedimentation profile of crab rAU B is shown in Figure 6. The different fractions of crab rAU B have a constant  $u/c$  ratio of 31.5, except for the small material near the meniscus. We believe this decrease in the  $u/c$  ratio for the small material is real, and we shall comment on it later.

The sedimentation profile of the total RNase  $T_1$  digest of crab rAU B is shown in Figure 7.

The final digest has a peak which cosediments with transfer RNA and a  $u/c$  ratio of 32.0 which is constant throughout the gradient if the lower values near the meniscus are corrected for the low  $u/c$  ratio of the pre-existing small material. This correction is made by assuming the original small material is not significantly digested; and, therefore, each small RNA makes the same mass contribution to the corresponding fraction of the sucrose gradient after digestion as before digestion. Let  $(u/c)_B$ ,  $(u/c)_A$ , and  $(u/c)_T$  be the ratio of  $u/c$  measured before digestion, measured after digestion, and the true ratio of the new small fragments after digestion, respectively; and let  $f_B$  and  $f_T$  be the mass fraction of material pre-existing and newly created at a given fraction of the sucrose gradient ( $f_B + f_T = 1$ ), then

$$(u/c)_A = (u/c)_T f_T + (u/c)_B f_B. \quad (9)$$

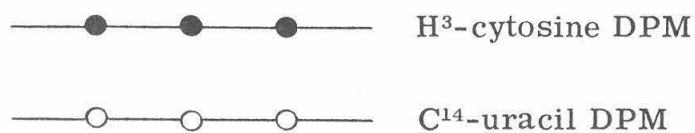
$(u/c)_B$  and  $(u/c)_A$  are measured, and  $f_B$  and  $f_T$  can be estimated so the calculation of  $(u/c)_T$  can be made. The corrected values are

Figure 6. Crab rAU B sedimented in a DMSO-sucrose gradient with yeast tRNA as a marker: 45 Krpm, 50 hours, 20° C.

(a) Yeast tRNA (100  $\mu$ l of 1.5 mg/ml) dripped into 0.5 ml DMSO and  $A_{280}$  read.

(b) The ratio of uracil of cytosine ( $C^{14}$ -DPM to  $H^3$ -DPM times the specific activities) for each fraction of the gradient.

(c) Crab rAU B



dripped directly into scintillation vials, Bray's solution added, and counted on a Packard Tri-Carb Scintillation counter.

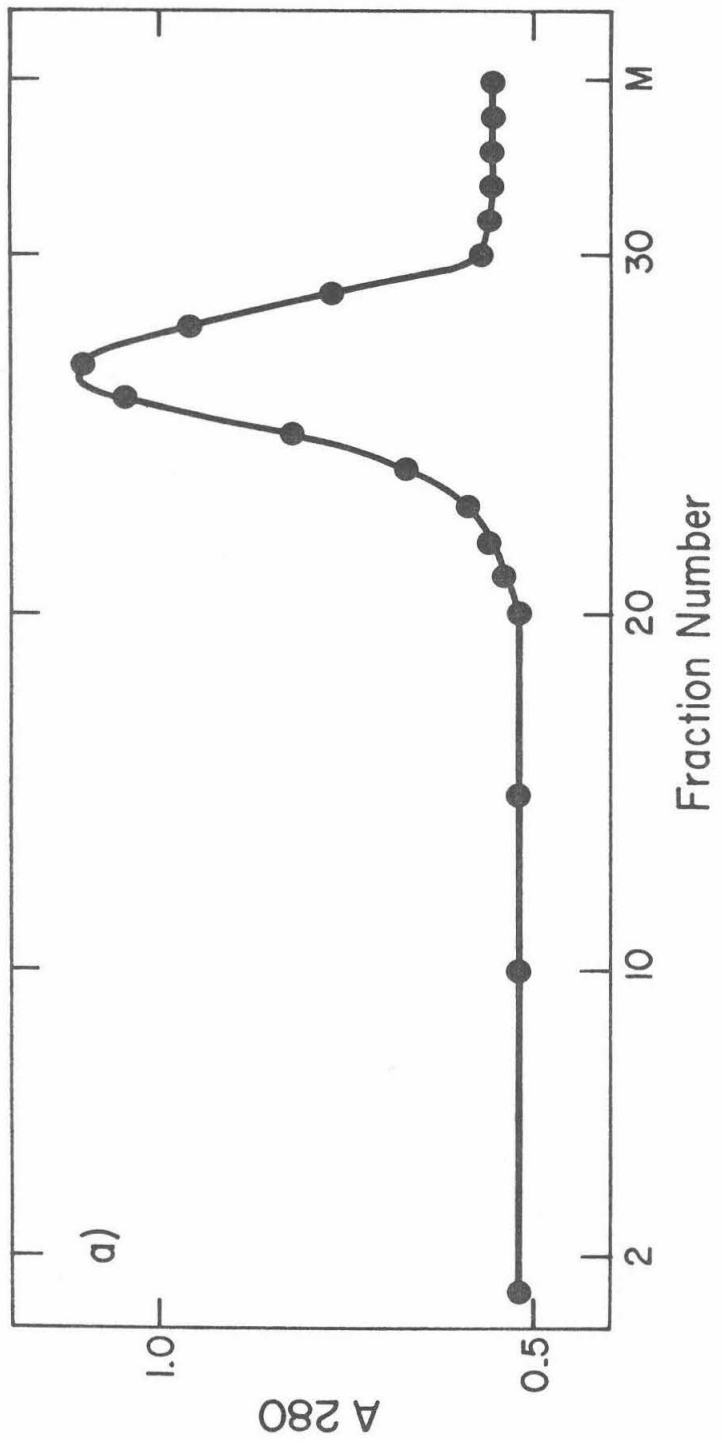


FIG 6a

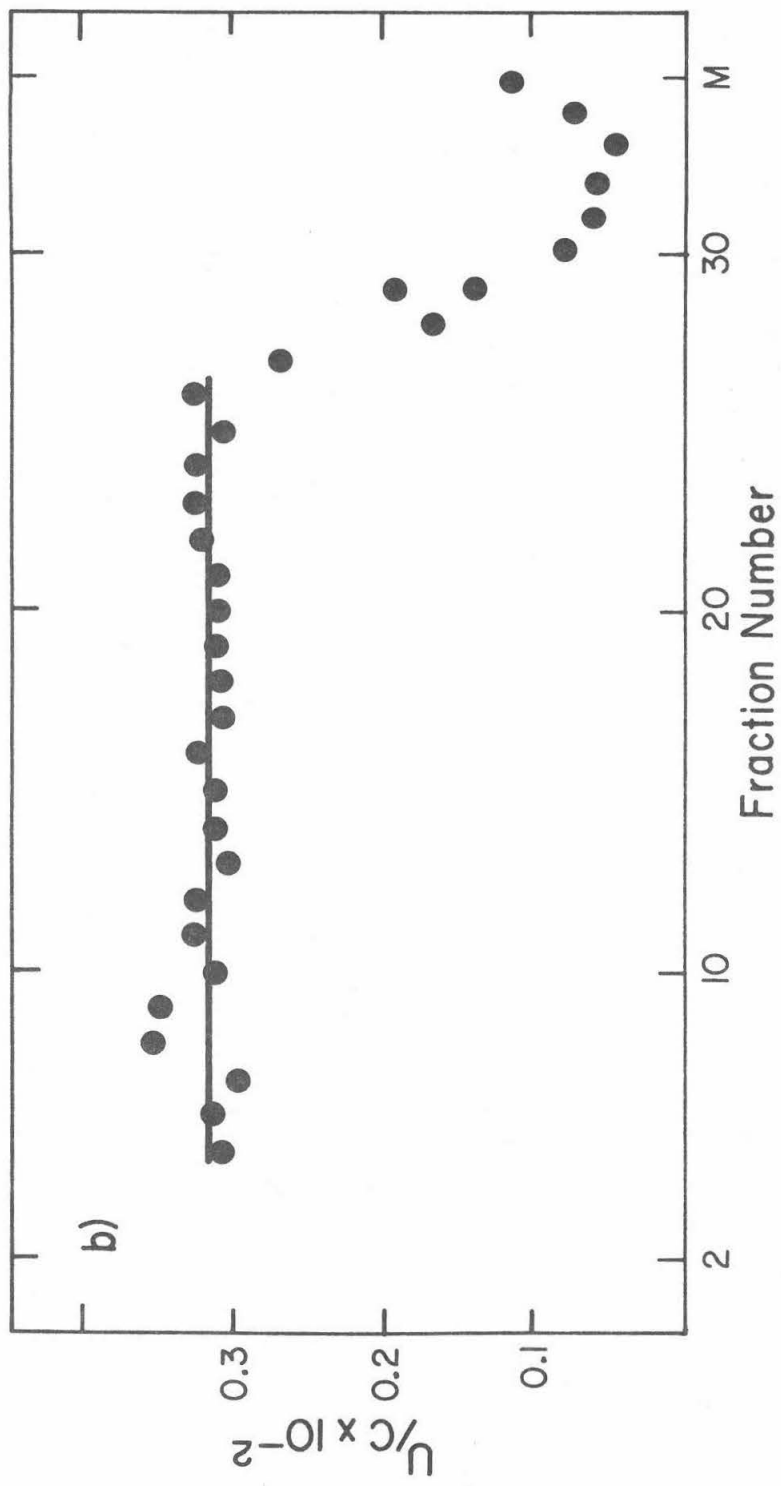


FIG 6b

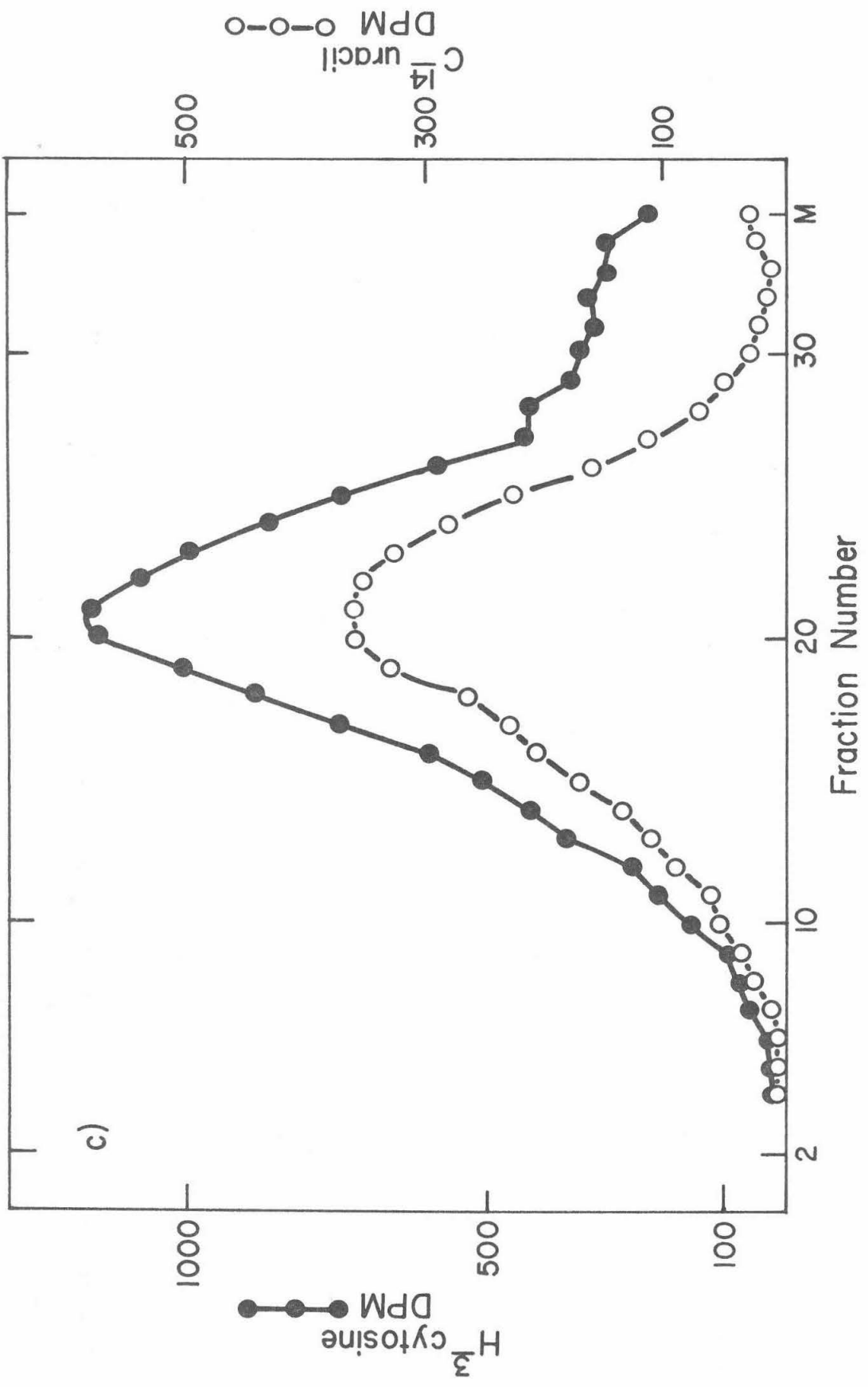


FIG 6c

Figure 7. The final RNase T<sub>1</sub> digest of crab rAU on a 5-20 w/v% sucrose gradient in DMSO and run for 65 hours at 40 Krpm and 20°C.

(a) Yeast tRNA (100 λ of 1.5 mg/ml) dripped into 0.5 ml DMSO.

(b) The final digest of crab rAU

—●—●—●— DPM of H<sup>3</sup>-cytosine

—○—○—○— DPM of C<sup>14</sup>-uracil.

(c) The ratio u/c; C<sup>14</sup>-DPM/H<sup>3</sup>-DPM

● data and reasonable error bars

○ corrections at low S value for the pre-existing small material of low u/c ratio (Equation 9).

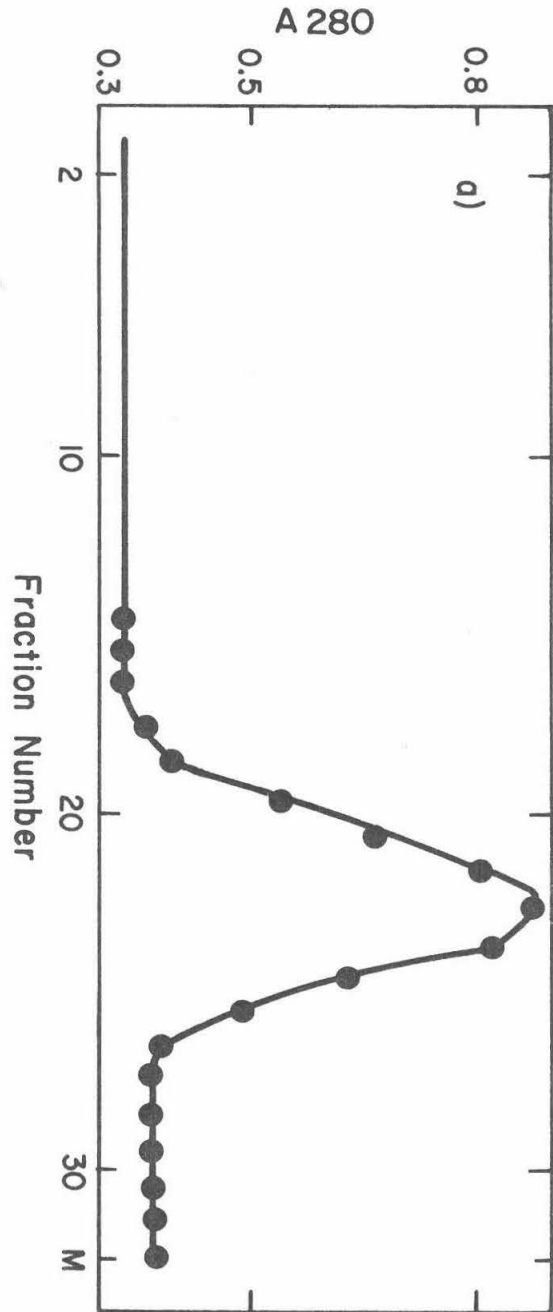


FIG 7a

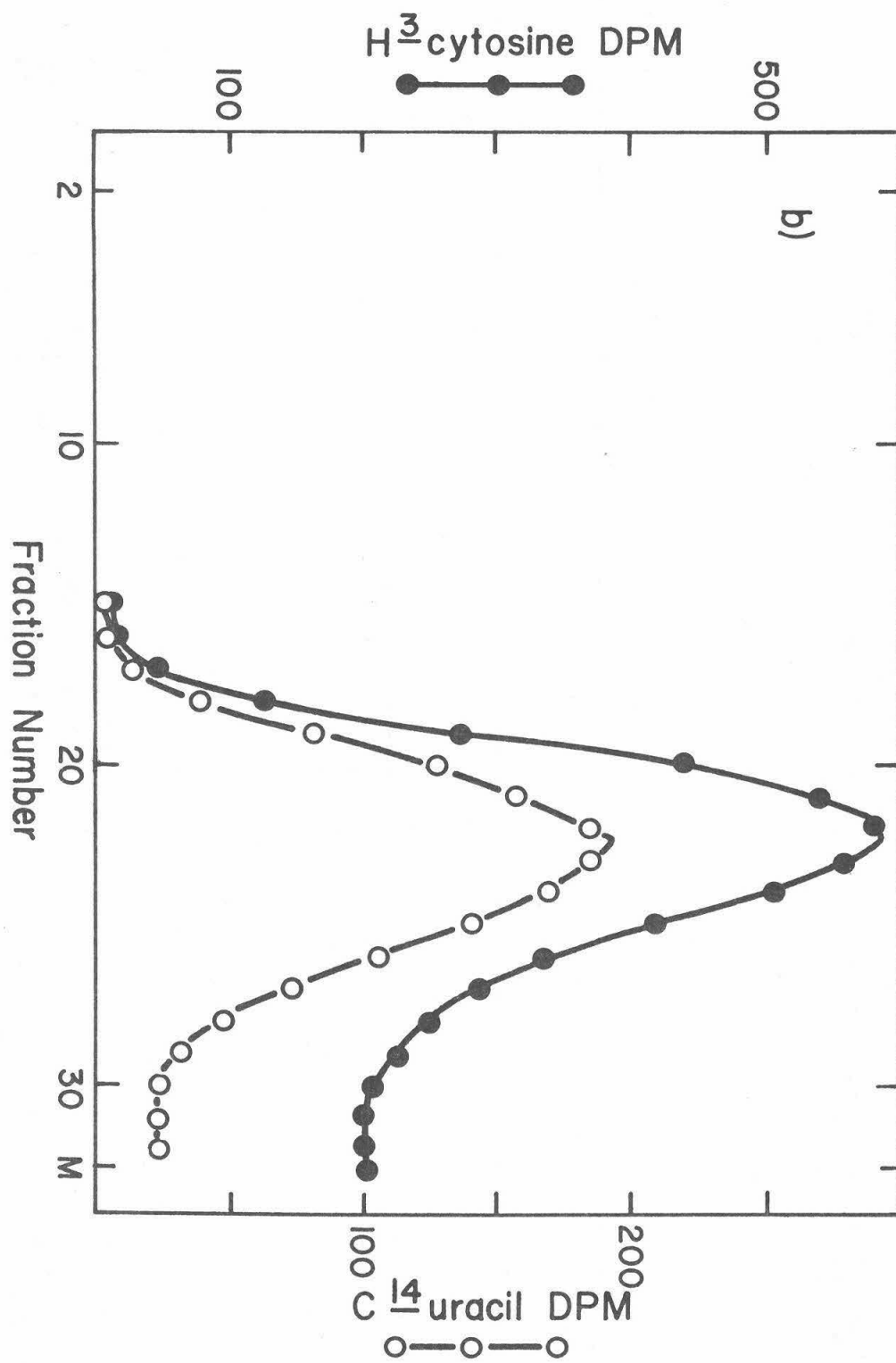


FIG 7b

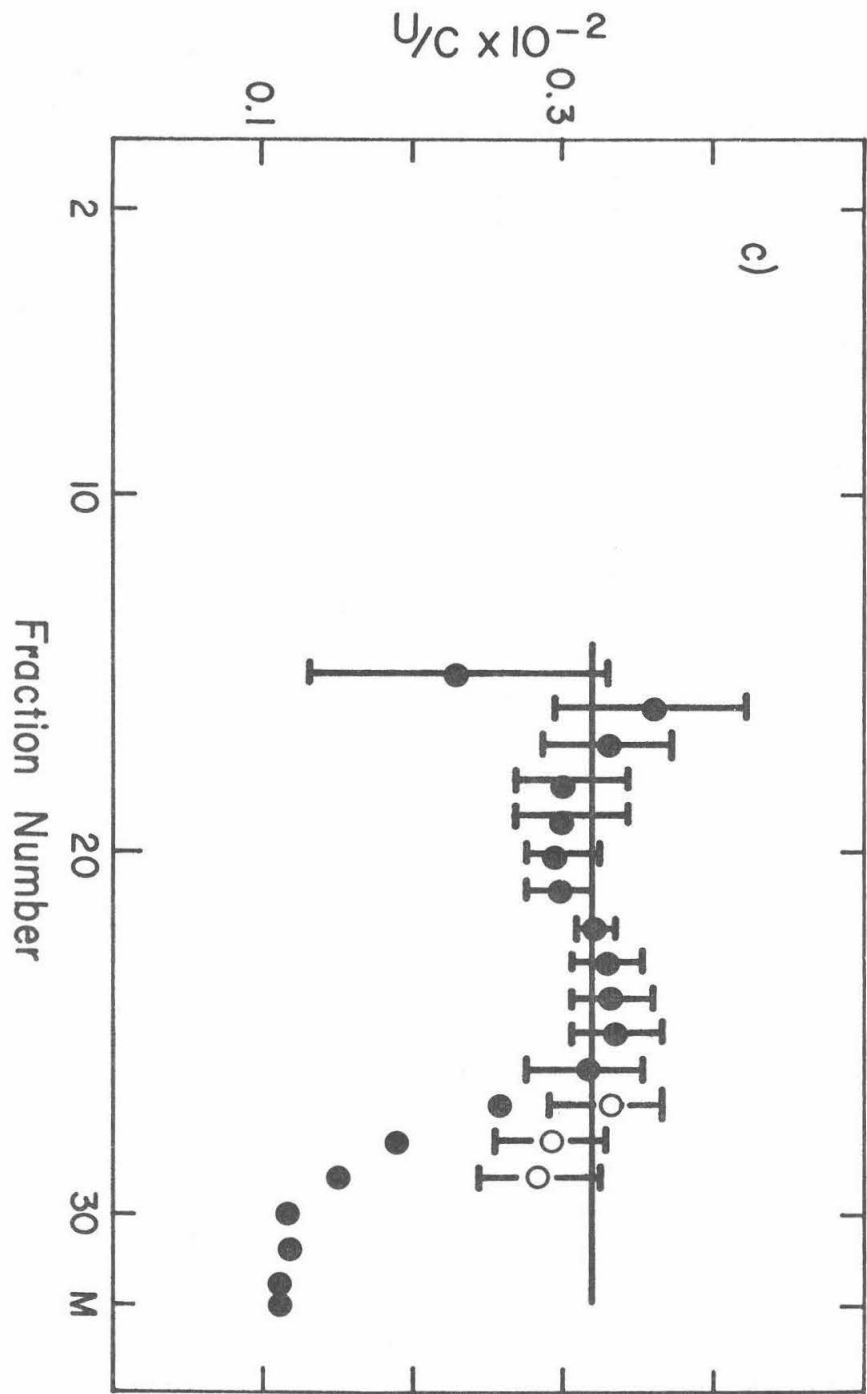


FIG 7c

plotted in Figure 7 and agree with the values from the other parts of the gradient. The constancy of the u/c ratio independently and importantly implies a random spacing of guanines between cytosines on the transcribing strand.

Since crab dAT is 3.0% GC, we expect one G for every 67 nucleotides and, hence, crab rAU fragments of 68 nucleotides after total RNase T<sub>1</sub> digestion, if the G's are randomly distributed in the template. The peak of the total RNase T<sub>1</sub> digest of crab rAU is coincident with the peak of tRNA (Figure 7). Yeast tRNA is composed of about 75 nucleotides (21, 17). In our experiment 68 and 75 are the same number, and this agreement strongly argues for the random distribution of the G's. If true, there should also be an average of one C per RNase T<sub>1</sub> fragment. This prediction is verified by calculations using the experimental values from Figure 7.

$$75 = a + u + g + c$$

$$u/c = 32.0$$

$$g = 1 \tag{10}$$

We assume that  $a = u$ , then

$$a = u = 36 \tag{11}$$

$$c = 1.1$$

Therefore, in the template crab dAT there is one GC base pair for every 36 AT base pairs on the average, where exactly random is 1 GC for every 33 base pairs. The GC base pairs appear to be randomly distributed in crab dAT.

We can enhance this last conclusion by comparing our results with those predicted for a random polymer. The calculation for a random polymer proceeds as follows. If we start with an infinite polymer of composition 1.5% guanine and degrade it to completion with RNase T<sub>1</sub>, and if we let

$$\begin{aligned}
 1 - P &\equiv \text{the probability of occurrence of guanine,} \\
 &\quad \text{an RNase T}_1 \text{ sensitive link} \\
 &= 0.015 \qquad \qquad \qquad (12)
 \end{aligned}$$

$$\begin{aligned}
 P &\equiv \text{the probability of finding any base not guanine} \\
 &\quad \text{and hence RNase T}_1 \text{ resistant} \\
 &= 0.985 \qquad \qquad \qquad (13)
 \end{aligned}$$

then the weight fraction of the total RNase T<sub>1</sub> digest is expressed as

$$W(n) = (n + 1) P^n (1 - P)^2. \quad n = 0, 1, 2, 3, \dots \quad (14)$$

We convert the weight fraction to a mole fraction and integrate the latter:

$$X(n) = \frac{W(n)}{(n+1)(1-P)} = P^n/(1-P) \quad (15)$$

$$\int_0^n X(n) dn = \left(\frac{P-1}{\ln P}\right)(1-P^n) \quad (16)$$

Since the starting crab rAU is not an infinite polymer, we can expect the experimental data to deviate from the curve (Eq. 16) at  $n \geq 100$ . The theoretical and experimental curves are plotted in Figure 8. The coincidence of the two curves is remarkable, and once again, suggests the randomness of the GC base pair distribution in crab dAT.

As a second, better theoretical approximation, we notice that the experimental curve of  $X(n)$  vs.  $n$  essentially reaches zero at  $n = 200$ . To better fit the experimental data, we truncate the theoretical curve of  $X(n)$  vs.  $n$  for a random polymer at  $n = 200$  and integrate graphically and normalize. The experimental results and the integrated truncated theoretical curve for a random polymer are graphed in Figure 9. The data from H<sup>3</sup>-cytosine exactly fit on the theoretical curve, and the C<sup>14</sup>-uracil data are in good agreement. This fit of the theoretical curve for a random polymer and the experimental data strongly argue for the randomness of the GC base pairs in crab dAT.

Figure 8. The experimental and theoretical curves for the integrated mole fraction,  $X(n)$ . The theoretical curve for a random, infinite polymer is calculated from Equation (16) and is the solid line.

- the data from H<sup>3</sup>-cytosine
- the data from C<sup>14</sup>-uracil
- the theoretical curve.

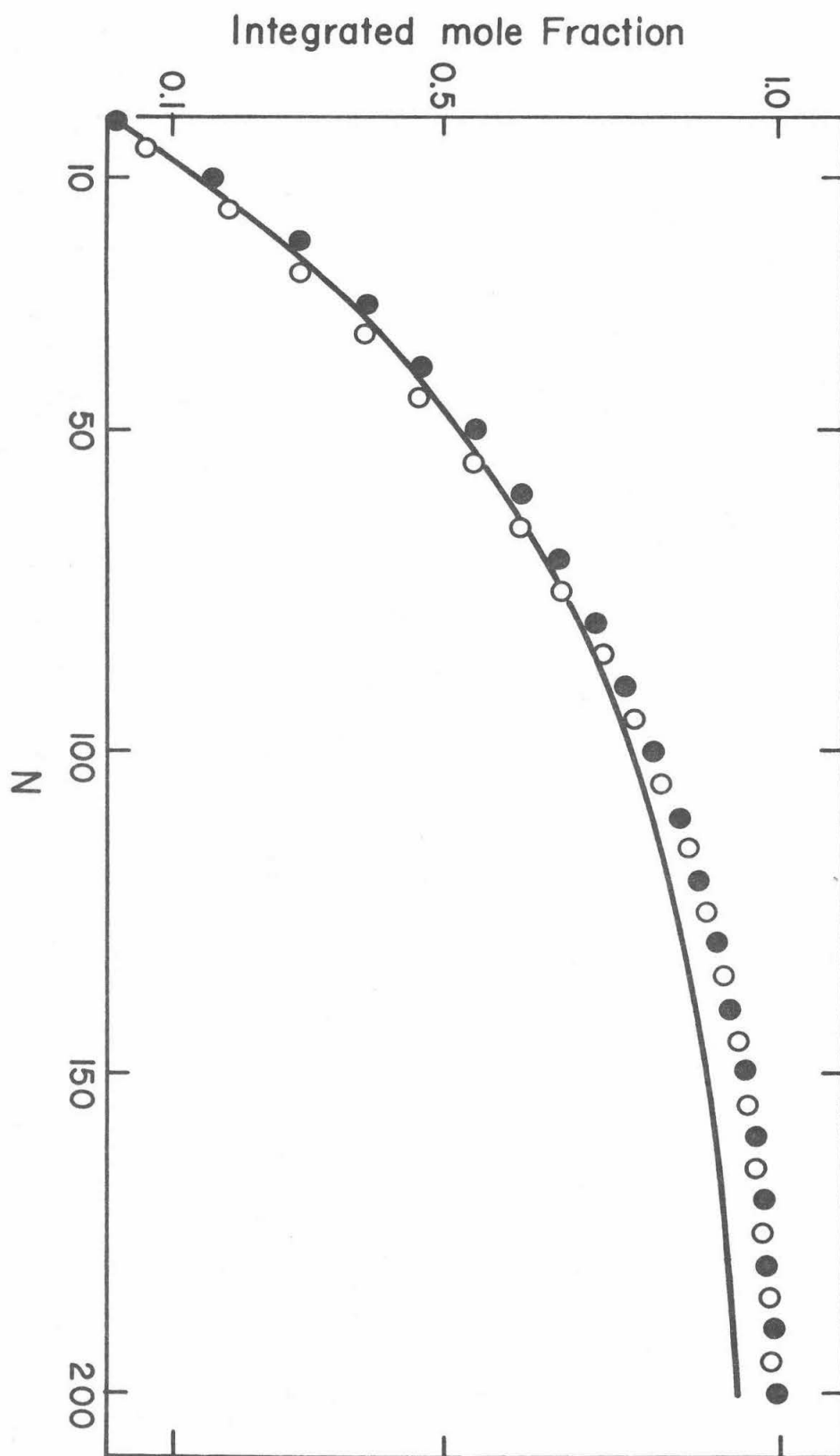


FIG 8

Figure 9. The curve is for the integrated, truncated random polymer.

- the data for H<sup>3</sup>-cytosine
- the data for C<sup>14</sup>-uracil from Figure 7.

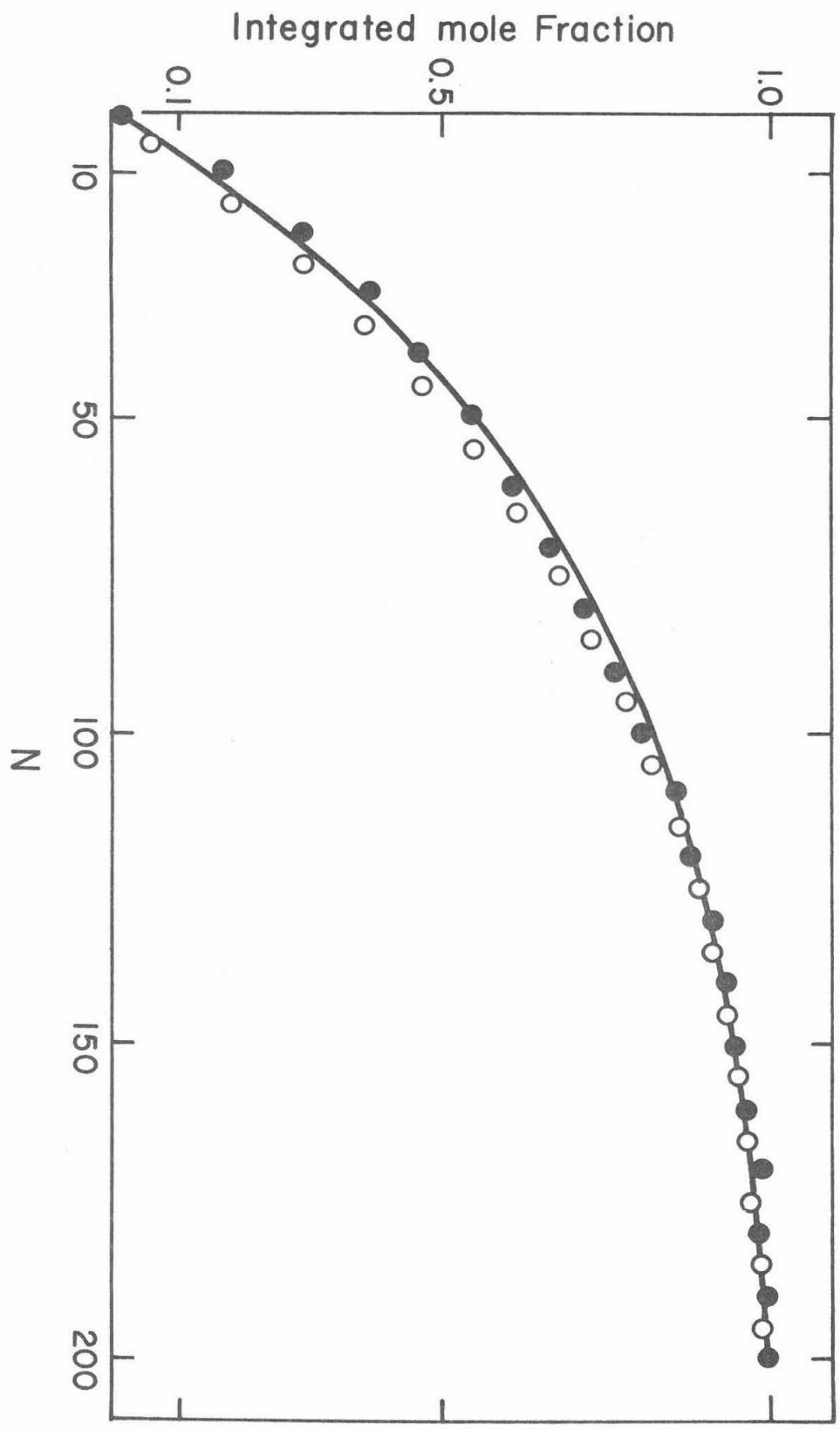
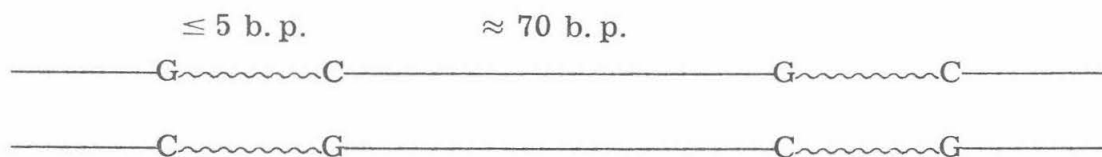


FIG 9

## DISCUSSION

The existence of small crab rAU may be related to the class of enzyme termed "early quitter" by Bremer, Konrad, Gaines and Stent (22). If so, the low u/c ratio implies that a relatively GC-rich region of the DNA provides a signal for chain termination (23).

The crab rAU data strongly suggest that the GC base pairs of crab dAT are randomly distributed. There is, however, one simple model for a nonrandom GC distribution which we could not detect as such by our experiment. If the GC base pairs themselves occur in pairs always in the trans configuration, and if these pairs of pairs are randomly distributed about an average of 70 base pairs apart,



there is a nonrandom GC distribution which would appear to be random in our test and would explain the AMD binding data on the basis of steric interference alone. This model is bizarre and, since we can explain the fact that 25-40% of the guanines of crab dAT are not binding sites without recourse to this model, we prefer to interpret Figure 9 to mean that the GC base pairs of crab dAT are randomly distributed.

In the digest (Figure 9) 12% of the fragments are eight bases or shorter; this fact means that at very most only 12% of the GC base

pairs of crab dAT are within the maximum distance whereby steric interference would rule out a guanine being an AMD binding site, and 12% is well below the 25-40% necessary to explain the crab dAT-AMD binding data. Therefore, steric interference alone is not the limiting factor in AMD binding. The strong AMD binding site must require either G within a particular favored sequence or G not within a disallowed sequence.

In our previous paper we suggested that guanine and a neighboring purine for the unique AMD binding site. This model is absolutely eliminated by the binding data of AMD to poly dAC:TG. In poly dAC:TG, guanine has only pyrimidines as neighbors and yet this polymer behaves as any irregular DNA.

The question of which guanines are (or are not) binding sites is not answered by considering nearest-neighbors on only one side. In this regard the recent measurement by Wells (1) of the binding of AMD by the synthetic DNA-like polymer poly dGAT:CTA is very important. Poly dGAT:CTA, wherein the guanine is contained in the sequence 5'TGA3', exhibits no strong binding sites. With certain assumptions we can calculate the frequency of occurrence of TGA in crab dAT from the normalized nearest-neighbor analysis data of Schwartz, Trautner and Kornberg (24):

TpG	0.72	GpA	0.29
ApG	0.14	GpT	0.55
GpG	0.07	GpG	0.06
CpG	<u>0.06</u>	GpC	<u>0.10</u>
	0.99		1.00

We assume that TpG occurs at random with respect to GpA; the frequency of occurrence of TGA is the frequency of TpG times the frequency of GpA:  $TGA = 0.72 \times 0.29 = 0.21$ . Twenty-one percent of the guanines of crab dAT are disallowed as AMD binding sites on this basis alone. If TGA is an example of the general phenomenon that 5' pyrimidine-guanine-purine 3' is disallowed as an AMD binding site, then 27% of the guanines of crab dAT are disallowed. (This generalization can be tested when the corresponding synthetic polymers become available.) We add to the fraction of disallowed guanines the small number that are too close together to be binding sites for steric reasons even though the guanines are randomly distributed, about 7% not including 5' pyrimidine-guanine-purine 3' (Figure 9). Thus, we estimate that 28% of the guanines of crab dAT are not strong binding sites, if only TGA is disallowed, or that 34% of the guanines of crab dAT are not strong binding sites if 5' pyrimidine-guanine-purine 3' is disallowed. We have then good agreement with the experimental binding data of AMD to crab dAT (Table 3), where 25 to 40% of the guanines are not sites, based on the knowledge: (a) the guanines of crab dAT are randomly distributed (Figure 9); (b) binding sites cannot be closer than about  $5 \pm 1$  base pairs because of steric interference (Table 3); and (c) TGA is disallowed as the AMD binding site (1). These observations are of general significance, indicating that for any ordinary DNA there are two constraints on strong AMD binding: steric interference and the occurrence of the sequence TGA (possibly pyrimidine-guanine-purine). Why TGA is a disallowed sequence for strong AMD binding is an open question.

**ACKNOWLEDGMENTS**

We are deeply grateful to Grace Kung Dahmus for the generous gift of RNA polymerase and to Dr. Michael Chamberlin for the gift of poly dAC:TG. We have profitted from counsel and conversation with M. Simon, J. Widholm, and D. Mohr. This research has been supported by U. S. Public Health Service Research Grant No. GM 10991. One of us (R. W. H. ) was a National Institutes of Health predoctoral trainee (GM 1262).

## REFERENCES

- 1 R. D. Wells, Science, 165 (1969) 75.
- 2 I. H. Goldberg, M. Rabinowitz and E. Reich, Proc. Nat. Acad. Sci. U.S., 48 (1962) 2094.
- 3 L. Cavalieri and R. Nemchin, Biochim. Biophys. Acta, 87 (1964) 641.
- 4 M. Gellert, C. E. Smith, D. Neville and G. Felsenfeld, J. Mol. Biol., 11 (1965) 445.
- 5 E. Kahan, F. M. Kahan and J. Hurwitz, J. Biol. Chem., 238 (1963) 2491.
- 6 W. Kersten, Biochim. Biophys. Acta, 47 (1961) 610.
- 7 R. W. Hyman and N. Davidson, Biochem. Biophys. Res. Comm., 26 (1967) 116.
- 8 N. Davidson, J. Widholm, U. S. Nandi, R. Jensen, B. M. Olivera and J. C. Wang, Proc. Nat. Acad. Sci. U.S., 53 (1965) 111.
- 9 H. Fraenkel-Conrat, Virology, 14 (1961) 54.
- 10 M. Chamberlin and P. Berg, Proc. Nat. Acad. Sci. U.S., 48 (1962) 81.
- 11 B. C. Westmoreland, W. Szybalski and H. Ris, Science, 163 (1969) 1343.
- 12 R. W. Davis, M. Simon and N. Davidson, in L. Grossman and K. Moldave, Methods in Enzymology, Vol. XII, Part C, Academic Press, New York, 1970, in the press.
- 13 A. G. So, E. W. Davie, R. Epstein and A. Tissieres, Proc. Nat. Acad. Sci. U.S., 58 (1967) 1739.

- 14 H. Bremer and M. W. Konrad, Proc. Nat. Acad. Sci. U.S., 51 (1964) 801.
- 15 J. H. Strauss, Jr., R. B. Kelly and R. L. Sinsheimer, Biopolymers, 6 (1968) 793.
- 16 R. G. Martin and B. N. Ames, J. Biol. Chem., 236 (1961) 1372.
- 17 H. Boedtker, J. Mol. Biol., 35 (1968) 61.
- 18 W. Müller and D. M. Crothers, J. Mol. Biol., 35 (1968) 251.
- 19 R. D. Wells and J. E. Larson, J. Mol. Biol., (1970) in the press.
- 20 R. W. Hyman and N. Davidson, J. Mol. Biol., (1970) submitted.
- 21 R. W. Holley, J. Apgar, G. A. Everett, J. T. Madison, M. Marquisee, S. H. Merrill, J. R. Penswick and A. Zamir, Science, 147 (1965) 1462.
- 22 H. Bremer, M. Konrad, K. Gaines and G. Stent, J. Mol. Biol., 13 (1965) 540.
- 23 R. L. Novack, Fed. Proc., 29 (1969) 660.
- 24 M. N. Schwartz, T. A. Trautner and A. Kornberg, J. Biol. Chem., 237 (1961) 1961.

CHAPTER 3

The Kinetics of the In Vitro Inhibition  
of Transcription of Actinomycin

The following paper has been submitted  
for publication to the Journal of Molecular Biology.

The Kinetics of the in Vitro Inhibition  
of Transcription by Actinomycin

RICHARD W. HYMAN AND NORMAN DAVIDSON

Summary

The kinetics of the in vitro transcription of DNA to RNA by RNA polymerase in the absence and presence of actinomycin D (AMD) have been studied. In the kinetics experiments, the total amount of RNA synthesized is measured by incorporation of a radioactive label, and the average RNA chain length as a function of time is measured by sedimentation analysis. Thus the number of growing chains can be calculated. Membrane filter retention experiments show that if RNA polymerase is added to T7 DNA in a low salt medium in the presence of ATP and GTP ( $2 \times 10^{-4}$  M) and the medium then adjusted to 0.4 M  $(\text{NH}_4)_2\text{SO}_4$ , a sufficient amount of the polymerase remains attached to the DNA so that the DNA is retained by the filter. If ATP and GTP are absent, most of the polymerase dissociates in the high salt medium, and the DNA is not retained. The membrane filter experiments and the kinetics experiments both suggest that there is an initiation complex, consisting of RNA polymerase and a purine triphosphate attached at a specific site on T7 DNA, which can be formed at low salt and does not dissociate at high salt. The formation of the initiation complex is not significantly inhibited by AMD. For the kinetics of transcription studies, the initiation complex was formed by mixing T7 DNA, RNA polymerase, ATP, GTP, and UTP in the low salt medium,

then adjusting to  $0.4 \text{ M } (\text{NH}_4)_2\text{SO}_4$ , adding AMD if desired, and starting propagation by adding CTP. Under these conditions, there is one RNA molecule synthesized per T7 DNA molecule. Thus, the conditions of initiation are quite specific, and there is no reinitiation. The main effect of AMD is to inhibit the rate of chain growth; it may have a small effect on termination. The effects of concentration of the four nucleoside triphosphate substrates on the rate of chain growth conform to Michaelis-Menten kinetics; the reciprocal of the rate of chain growth is a linear function of the reciprocal substrate concentrations. AMD inhibits propagation by affecting the rate terms for both GTP and CTP, but not for ATP and UTP. This result shows that AMD is interacting in a special way with GC base pairs; several plausible models for the mode of action of AMD are eliminated by these kinetics results.

### 1. Introduction

Actinomycin D (AMD) functions as an antibiotic by binding reversibly to DNA. In the bound state, it inhibits DNA directed transcription by RNA polymerase, in vivo and in vitro (Kersten, Kersten & Rauen, 1960; Goldberg, Rabinowitz & Reich, 1962; Hurwitz, Furth, Malamy & Alexander, 1962; Harbers & Müller, 1962).

Transcription may be considered as a three-step process (Anthony, Zeszotek & Goldthwait, 1968), as represented below:

(1) initiation



(where E = RNA polymerase, and PuTP is a purine triphosphate, and E · DNA · PuTP is the initiation complex)

(2) propagation



⋮



(where growing chain (i) signifies a growing RNA chain of length i)

(3) termination



The effect of AMD could be on any or all of these three steps. Previous evidence has suggested that the major effect of AMD is not on step (1) (Maitra, Nakata & Hurwitz, 1967). In the present investigation, we show that the major in vitro effect of AMD is to inhibit

step (2).

The propagation step (2) must be considered as at least four separate reactions, one for each of the nucleoside triphosphates. We have studied the effect of AMD on each of these steps in vitro, and have discovered that inhibition by AMD occurs only for the incorporation of G and of C.

## 2. Materials and Methods

### (a) Materials

Coliphage T7 and the E. coli strains were from the stocks of Professor R. S. Edgar and the late Dr. J. J. Weigle. T7 was grown on E. coli B/5 in K medium. At a bacterial concentration of  $6 \times 10^8$  / ml, T7  $\phi$  was added at a multiplicity of infection of 0.01. Glucose was added to increase the concentration by 0.5%. Vigorous aeration was continued until there were three successive lyses spaced about 25 minutes apart. The culture had then completely cleared ( $A_{600} \leq .05$ ). Several drops of  $\text{CHCl}_3$  were added, and the culture was cooled to  $15^\circ \text{C}$ . Because of the clarity of the culture after the final lysis, no preliminary centrifugation to remove bacteria was needed. The phage were pelleted by centrifugation for about 3 hours at 45,000 g. The phage pellet was resuspended in 1 M NaCl, 0.01 M  $\text{MgSO}_4$ , 0.01 M Tris, pH 7 and then banded in CsCl. Bacterial debris either floated on the top of the gradient or pelleted at the bottom, leaving only a viscous phage band within the gradient. The phage band was collected by puncturing the side of the tube well above the bacterial debris, and dialyzed against 0.5 M NaCl, 0.01 M  $\text{MgSO}_4$ , 0.01 M Tris, pH 7.

That the phage so grown and purified was indeed T7 was demonstrated by testing the phage preparation on the sensitive and resistant strains of E. coli, B/5 and B/3, 4, 7, respectively. At a dilution that gave almost confluent lysis on the sensitive strain, there were no plaques on the resistant strain. Furthermore, the phage morphology, as observed in the electron microscope, was identical to that reported for T7 by Davison & Freifelder (1962).

T7 DNA was extracted from the phage by gentle rocking, firstly with freshly distilled, buffered phenol and secondly with fresh diethyl ether, followed by dialysis against 0.05 M Tris, pH 7. T7 DNA so prepared gave only a homogeneous band corresponding to the correct molecular weight in a neutral or alkaline band sedimentation experiment. When labeled T7 DNA was required, thymine-2-C<sup>14</sup> at a final concentration of 1  $\mu$ c/ml (2  $\mu$ g/ml) was added to the culture one-half hour before infection.

Thymine-2-C<sup>14</sup>, UTP-C<sup>14</sup>, and the unlabeled nucleoside triphosphates (NTP's) were purchased from Schwartz Bioresearch Corporation. AMD was a gift from Merck, Sharp, and Dohme.

RNA polymerase, fraction f<sub>4</sub> of Chamberlin & Berg (1962), was a gift from Dr. Michael Dahmus. We are grateful to him for his generosity. The polymerase had an absolute dependence on exogenous DNA. Its specific activity was 500 units/mg when assayed under the conditions described by Burgess (1969). When sedimented in a 10-30% glycerol gradient over a 50% glycerol shelf in a low salt medium (0.02 M Tris, 0.01 M MgCl<sub>2</sub>, 0.002 M glutathione,

0.012 M  $(\text{NH}_4)_2\text{SO}_4$ ), about 50% of the  $A_{280}$  absorbing material sedimented in a band with the expected sedimentation coefficient of ca. 22 s. All of the polymerase activity was in this band. The enzyme prepared by Burgess had a specific activity of 600 units/mg and was 95% pure by the gel electrophoresis criterion. For purposes of calculating the active enzyme concentration in reaction mixtures, we have assumed that our polymerase preparation was 40% pure, that  $\frac{A_{280}^{1\%}}{A_{280}} = 6.2$  (Richardson, 1966), and that the molecular weight of RNA polymerase is  $0.5 \times 10^6$  under the high salt conditions used for our studies (Burgess, 1969). The concentration of polymerase quoted in later sections is always 40% of the total protein added.

#### (b) Methods

The binding curve of actinomycin with T7 DNA was measured by a spectrophotometric titration method (Gellert, Smith, Neville & Felsenfeld, 1965; Hyman & Davidson, 1970).

The formation and stability of the initiation complex of RNA polymerase, DNA, and purine nucleoside triphosphates were studied by a slight modification of the Millipore filter method of Jones & Berg (1966). A fixed amount of  $C^{14}$ -labeled T7 DNA was titrated with increasing amounts of polymerase in low salt buffer (LSB, 0.05 M Tris, 0.004 M  $\text{MgCl}_2$ ,  $10^{-4}$  M glutathione, pH 7.8) at 37° in the presence or absence of ATP plus GTP, and/or AMD. After a 15-minute incubation, which is, we believe, more than sufficient for the establishment of binding equilibrium,  $(\text{NH}_4)_2\text{SO}_4$  is added to a final concentration of 0.4 M. After 15 minutes incubation at 37° C, the reaction

mixture is poured through a Millipore filter (HAWP, 0.45 $\mu$  pore-diameter) and gently washed with ice-cold high salt buffer (HSB, 0.05 M Tris, 0.004 M MgCl<sub>2</sub>, 10<sup>-4</sup> M glutathione, 0.4 M (NH<sub>4</sub>)<sub>2</sub>SO<sub>4</sub>, pH 7.8). After extensive washing, the filter is dried and counted in a toluene-based scintillation fluid in a scintillation counter.

For the kinetics of propagation experiments, T7 DNA, RNA polymerase, ATP, GTP, and C<sup>14</sup>-labeled UTP are mixed in low salt buffer and allowed to stand for 15 minutes at 37° C. (NH<sub>4</sub>)<sub>2</sub>SO<sub>4</sub> is added to a final concentration of 0.4 M. This high salt concentration washes any noninitiated polymerase off the DNA, leaves the initiation complex intact, and severely slows the rate of reinitiation when the initiation sites are later made reavailable. At this point (after initiation has occurred) AMD is added. Thus, only the effect of AMD on propagation is measured. The solution is incubated for 15 minutes at 37° C to ensure equilibrium in the addition of AMD to the DNA. Propagation is started by the addition of CTP. At convenient time intervals either a 100  $\mu$ l aliquot or the entire reaction mixture (usually 0.5 ml) is added to 100  $\mu$ l of cold carrier yeast high molecular weight RNA (1 mg/ml, Calbiochem), and 0.5 ml of cold 5% TCA is added. After 20 minutes at 4° C the precipitate is washed onto a Whatman GF/C glass filter with cold 1% TCA. The filter is washed thoroughly with cold 1% TCA and then cold 95% ethanol, dried, and counted.

The total amount of RNA synthesized is calculated from the measured radioactivity, using the measured efficiency of the counter for a precipitated sample, the specific activity of the UTP calculated

from the specific activity of the stock UTP solution quoted by Schwarz Bioresearch Corporation and the dilution factor for the reaction mixture, and by assuming that the mole fraction of ribonucleotides incorporated is 0.24 for G and for C, and 0.26 for A and for U in accordance with the base composition of the DNA (Wyatt & Cohen, 1953). Initial rates of incorporation were estimated from the initial slopes of plots such as that shown in Fig. 3.

For experiments in which the average RNA chain length as well as the total incorporation is measured, the procedure for starting the propagation reaction is the same as above. Then 100  $\mu$ l aliquots are alternately either precipitated as above or added to 100  $\mu$ l of 1% SDS, 0.01 M EDTA, pH 8 for subsequent sedimentation analysis. The samples for sedimentation analysis are allowed to stand at room temperature for one hour before storage at 4° C. The EDTA stops propagation immediately by removing  $Mg^{++}$  from the reaction mixture, and the SDS dissociates the RNA from the enzyme and from the T7 DNA. Samples of the RNA are sedimented on 5 ml 5-20 w/v % sucrose gradients containing 0.1 M NaCl,  $10^{-3}$  M Tris,  $10^{-3}$  M EDTA, pH 8. The sucrose is 50% sterile aqueous solution, density gradient grade, RNase free, from Mann Research Corporation. Wheat germ ribosomal RNA (25 + 18S), a gift from Professor James Bonner, is used as a marker in a separate tube. The fractions are dripped into cold carrier RNA, precipitated and counted as before.

An essential feature of all these experiments is the employment of a high salt concentration to minimize nonspecific initiation and propa-

gation, and to minimize reinitiation by the excess polymerase after propagation has moved the already initiated enzyme away from the initiation site. The results show that high salt concentration slows the process of initiation sufficiently that it is negligible over our short time scale (less than one-half hour).

### 3. Results

#### (a) Binding of AMD to T7 DNA

A spectrophotometric titration, in a medium consisting of 0.01 M NaCl, 0.001 M phosphate buffer, pH 7.0, at 25° C, gives the result that the equilibrium association constant of AMD to T7 DNA is  $2 \times 10^6$  M<sup>-1</sup> and there is one binding site for every 7(±2) base pairs. These results are entirely concordant with measurements on other DNA's reported in the literature (Gellert et al., 1965; Hyman & Davidson, 1967, 1970; Müller & Crothers, 1968). It should be recalled that these data pertain to the "strong binding" sites on DNA. If the concentration of free AMD rises above about  $10^{-5}$  M, more AMD is bound to the DNA at other sites.

The quantity r is defined as the ratio of the amount of AMD bound to the number of base pairs; for T7 DNA, at saturation of the strong binding sites, r = 0.143.

The experiments reported in later sections are at 37° and either at "low" salt (LSB) or at "high" salt (HSB). Furthermore, GTP is present in these experiments, and G derivatives are known to bind AMD. Müller & Crothers (1968) report that the association constants

of actinomycin C<sub>3</sub> to calf-thymus DNA at 25° C are  $2.4 \times 10^6 \text{ M}^{-1}$  and  $1.2 \times 10^7$  in  $0.2 \text{ M Na}^+$  and  $0.01 \text{ M Na}^+$  media, respectively. Gellert *et al.* (1965) report binding constants of AMD to calf-thymus DNA of  $4 \times 10^6$  and  $6 \times 10^6$  at 4° C and 22° C, respectively. From all these data, we estimate binding constants of  $5 \times 10^6 \text{ M}^{-1}$  and  $1 \times 10^6 \text{ M}^{-1}$  at 37° at low and high salt, respectively. Gellert *et al.* report binding constants of AMD to deoxyguanosine of  $5 \times 10^3$ ,  $2.2 \times 10^3$ , and  $1 \times 10^3 \text{ M}^{-1}$  at 10°, 25° and 37°; they report a binding constant to riboguanosine of  $10^2$  at 20° C. We assume that ribo GTP has the same binding constant as does ribo G, and take a constant of  $30 \text{ M}^{-1}$  at 37° C for GTP. (The correction for AMD·GTP complexes is less than 10% anyway.)

The binding of AMD to DNA can then be calculated for any given experiment.

#### (b) Membrane Filter Experiments

Measurements of the retention of T7 DNA by a membrane filter as a function of the concentration of added RNA polymerase, in the presence and absence of ATP and GTP, and of AMD are presented in Fig. 1.

When the protein and DNA are mixed in LSB, and  $(\text{NH}_4)_2\text{SO}_4$  added to convert the medium to HSB, in the absence of ATP plus GTP, irrespective of the presence or absence of UTP plus CTP, no DNA is retained on the filter. If ATP and GTP are present in the LSB, the amount of DNA retained increases with increasing enzyme concentration. At the point marked by an arrow in Fig. 1 where all the DNA is retained, the weight ratio of protein to DNA in the solution that was

Fig. 1. The fractional retention of 1.40  $\mu\text{g}$  of T7 DNA on a Millipore filter (HAWP, 0.45  $\mu$  pore diameter) by complexing with RNA polymerase, in the presence and absence of ATP plus GTP, and of AMD.

●, (ATP) = (GTP) =  $2 \times 10^{-4}$  M present in LSB as the polymerase is added; the medium is then adjusted to HSB, and washed through the filter; □, no ATP or GTP, otherwise as above;  $2 \times 10^{-4}$  M UTP and CTP were present in some experiments; O, (ATP) = (GTP) =  $2 \times 10^{-4}$  M, AMD to r = 0.12 added to LSB before addition of the polymerase.

---

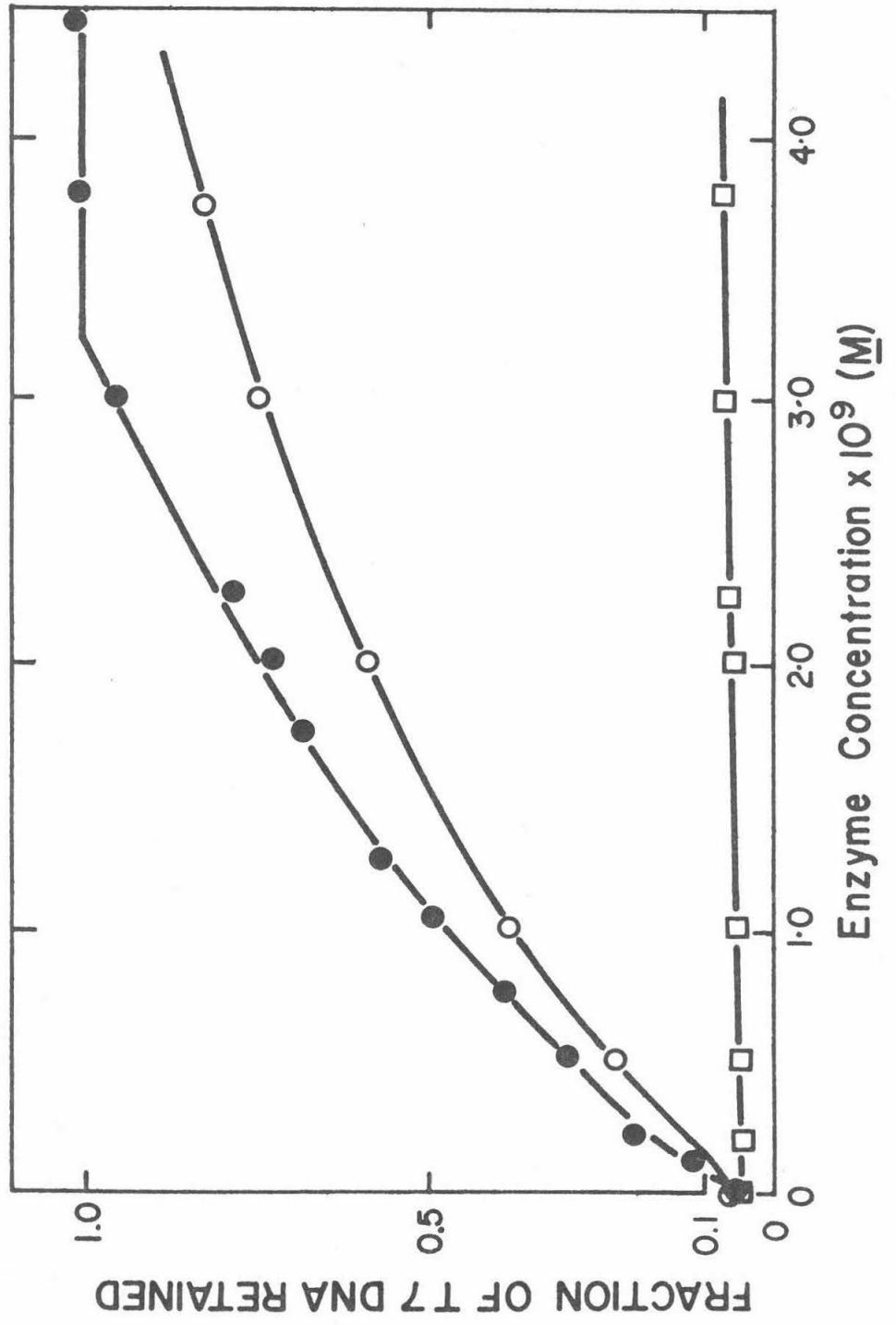


FIG 1

passed through the filter was 0.57. Using a molecular weight of  $0.5 \times 10^6$  for RNA polymerase, this corresponds to a ratio of 1300 base pairs per enzyme molecule.

If the actinomycin is present in the solution before the protein is added and the salt concentration raised, there is a small decrease in the retention of DNA on the filter (Figs. 1 and 2). This decrease is about 20% for an  $r$  value of 0.12. If the AMD is added after the polymerase, and then the salt concentration is raised, there is no effect on the retention (Fig. 2). As will be seen later, under typical conditions, the total rate of transcription is reduced by a factor of 30 to 50 by this amount of AMD.

We do not know how to make a quantitative interpretation of these experiments, since we do not understand quantitatively how the probability of retention of DNA on the filter varies with the amount of protein bound. Nevertheless, the results strongly suggest that the RNA polymerase-DNA complex is largely dissociated in HSB, unless GTP and ATP are present. This is in agreement with previous work (Anthony *et al.*, 1966; Jones & Berg, 1966). Furthermore, the effect of AMD added to the low salt medium before adding the protein on the binding of polymerase to DNA is comparatively small compared to the effects on the rate of transcription reported in a later section. Furthermore, AMD added after adding the polymerase has no effect on the binding curve. In the rate of transcription experiments reported in a later section, the AMD was added after adjusting to HSB. Thus, the possibility that it affected the initiation process was still less.

Fig. 2. Retention of 1.40  $\mu\text{g}$  of T7 DNA by  $1.26 \times 10^{-9}$  M RNA polymerase in the presence of (ATP) = (GTP) =  $2 \times 10^{-4}$  M.

●, AMD added to the LSB before adding polymerase; O, AMD added to the LSB after adding polymerase; for each case, the medium is then converted to HSB.

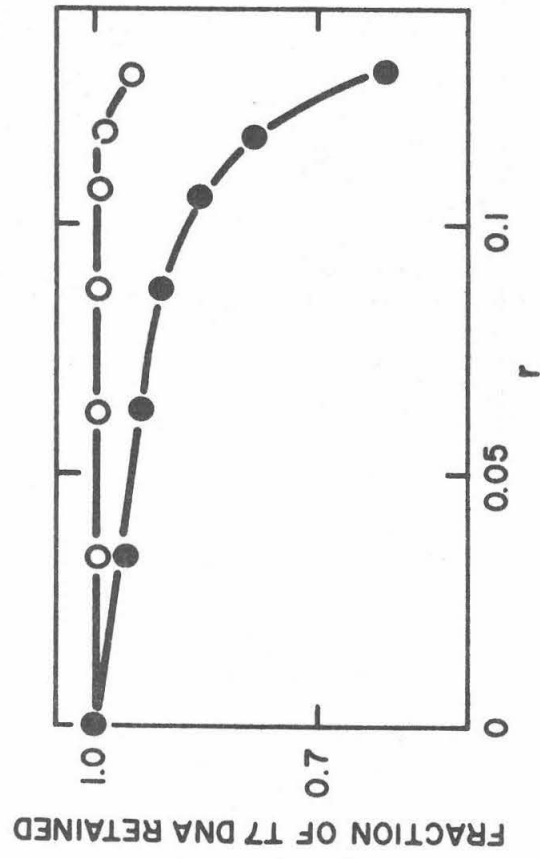


FIG 2

(c) Effects of AMD on Initiation, Propagation, and Termination

In these experiments the rate of in vitro propagation is measured under high salt conditions as described in Methods. At varying times after starting the reaction, the average chain length of the RNA is measured by sedimentation analysis and the total amount of nucleotide incorporation into an acid insoluble form is also measured. Thus, the average chain length and the total number of growing chains can be calculated.

The average chain length,  $\bar{n}$ , is calculated from the sedimentation coefficient by Spirin's equation (Spirin, 1963; Boedtker, 1968)

$$\log_{10} \bar{n} = 2.10 \log_{10} s_{20,w} + 0.644 \quad (1)$$

Data on the rate of nucleotide incorporation in the presence and absence of AMD at an  $r$  value of 0.0037 are shown in Fig. 3.

Sedimentation profiles for two different incorporation times are shown in Fig. 4. The sedimentation coefficients were calculated by comparison with the sedimentation velocities of the 25s and 18s wheat germ rRNA mixture measured in a separate tube.

As a control against the possibility of interstrand interactions which would affect the sedimentation velocity of the synthesized RNA, a 5- and a 15- minute sample were mixed; wheat germ ribosomal RNA was added, and the mixture sedimented. As shown in Fig. 5, the sedimentation profile of the radioactivity is the sum of the sedimentation profiles of the two components. Thus, there is no evidence for intermolecular interactions in the synthesized RNA or with the ribo-

Fig. 3. Time course of the propagation reaction. (T7 DNA) = 10  $\mu\text{g}/\text{ml}$ , (RNA polymerase) = 2.5  $\mu\text{g}/\text{ml}$ , (ATP) = (GTP) = (CTP) =  $0.8 \times 10^{-4}$  M, (UTP) =  $0.3 \times 10^{-4}$  M. Closed symbols are samples precipitated and counted; open symbols, the activity incorporated was calculated by summing cpm over the sucrose gradient. The squares and triangles were run side by side, with AMD at  $\underline{r} = 0.0037$  present in the latter case. The circles are a previous experiment with no AMD; the curve should agree with the square curve.

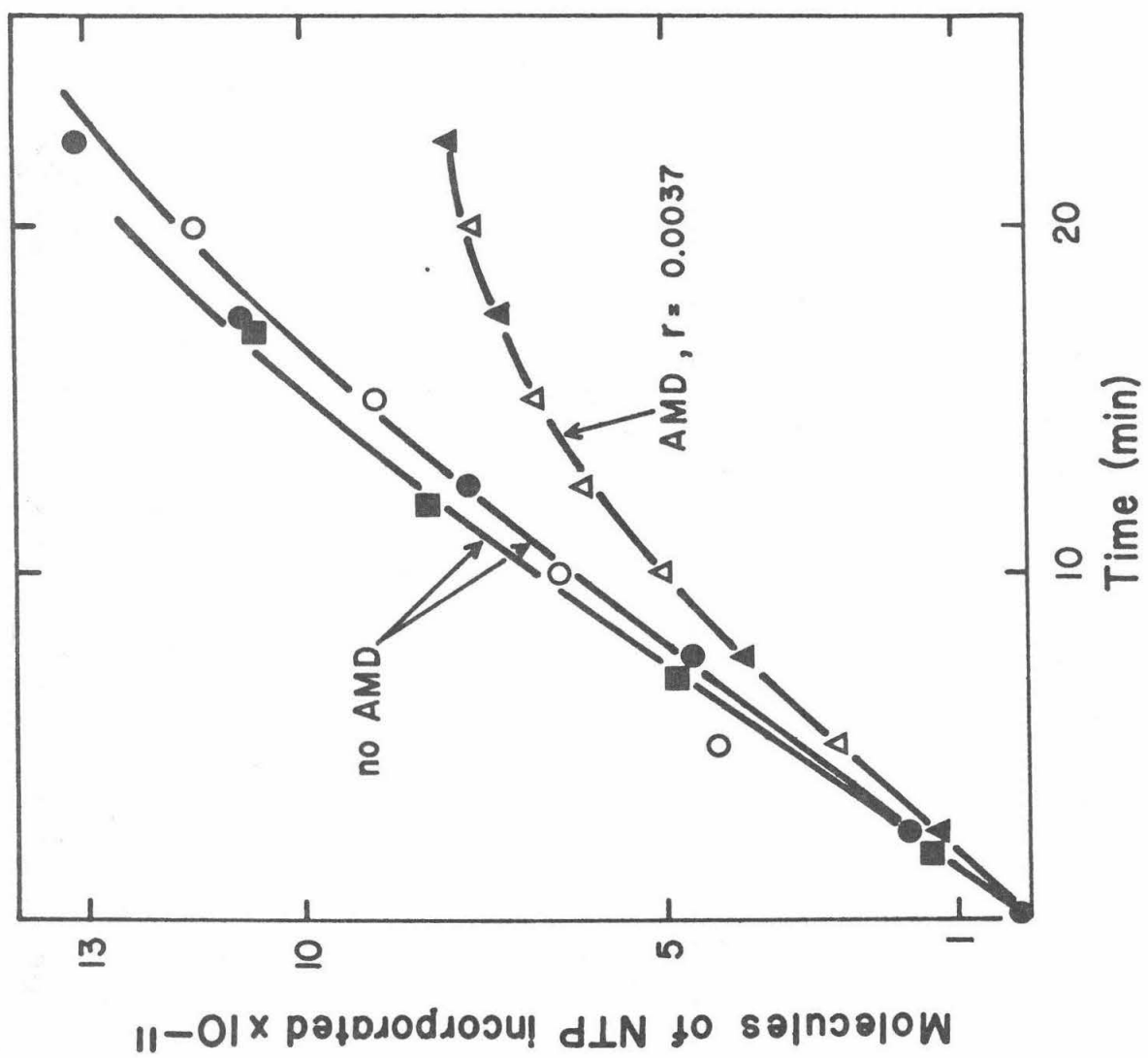


FIG 3

Fig. 4. Sucrose gradient sedimentation of transcribed T7 RNA. The conditions of synthesis are given in Fig. 3. 100  $\mu$ l of 5 min (o) and 10 min (●) samples were separately sedimented through a 5-ml, 5-20% w/v sucrose gradient in 0.1 M NaCl,  $10^{-3}$  M Tris,  $10^{-3}$  M EDTA, pH 8. 60,000 rpm, 1 3/4 hours, 20° C. The marker was wheat germ ribosomal RNA (25 + 18 s) in a separate tube.

---

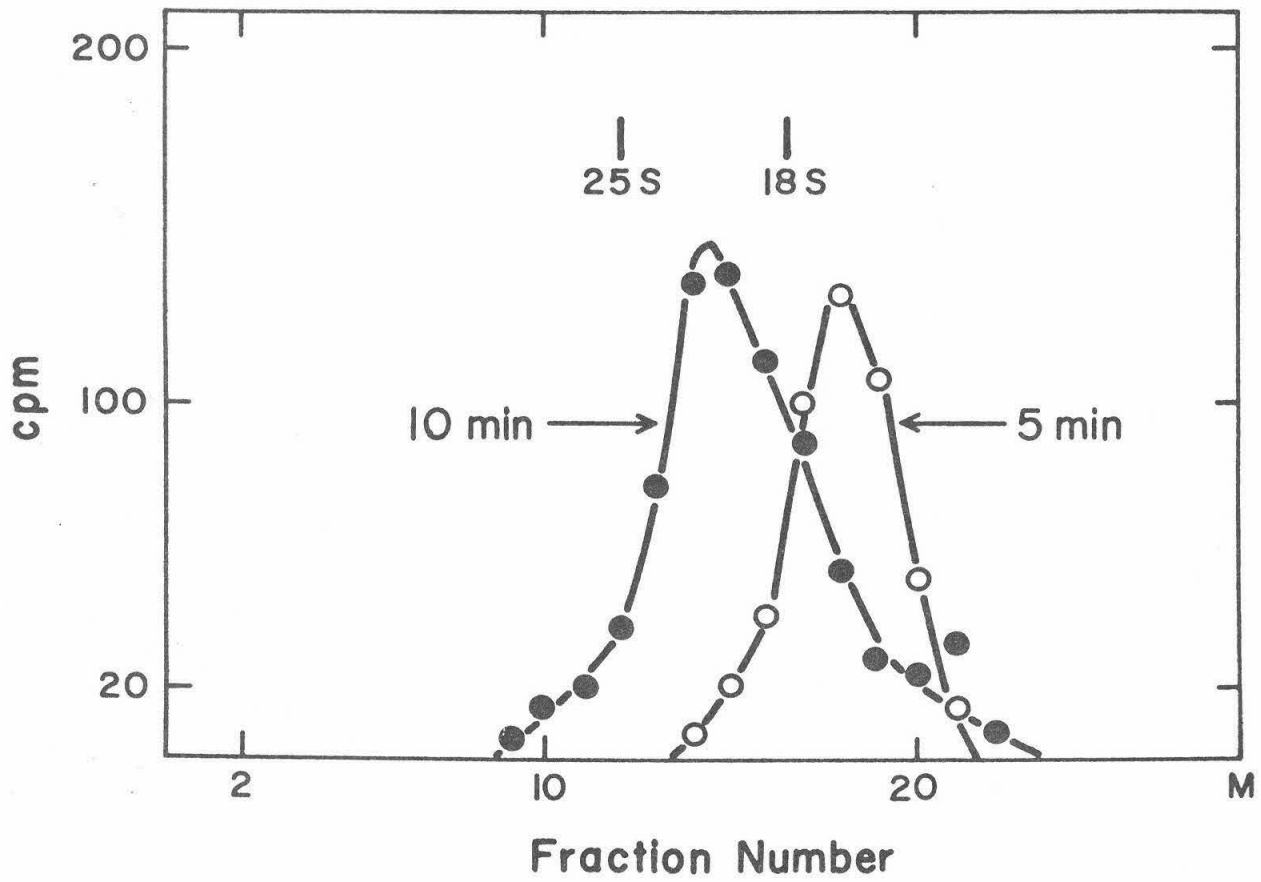


FIG 4

Fig. 5. Sucrose gradient sedimentation as in Fig. 4 of 50  $\mu$ l of a 5-min sample of T7 RNA mixed with 50  $\mu$ l of a 15-min sample of T7 RNA and mixed with 20  $\mu$ l of ribosomal RNA (1.5 mg/ml). The conditions of synthesis are given in Fig. 3. The curve is the sum of the patterns of the 5- and 15-min T7 RNA samples sedimented separately in the absence of the ribosomal marker.

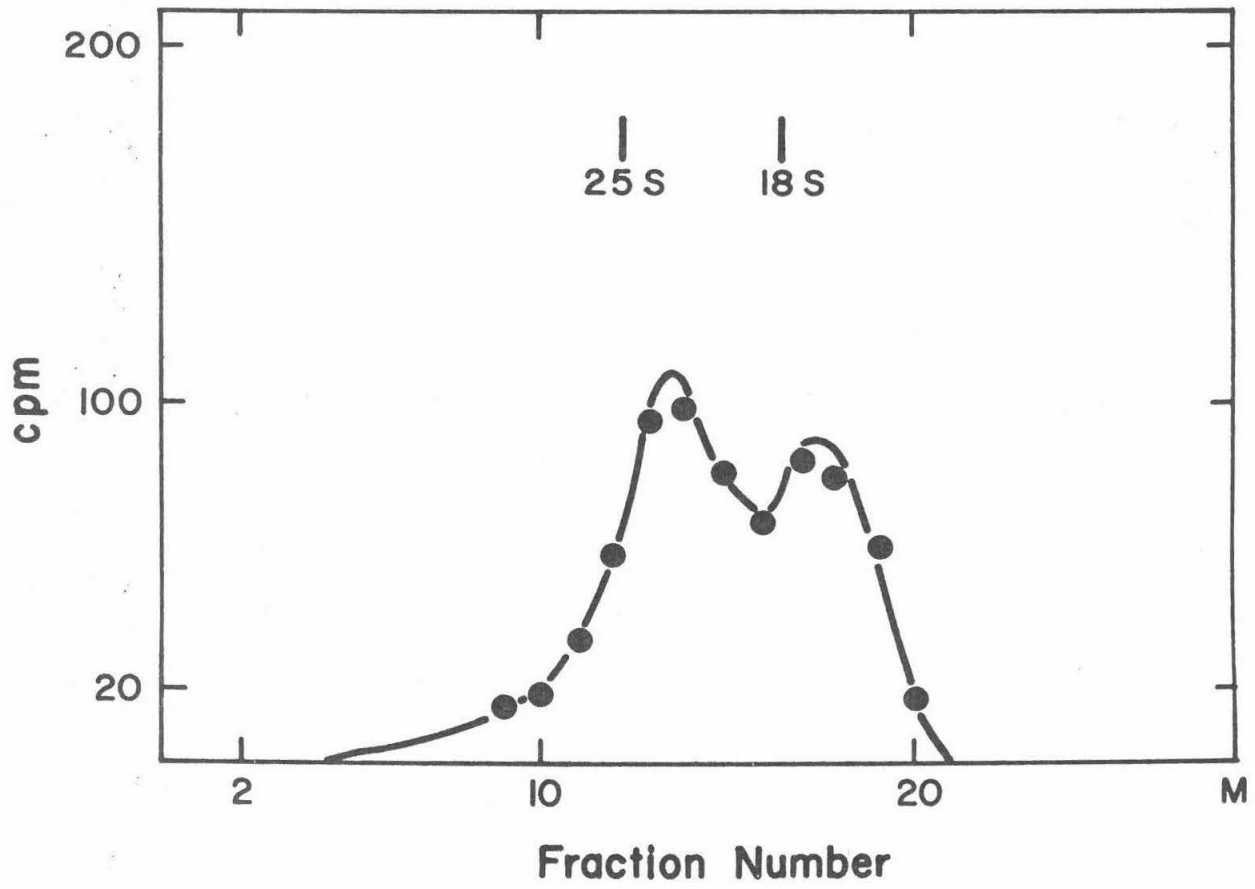


FIG 5

somal markers.

The calculated average chain length as a function of time of synthesis in the absence and presence of AMD is shown in Fig. 6.

From the average chain length and the total incorporation, the number of chains per DNA molecule can be calculated. These results are presented in Table 1.

The following conclusions are drawn from all these results.

Since the number of chains per DNA molecule are constant within experimental error during synthesis (Table 1) and since the bandwidths of the sedimentation profiles (Fig. 4) indicate a reasonably narrow chain length distribution for the reaction product, the conditions chosen are effective for preventing reinitiation of synthesis.

Although the ratio of polymerase molecules to DNA molecules in the reaction mixture is 15 to 1, there is only one growing chain per DNA molecule. This suggests, but does not prove, that there is one and only one initiation site per T7 DNA molecule under the conditions of synthesis used here.

With the amount of actinomycin used in this experiment, the rate of incorporation is reduced by 30 % (Fig. 3). The average number of chains in the presence and absence of actinomycin is  $1.2(\pm 0.1)$  and  $1.0_5(\pm 0.1)$ , respectively. This is an additional confirmation of the conclusion from the membrane filter experiments that actinomycin does not reverse the initiation reaction.

The downward curvatures of the incorporation plots (Fig. 3) and of the chain length plots (Fig. 6) may indicate that some termin-

Fig. 6. Chain length,  $\underline{n}$ , in nucleotides, as a function of time.  
The conditions of synthesis are given in Fig. 3.  
●, Control; O, with AMD at  $\underline{r} = 0.00037$ .

---

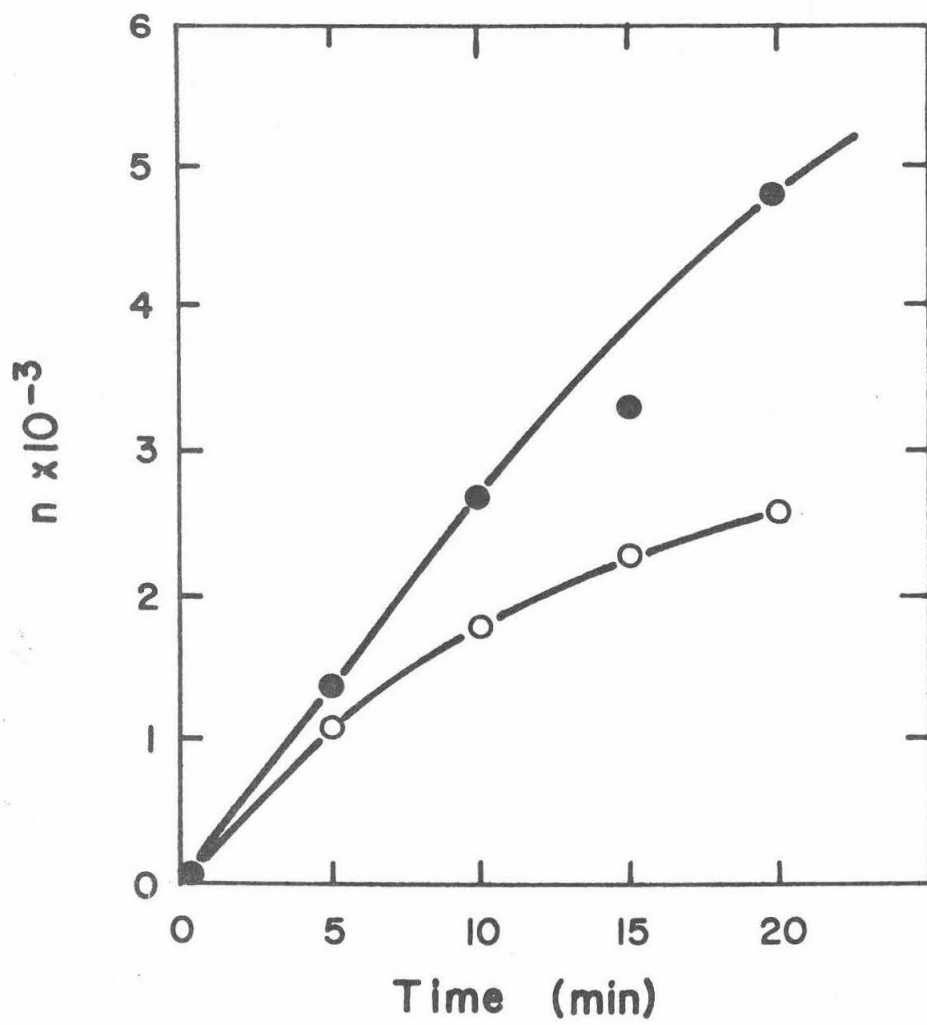


FIG 6

TABLE 1

Calculated ratio of RNA chains to DNA molecules  
during RNA synthesis<sup>a, b</sup>

Time (min.)	Ratio	
	$r = 0.0$	$r = 0.0035^c$
5	0.95	1.0
10	1.0	1.2
15	1.2	1.3
20	1.0	1.3

<sup>a</sup> Ratio calculated from mean chain length and total RNA synthesis as described in the text.

<sup>b</sup> Conditions of synthesis given in text.

<sup>c</sup> Ratio of AMD molecules bound to DNA base pairs present.

ation is occurring. Alternatively, the propagation rate may decrease as transcription proceeds down the T7 molecules due to deterioration of the enzyme. Alternatively, the effect may be due to nuclease action. The data are not sufficiently accurate to decide this issue. In the actinomycin experiment, the antibiotic was present at a level of one molecule per 270 base pairs. After 10 minutes of synthesis, the average chain length in the presence of AMD was 1800 nucleotides. Thus, it is quite clear that the growing chains have passed several AMD molecules. We conclude that the primary inhibiting effect of AMD is on chain propagation, not termination. However, the downward curvatures in Figs. 3 and 6 are somewhat greater in the presence of AMD; thus, the data do not exclude the possibility that AMD somewhat increases the termination rate.

#### (d) Effects of AMD on the Kinetics of the Propagation Step

The experiments reported so far show that the main, if not the only, inhibiting effect of AMD on transcription is on the propagation step and not on the initiation or termination steps. A detailed study of the kinetics of incorporation of each individual nucleotide and of the effects of AMD on each step is reported in this section.

A theoretical rate equation used to interpret the data will first be derived. This analysis is similar to one already presented by Bremer (1967).

Transcription proceeds by stepwise motion of the polymerase along the DNA chain and stepwise addition of ribonucleotide  $\alpha$  ( $\alpha = A,$

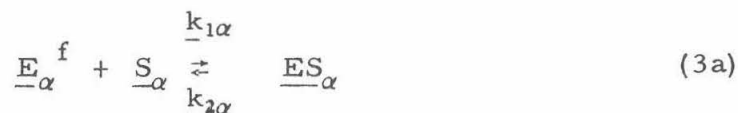
G, C, U) to the growing RNA chain, as dictated by the nucleotide sequence in the transcribing DNA strand.

Let  $f_{\alpha}$  be the mole fraction of nucleotide  $\alpha$  in the product RNA chain. Let  $t_{\alpha}$  be the mean time for addition of ribonucleotide  $\alpha$  to the chain, after the previous nucleotide has been incorporated. Then the average velocity of incorporation,  $\underline{v}$ , in units of nucleotides per unit time per chain, and the average time of incorporation per nucleotide  $\langle t \rangle$ , are given by

$$(1/\underline{v}) = \langle t \rangle = \sum_{\alpha} f_{\alpha} t_{\alpha} \quad (2)$$

The quantities  $t_{\alpha}$  are calculated as follows: Consider a polymerase-DNA-RNA complex,  $\underline{E}_{\alpha}$ , which is at a site where nucleotide  $\alpha$  is to be incorporated. The site is either free, denoted by  $\underline{E}_{\alpha}^f$ , or has the nucleoside triphosphate, denoted by  $\underline{S}_{\alpha}$ , bound in an enzyme-substrate complex, denoted by  $\underline{ES}_{\alpha}$ . We denote the corresponding concentrations by  $[\underline{E}_{\alpha}]$ ,  $[\underline{E}_{\alpha}^f]$ ,  $[\underline{S}_{\alpha}]$ ,  $[\underline{ES}_{\alpha}]$ .

The reactions for the reversible formation of the enzyme-substrate complex are



$$\text{and} \quad [\underline{E}_{\alpha}] = [\underline{E}_{\alpha}^f] + [\underline{ES}_{\alpha}] \quad (3b)$$

The nucleotide  $\alpha$  becomes covalently attached to the RNA chain, and the enzyme moves on to the next site on the DNA in the reaction denoted by



The overall velocity of reactions (3) and (4) is obtained by the standard Michaelis-Menten argument as

$$\frac{1}{[\underline{E}_\alpha]} \frac{d[\underline{P}]}{dt} = \frac{k_{3\alpha} [\underline{S}_\alpha]}{\underline{K}_\alpha + [\underline{S}_\alpha]} \quad (5a)$$

where

$$\underline{K}_\alpha = \frac{k_{2\alpha} + k_{3\alpha}}{k_{1\alpha}} \quad (5b)$$

Thus, the velocity and propagation time for step  $\alpha$  per chain are given by

$$(1/\underline{v}_\alpha) = \underline{t}_\alpha = \frac{\underline{K}_\alpha + [\underline{S}_\alpha]}{k_{3\alpha} [\underline{S}_\alpha]} = \frac{\underline{K}_\alpha}{k_{3\alpha} [\underline{S}_\alpha]} + \frac{1}{k_{3\alpha}} \quad (6)$$

Then, using (2), the overall rate of incorporation per chain is given by

$$(1/\underline{v}) = \langle \underline{t} \rangle = \sum_\alpha \frac{f_\alpha}{k_{3\alpha}} + \frac{f_\alpha \underline{K}_\alpha}{k_{3\alpha} [\underline{S}_\alpha]} \quad (7)$$

The quantities  $f_\alpha$  are known. For T7 DNA we take  $f_{\underline{A}} = f_{\underline{U}} = 0.26$ ,  $f_{\underline{G}} = f_{\underline{C}} = 0.24$  (Wyatt & Cohen, 1953).

In a typical experiment, one nucleoside triphosphate,  $\underline{S}_\beta$ , is adjusted to a lower concentration than are the other three, and this concentration is varied. Equation (7) predicts that a Lineweaver-Burke plot of  $1/\underline{v}$  vs.  $1/[\underline{S}_\beta]$  should be a straight line with a slope of  $f_\beta \underline{K}_\beta / k_{3\beta}$ . The intercept on the  $1/\underline{v}$  axis at  $(1/[\underline{S}_\beta]) = 0$  is

$$\left(\frac{1}{\underline{v}}\right)_{(1/S_3)=0} = \sum_{\alpha=A, G, C, U} \frac{f_{\alpha}}{k_{3\alpha}} + \sum_{\alpha \neq \beta} \frac{f_{\alpha} K_{\alpha}}{k_{3\alpha} [S_{\alpha}]} \quad (7)$$

Bremer (1967) has already presented data which confirm the rate law (8).

We now assume that each AMD molecule is bound at a particular site where it inhibits the incorporation of one or several nucleotides in the vicinity of the site. Let  $\underline{r}$  be the ratio of AMD molecules bound to base pairs. We assume that the binding sites are homogeneous, so that the degree of inhibition of incorporation of a particular nucleotide, say C, by one of the first AMD molecules bound and by one of the AMD molecules bound later is, on the average, the same. Thus, the inhibiting effect on incorporation of each nucleotide will be a linear function of  $\underline{r}$ . Let  $t_{\alpha 0}$  and  $t_{\alpha A}$  represent the mean incorporation time of nucleotide  $\alpha$  in the absence of AMD and for the hypothetical state of  $\underline{r} = 1.0$ , respectively. Then

$$\underline{t}_{\alpha}(\underline{r}) = (1-\underline{r})t_{\alpha 0} + \underline{r}t_{\alpha A} = t_{\alpha 0} + \underline{r}(t_{\alpha A} - t_{\alpha 0}) \quad (9)$$

where  $\underline{t}_{\alpha}(\underline{r})$  is the mean incorporation time for nucleotide  $\alpha$  with a binding ratio of  $\underline{r}$  for the AMD.

Equation (2) is now modified to read

$$\langle \underline{t}(\underline{r}) \rangle = \sum_{\alpha} \frac{f_{\alpha}}{k_{3\alpha}} t_{\alpha 0} + \underline{r} \sum_{\alpha} \frac{f_{\alpha}}{k_{3\alpha}} (t_{\alpha A} - t_{\alpha 0}) \quad (10)$$

where  $\langle \underline{t}(\underline{r}) \rangle$  is the mean time of incorporation of a nucleotide when

there are  $\underline{r}$  AMD molecules bound per base pair.

Furthermore, let the kinetic parameters in the absence of AMD and for the hypothetical case of  $\underline{r} = 1$  AMD per base pair be denoted by  $\underline{k}_{-3\alpha 0}$ ,  $\underline{K}_{\alpha 0}$ , and  $\underline{k}_{-3\alpha A}$ ,  $\underline{K}_{\alpha A}$ , respectively. Then,

$$\underline{t}_{\alpha 0} = \frac{\underline{K}_{\alpha 0}}{\underline{k}_{-3\alpha 0} [\underline{S}_{-\alpha}]} + \frac{1}{\underline{k}_{-3\alpha 0}} \quad (11a)$$

$$\underline{t}_{\alpha A} = \frac{\underline{K}_{\alpha A}}{\underline{k}_{-3\alpha A} [\underline{S}_{-\alpha}]} + \frac{1}{\underline{k}_{-3\alpha A}} \quad (11b)$$

so that, using equations (9), (10), and (11), the final rate equation is

$$\begin{aligned} (1/\underline{v}) = \langle \underline{t}(\underline{r}) \rangle &= \sum_{\alpha} \underline{f}_{\alpha} \left( \frac{\underline{K}_{\alpha 0}}{\underline{k}_{-3\alpha 0} [\underline{S}_{-\alpha}]} + \frac{1}{\underline{k}_{-3\alpha 0}} \right) + \\ &\underline{r} \sum_{\alpha} \underline{f}_{\alpha} \left[ \left( \frac{\underline{K}_{\alpha A}}{\underline{k}_{-3\alpha A}} - \frac{\underline{K}_{\alpha 0}}{\underline{k}_{-3\alpha 0}} \right) \frac{1}{[\underline{S}_{-\alpha}]} + \left( \frac{1}{\underline{k}_{-3\alpha A}} - \frac{1}{\underline{k}_{-3\alpha 0}} \right) \right] \quad (12) \end{aligned}$$

This rather cumbersome formal analysis predicts that the reciprocal of the reaction velocity will be a linear function of the AMD bound (Eq. 10) and that the Lineweaver-Burke plot of  $1/\underline{v}$  vs.  $1/[\underline{S}_{\beta}]$  will still be linear, but that each slope and intercept will be a linear function of the AMD bound (Eq. 12).

Rate data from two experiments at two different sets of fixed nucleoside triphosphate concentrations at varying AMD concentrations are displayed in Fig. 7. The vertical coordinate in Fig. 7 is the recip-

Fig. 7. The inverse initial rate as a function of  $\underline{r}$  (equation 10). For convenience, the initial rate is taken as 1.0 when  $\underline{r} = 0.0$ ,  $(\text{ATP}) = (\text{GTP}) = (\text{CTP}) = 0.8 \times 10^{-4} \underline{\text{M}}$ ,  $(\text{UTP}) = 0.3 \times 10^{-4} \underline{\text{M}}$ ,  $(\underline{\text{E}}_{\alpha}) = 3.85 \times 10^{-10} \underline{\text{M}}$ . The measured incorporation rate under these conditions is  $20 \times 10^{-10} \underline{\text{M}} \text{ sec}^{-1}$ , or 5.1 nucleotides/sec/RNA chain. Note that  $(\underline{\text{E}}_{\alpha})$  is taken as the concentration of T7 DNA molecules. Thus, the scale factor to convert arbitrary units to "seconds" is 0.193. Both curves have been normalized against the same value.  $(\text{DNA}) = 10 \mu\text{g/ml}$ ;  $(\text{RNA polymerase}) = 2.5 \mu\text{g/ml}$ .  $\circ$ ,  $(\text{ATP}) = (\text{GTP}) = (\text{CTP}) = 0.8 \times 10^{-4} \underline{\text{M}}$ ,  $(\text{UTP}) = 0.3 \times 10^{-4} \underline{\text{M}}$ .  $\square$ ,  $(\text{ATP}) = (\text{GTP}) = (\text{CTP}) = 0.8 \times 10^{-3} \underline{\text{M}}$ ,  $(\text{UTP}) = 0.3 \times 10^{-4} \underline{\text{M}}$ .

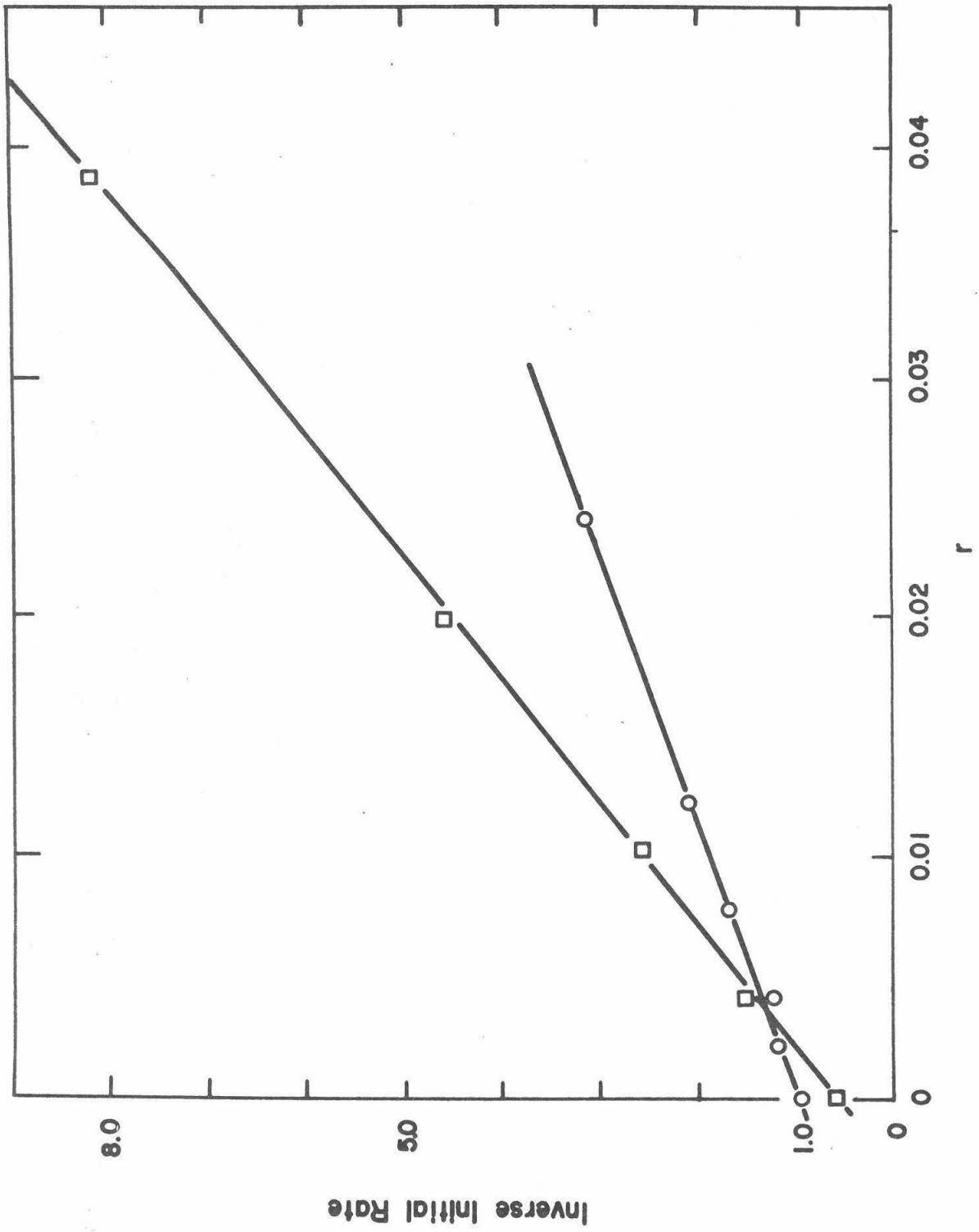


FIG 7

reciprocal of the rate in arbitrary units. The main point is that the reciprocal of the rate is a linear function of the amount of AMD bound as predicted by Eq. (10).

Assuming, in accordance with evidence already presented, that there is one growing RNA chain per DNA molecule, the rate data in nucleotides per sec per chain can be calculated, and are presented in Table 2. As expected from Eq. (12), the ratio  $\langle t(1) \rangle / \langle t(0) \rangle$  is dependent on the substrate concentrations.

The rate of growth of the RNA chain can also be calculated in a completely independent way from the time rate of change of the sedimentation coefficient. These data are essentially presented in Fig. 6. The conditions of synthesis are the same for the experiment of Fig. 6 and the right hand column of Table 2. The calculated chain growth rates (in the absence of AMD) are 4.6 and 5.1 nucleotides per sec, respectively. This good agreement confirms the assumption of one growing chain per T7 DNA molecule.

Reciprocal reaction rate plots when one nucleoside triphosphate is at a low and variable concentration,  $[S_3]$  in the presence and absence of AMD, are given in Fig. 8. The predicted linear dependence on  $1/[S_3]$  is observed. In the case of guanosine triphosphate, two different  $r$  values were studied and the slope

$$\left( \frac{f_{\underline{G}} K_{\underline{G}o}}{k_{\underline{3}G\text{O}}} \right) + \frac{r}{r_{\underline{G}}} \left[ \left( \frac{K_{\underline{G}A}}{k_{\underline{3}GA}} \right) - \left( \frac{K_{\underline{G}o}}{k_{\underline{3}G\text{O}}} \right) \right]$$

is indeed a linear function of the amount of AMD bound, as predicted by Equation (12) (Fig. 9).

TABLE 2

Chain growth rate calculations from Fig. 7

	Substrate concentration	
	(ATP) = (GTP) = (CTP) = $0.8 \times 10^{-3}$ M, (UTP) = $0.3 \times 10^{-4}$ $\bar{M}$	(ATP) = (GTP) = (CTP) = $0.8 \times 10^{-4}$ M, (UTP) = $0.3 \times 10^{-4}$ $\bar{M}$
initial rate of UTP incorporation at $r = 0$ ; ( $\bar{\mu}$ mole/min/ml)	0.054	0.036
growth rate per chain at $r = 0$ ; ( $1/\langle \bar{t}(0) \rangle$ ); (nucleotides/sec/RNA)	7.8	5.1
<sup>a</sup> $\frac{\langle \bar{t}(1) \rangle}{\langle \bar{t}(0) \rangle}$ (eq. 10)	290	90

<sup>a</sup> Ratio of incorporation time per nucleotide for the hypothetical state of one AMD per base pair and no AMD's.

Fig. 8. The inverse of the initial rate in arbitrary units as a function of the inverse substrate concentration (eq. 12) when in turn only one of the four nucleoside triphosphate concentrations is varied. For convenience, the initial rate is taken as 1.0 when  $\underline{r} = 0.0$ ,  $(\underline{E}_\alpha) = 3.85 \times 10^{-10} \underline{M}$ ,  $(\text{ATP}) = (\text{GTP}) = (\text{CTP}) = 0.8 \times 10^{-4} \underline{M}$ ,  $(\text{UTP}) = 0.3 \times 10^{-4} \underline{M}$ . The measured incorporation rate is then  $20 \times 10^{-10} \underline{M} \text{ sec}^{-1}$ . The scale factor to convert arbitrary units to "seconds" is 0.193.  $(\text{DNA}) = 10 \mu\text{g/ml}$ ;  $(\text{enzyme}) = 2.5 \mu\text{g/ml}$ .  $\circ$ ,  $\underline{r} = 0.0$ ,  $\square$ ,  $\underline{r} = 0.0017$ ,  $\Delta$ ,  $\underline{r} = 0.0041$ , (a)  $(\text{ATP}) = (\text{CTP}) = 0.8 \times 10^{-4} \underline{M}$ ,  $(\text{UTP}) = 0.3 \times 10^{-4} \underline{M}$ ,  $(\text{GTP})$  varied. (b)  $(\text{ATP}) = (\text{GTP}) = 0.8 \times 10^{-4} \underline{M}$ ,  $(\text{UTP}) = 0.3 \times 10^{-4} \underline{M}$ ,  $(\text{CTP})$  varied. (c)  $(\text{GTP}) = (\text{CTP}) = 0.8 \times 10^{-4} \underline{M}$ ,  $(\text{UTP}) = 0.3 \times 10^{-4} \underline{M}$ ,  $(\text{ATP})$  varied. (d)  $(\text{ATP}) = (\text{GTP}) = (\text{CTP}) = 0.8 \times 10^{-4} \underline{M}$ ,  $(\text{UTP})$  varied.

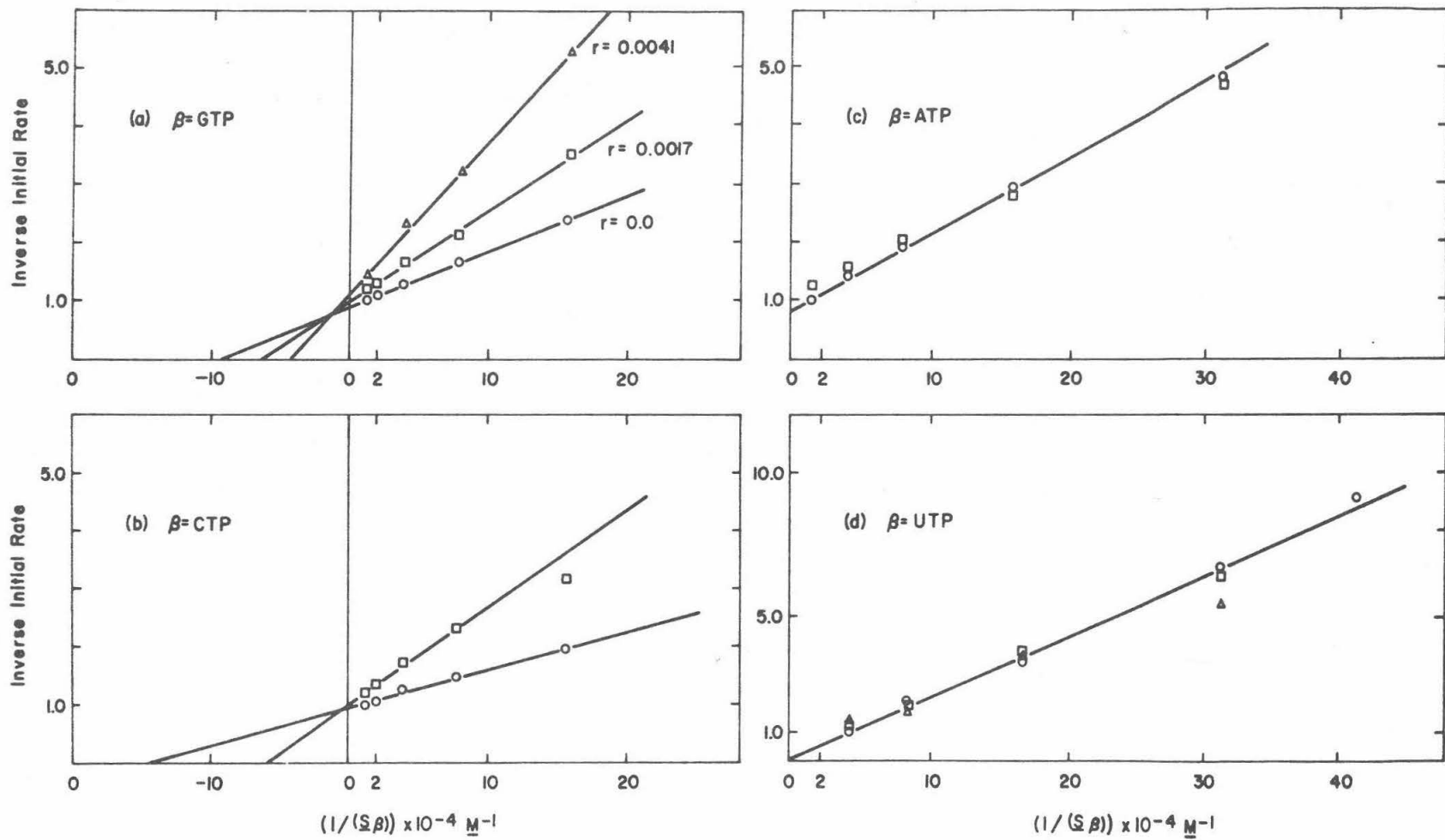


FIG 8

Fig. 9. The slopes of Fig. 8a,  $(f_{\underline{G}} K_{\underline{Go}} / k_{\underline{3Go}}) +$   
 $\underline{r} f_{\underline{G}} [(K_{\underline{GA}} / k_{\underline{3GA}}) - (K_{\underline{Go}} / k_{\underline{3Go}})]$ , divided by  $f_{\underline{G}}$  ( $= 0.24$ ), as a  
 function of  $\underline{r}$ . Conditions of synthesis as given in the legend to Fig. 8.

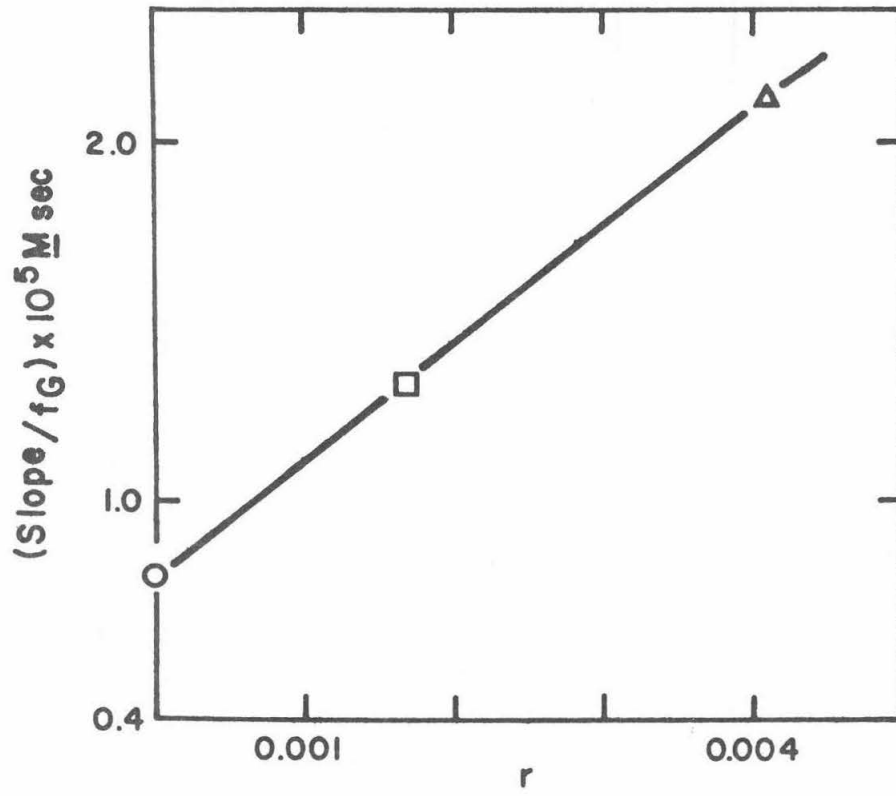


FIG 9

The most striking and significant results is that AMD acts by inhibiting the rate of incorporation of G and C, but not of A and U. The ratios  $t_{\alpha A}/t_{\alpha 0}$  are 390 for G and 980 for C, as calculated from the data of Fig. 8.

As already noted, the vertical intercepts of the reciprocal plots give the quantity

$$\sum_{\alpha} (f_{-\alpha}/k_{-3\alpha}) + \sum_{\alpha \neq \beta} f_{-\alpha} (K_{-\alpha}/k_{-3\alpha} [S_{\alpha}])$$

The second term of this expression can be evaluated when all four slopes have been measured. We then find, for the experiments in the absence of AMD, values of  $\sum f_{-\alpha} (1/k_{-3\alpha})$  in the neighborhood of  $-0.04$  sec (Table 3), which is, within experimental error, zero. This says, in effect, that at the upper limits of nucleoside triphosphate concentrations studied in this work,  $[ATP] = [GTP] = [CTP] = 0.8 \times 10^{-4}$  M,  $[UTP] = 0.3 \times 10^{-4}$  M, the reaction rate is, within experimental error, still proportional to nucleoside triphosphate concentration. Correspondingly, the observed effects of AMD are on the constants  $K_{-\alpha}/k_{-3\alpha}$  which have thus been shown to be linear functions of the  $r$  value.

The final numerical results for the slopes and intercepts in Fig. 8 are presented in Tables 3 and 4.

#### 4. Further Discussion

The results reported here show that AMD has only a small inhibiting effect on initiation of transcription, at least under the rather

TABLE 3

Kinetic data from Fig. 8

NTP	Slope <sup>a</sup> arbitrary units	$\frac{K_{\alpha 0}}{k_{-3\alpha 0}}$ (M sec) <sup>b</sup>	$\sum_{\alpha \neq \beta} \frac{f_{\alpha} K_{\alpha 0}}{k_{-3\alpha 0} S_{\alpha}}$ (sec) <sup>c</sup>	Vertical intercept (sec)	$\sum_{\alpha} \frac{f_{\alpha}}{k_{-3\alpha 0}}$ (sec) <sup>d</sup>
GTP	$0.98 \times 10^{-5}$	$0.79 \times 10^{-5}$	0.21	0.17	-0.04
CTP	$0.64 \times 10^{-5}$	$0.51 \times 10^{-5}$	0.22	0.18	-0.04
UTP	$2.16 \times 10^{-5}$	$1.6 \times 10^{-5}$	0.070	0.012	-0.06
ATP	$1.30 \times 10^{-5}$	$0.96 \times 10^{-5}$	0.21	0.16	-0.05

<sup>a</sup> Data from Fig. 8..

<sup>b</sup> The explanation of converting arbitrary units to real units is given in the legend to Fig. 8.

<sup>c</sup> Calculated from the slopes given in the third column for the other three nucleoside triphosphates.

<sup>d</sup> Fifth column minus fourth column, as dictated by eq. 8.

TABLE 4

The reciprocal rate constant,  $\frac{K_{\alpha A}}{k_{3\alpha A}}$ ,  
in the presence of AMD, from Fig. 8

NTP	$\underline{r}$	Slope (arbitrary units)	Slope <sup>a</sup> $\underline{M}(\text{sec})$	$\frac{K_{\alpha A}}{k_{3\alpha A}}$ ( $\underline{M}$ sec)
GTP	0.0	$0.98 \times 10^{-5}$	$0.79 \times 10^{-5}$	
	0.0017	$1.57 \times 10^{-5}$	$1.26 \times 10^{-5}$	$310 \times 10^{-5}$
	0.0041	$2.66 \times 10^{-5}$	$2.13 \times 10^{-5}$	
CTP	0.0	$0.64 \times 10^{-5}$	$0.51 \times 10^{-5}$	
	0.0017	$1.70 \times 10^{-5}$	$1.36 \times 10^{-5}$	$500 \times 10^{-5}$

<sup>a</sup> As explained in the text, this slope is (eq. 12):

$$\left( f_{\beta} \frac{K_{\beta 0}}{k_{3\beta 0}} \right) + \frac{r f_{\beta}}{1 - \beta} \left[ \left( \frac{K_{\beta A}}{k_{3\beta A}} \right) - \frac{K_{\beta 0}}{k_{3\beta 0}} \right]$$

specific conditions of initiation used here. Previous experiments by the  $\gamma$  -  $P^{32}$  labeling method (Maitra, Nakata & Hurwitz, 1967) had already suggested this result.

Furthermore, AMD has little or no effect on chain termination; the major inhibiting effect is on chain propagation.

The membrane filter experiments show that only ATP and GTP are needed for the quasi-irreversible binding of RNA polymerase to T7 DNA at high salt conditions; added CTP and UTP have no effect. These facts are consistent with the finding that ATP and GTP are the first nucleotides of RNA chains transcribed from a T7 DNA template, in vivo and in vitro (Maitra, Cohen & Hurwitz, 1966). We have not measured the number of polymerase molecules bound to one T7 DNA molecule in the membrane filter experiments and the chemistry of the retention process is not understood; thus, the precise bearing of these experiments on the nature of the true initiation complex is not known.

Our measurements show that there is on the average one RNA chain transcribed per T7 DNA molecule, even in the presence of excess polymerase, under the high salt conditions of initiation used here. The possibility that this number is the accidental average of equal numbers of DNA molecules with two and no RNA chains is eliminated by the work of R. W. Davis (1969), who observes one RNA bush per T7 molecule in electron micrographs of samples initiated under conditions similar to those used here.

The main inhibiting effect of AMD is on the propagation step.

It does not affect the rate of incorporation of U and of A; it does affect the rate of incorporation of G and of C.

This result is in a general way consistent with the idea that GC base pairs are essential for the binding of AMD (Goldberg, Rabinowitz & Reich, 1962; Gellert et al., 1965; Kahan, Kahan & Hurwitz, 1963; Kersten, 1961). However, it is difficult to draw more specific mechanistic conclusions.

Müller and Crothers (1968) suggest that the rate limiting step in the inhibiting action of AMD is its dissociation from the DNA. They present an analysis which is equivalent to our eq. (10). They observed dissociation times of AMD from DNA in the absence of RNA polymerase of the order of 500 sec. With a CTP concentration of  $10^{-4}$  M, which is close to the highest concentration studied in Fig. 8, the passage time for addition of a C residue to the RNA chain is calculated as  $\frac{K_{CA}}{k_{3CA}} [CTP] = 50$  sec (Table 4). This is considerably shorter than 500 sec. The Müller and Crothers model is however consistent with our results if the AMD is in effect pushed off the DNA by the transcription complex as it moves along the DNA, so that the dissociation time of an AMD in the path of a transcription complex is less than that of AMD attached to DNA alone.

Several lines of evidence (Müller & Crothers, 1968), and especially the observation that AMD changes the winding angle of a DNA by the same amount as does an ethidium dye (Wang, 1970), suggest the AMD binds to DNA by intercalation. In the simplest intercalation model the phenoxazone chromophore of AMD would be symmetrically placed between a GC base pair and an adjoining base pair. The pre-

cise site requirements as to the nature of the neighboring base pairs for AMD binding are not known. However, it is probable that the adjoining pair need not be GC (Müller and Crothers, 1968; Hyman and Davidson, 1970; Wells, 1969). If intercalation is a symmetrical phenomenon, so that the AMD interacts equally with the GC base pair and an adjoining AT base pair, one would expect AMD to exert an inhibiting effect on the incorporation of A and/or U, in disagreement with the observations.

A related difficulty with a simple intercalation model may be expressed as follows: Suppose, for example, that AMD intercalates with a GC base pair on the 3' side of the G, and therefore on the 5' side of the C. If the G containing strand happens to be the transcribing strand, the AMD is located so that, as transcription proceeds, the RNA polymerase encounters the AMD before it encounters the G. If the C containing strand happens to be the transcribing strand, the RNA polymerase encounters the AMD after it encounters the C. This kind of model therefore suggests that the incorporation of A and/or of U should also be inhibited by AMD.

We conclude that, in an acceptable intercalation model, the AMD must be interacting more strongly with the GC base pair than with the other base pair of the intercalated structure.

Hamilton, Fuller & Reich (1963) have proposed a model for AMD binding in which the AMD chromophore interacts mainly with a guanine residue of the DNA, without intercalation. The interaction is

thus quite unsymmetrical with respect to G and C. Our observations are that the rate of incorporation of C is inhibited about twice as effectively as is that of G. This model may not be readily reconciled with other physical evidence (Müller & Crothers, 1968; Wang, 1970). However, the kinetic data do not contradict this model.

We believe that the kinetic data do eliminate one plausible general model for AMD action. Suppose that as the RNA polymerase-RNA chain complex moves along the DNA, it opens up a small loop of deoxynucleotides, consisting of, for example, five to ten base pairs. When one more ribonucleotide becomes covalently attached, the polymerase moves along the DNA chain, one base pair in the front of the loop opens up, and one base pair at the rear of the loop reforms. It is known that AMD stabilizes DNA base pairs against denaturation (Gellert *et al.*, 1965; Kersten, Kersten & Szybalski, 1966). This base-pair stabilizing effect raises the free energy of the transition state for the propagation reaction when an AMD is interacting with the first base pair in front of the loop and thus reduces the reaction rate. However, in such a model the driving force for the propagation reaction is the incorporation of a nucleotide at the back of the loop, and thus five or ten base pairs behind the GC base pair to which the AMD is bound. Thus, we would predict inhibition of the A and U incorporation steps too, in contradiction with the observed facts. (We are indebted to Dr. Richard Burgess for a stimulating discussion of this loop model.)

One model for the mode of action of AMD asserts that the antibiotic induces a conformational change in the DNA structure for a segment of nucleotides close to the bound AMD and that this altered structure resists transcription (Wells, R. D., 1969; Müller & Crothers, 1968). For this model, just as for the loop model, it is predicted that AMD will inhibit the incorporation of any nucleotide in the altered segment, in contradiction to the experimental results.

We conclude that the kinetic results do not lead to a unique model for the mechanism of inhibition by AMD. The results eliminate symmetrical intercalation models and the loop model discussed above. In the AMD-DNA complex, the AMD is interacting particularly with a GC base pair. The kinetic results place significant constraints on and must ultimately be consistent with an acceptable detailed model of the structure of the AMD-DNA complex.

#### Acknowledgments

As already indicated, we are deeply grateful to Dr. Michael Dahmus for the generous gift of RNA polymerase. We are grateful to Merck, Sharp, and Dohme, Inc., for the gift of the actinomycin. We have profited from counsel and conversation with Ronald W. Davis. This research has been supported by grant GM 10991 from the United States Public Health Service. One of us (R. W. H.) was a National Institutes of Health predoctoral trainee (GM 1262).

This is contribution no. 3952 from the Gates, Crellin, and Church Laboratories of Chemistry.

## REFERENCES

- Anthony, D. D., Zeszotek, E. & Goldthwait, D. A. (1966). Proc. Nat. Acad. Sci., Wash. 56, 1626.
- Boedtker, H. (1968). J. Mol. Biol. 35, 61.
- Bremer, H. (1967). Mol. Gen. Genetics 99, 362.
- Burgess, R. A. (1969). Ph.D. Thesis, Harvard University.
- Chamberlin, M. & Berg, P. (1962). Proc. Nat. Acad. Sci., Wash. 48, 81.
- Davison, P. F. & Freifelder, D. (1962). J. Mol. Biol. 5, 635.
- Davis, R. W. (1969). Ph.D. Thesis, California Institute of Technology.
- Gellert, M., Smith, C. E., Neville, D. & Felsenfeld, G. (1965). J. Mol. Biol. 11, 445.
- Goldberg, I. H., Rabinowitz, M. & Reich, E. (1962). Proc. Nat. Acad. Sci., Wash. 48, 2094.
- Hamilton, L., Fuller, W. & Reich, E. (1963). Nature 198, 538.
- Harbers, E. & Müller, W. (1962). Biochem. Biophys. Res. Commun. 7, 107.
- Hurwitz, J., Furth, J. J., Malamy, M. & Alexander, M. (1962). Proc. Nat. Acad. Sci., Wash. 48, 122.
- Hyman, R. W. & Davidson, N. (1967). Biochem. Biophys. Res. Commun. 26, 116.
- Hyman, R. W. & Davidson, N. (1970). Manuscript in preparation.
- Jones, O. W. & Berg, P. (1966). J. Mol. Biol. 22, 199.
- Kahan, E., Kahan, F. M. & Hurwitz, J. (1963). J. Biol. Chem. 238, 2491.

- Kersten, W. (1961). Biochem. Biophys. Res. Commun. 47, 610.
- Kersten, W., Kersten, H. & Rauen, H. M. (1960). Nature, 187, 60.
- Kersten, W., Kersten, H. & Szybalski, W. (1966). Biochemistry,  
5, 236.
- Maitra, W., Cohen, S. N. & Hurwitz, J. (1966). Cold Spring Harbor  
Symp. Quant. Biol. 31, 113.
- Maitra, W., Nakata, Y. & Hurwitz, J. (1967). J. Biol. Chem. 242,  
4908.
- Müller, N. & Crothers, D. M. (1968). J. Mol. Biol. 35, 251.
- Richardson, J. P. (1966). J. Mol. Biol. 21, 83.
- Spirin, A. S. (1963). Prog. Nucleic Acid. Res. 1, 301.
- Wang, J. C. (1970). Manuscript in preparation.
- Wells, R. D. (1969). Science, 165, 75.
- Wyatt, G. R. & Cohen, S. S. (1953). Biochem. J. 55, 773.

## PROPOSITION I

THE INITIATION SITES FOR RNA SYNTHESISABSTRACT

An experimental procedure is described that will allow the isolation of the E. coli RNA polymerase recognition sites of T7 DNA. It is proposed to measure the number of those sites per T7 DNA and to measure the base composition of those sites. The possibility exists that the E. coli RNA polymerase recognition sites of  $\lambda$  DNA have identical sequences to those of T7 DNA; two experiments are proposed to test this possibility.

RNA polymerase initiates RNA synthesis at specific site(s) on a DNA and must, therefore, recognize those sites. One possibility is that the enzyme can recognize unique nucleotide sequences. It is then of interest (a) to determine the number of sites per DNA; (b) to isolate those sites and determine their base composition; and (c) to compare the sites from different DNA's.

These measurements have been attempted previously, starting from the fact that the RNA polymerase-DNA complex is resistant to DNase (1, 2). However, in both attempts there were basic and substantial flaws: (a) bacterial DNA, which contains single-stranded regions, chain nicks, and free ends, was employed, and RNA polymerase demonstrates a preference for denatured, rather than native, bacterial DNA (3); (b) the enzyme and DNA were simply mixed together in low salt buffer which does yield a complex, but there is no assurance that this complex is the true initiation complex (4, 5); and (c) the excess polymerase present could bind to the new free ends being produced by the nuclease (6). Any of these flaws would lead to artifactual results.

The experiment proposed here surmounts those difficulties and others by using T7 DNA, a coherent DNA, by initiating specifically under defined conditions, and by removing the excess polymerase.

E. coli RNA polymerase is allowed to initiate on P<sup>32</sup> labeled T7 DNA in low salt buffer in the presence of ATP and GTP. These conditions select for the true initiation complex (5, 7). In this and all subsequent reaction mixtures containing polymerase, there is present

dithiothreitol,  $5 \times 10^{-3}$  M, 5% glycerol, and whenever possible the temperature is  $4^{\circ}\text{C}$ ; all these stabilize the enzyme (8).  $(\text{NH}_4)_2\text{SO}_4$  is added to a final concentration of 0.4 M. The high salt concentration causes the removal of noninitiated polymerase from the DNA and leaves the initiation complex intact. The initiation complex is separated from the excess polymerase by gel filtration. Since the complex has a minimum molecular weight of  $26.5 \times 10^6$  and the enzyme has a molecular weight of  $0.5 \times 10^6$ , this separation is easily accomplished. Thus, when the  $\text{P}^{32}$  decays and produces a single-strand break, there is no enzyme available to complex with that region. The complex is dialyzed into low salt buffer (0.05 M Tris, pH 7, 0.01 M  $\text{MgCl}_2$ ) preparatory to nuclease digestion, and then digested to completion with pancreatic DNase and snake venom phosphodiesterase. The digestion will have to be calibrated and followed closely. Dialysis is then employed to remove the small oligonucleotides, and then gel filtration to exclude the polymerase-binding site complex (molecular weight  $> 0.5 \times 10^6$ ) and to retard the nucleic acid breakdown products (molecular weight  $\leq 0.05 \times 10^6$ ). The fraction of  $\text{P}^{32}$ -T7 DNA resistant to nuclease tells us the average number of base pairs per DNA resistant to attack.

To separate the DNA from the enzyme, we treat the complex with SDS and phenol followed by dialysis of the DNA into a reasonable buffer.

The molecular weight of the DNA can be determined by polyacrylamide gel electrophoresis (9). From the molecular weight, we

can calculate the average number of base pairs per binding site and, combining this datum with our previous result of the number of base pairs resistant to nuclease per DNA, we get a measure of the number of RNA polymerase initiation sites per DNA:

$$\frac{\# \text{ base pairs resistant/DNA}}{\# \text{ base pairs/site}} = \# \text{ sites/DNA}.$$

Previous measurements indicate one site per T7 DNA (7).

Parallel and informative experiments can be accomplished with unlabeled material if the quantities of enzyme and DNA are increased. A 100 ml culture of T7 $\phi$  yields 2 mg of T7 DNA. A 10 l culture would produce 200 mg of T7 DNA. Frozen E. coli cells are sold by the kg, and a large scale purification procedure for RNA polymerase is in use (8). Therefore, acquiring large amounts of polymerase and T7 DNA requires only time, money, and work. If the enzyme protects 30-50 base pairs from digestion, about 0.1% of the DNA is resistant. 60 mg of T7 DNA yields 6  $\mu$ g of initiation sites. The actual fraction resistant to attack is calculated from the  $A_{260}$ . The molecular weight of the resistant base pairs is measured by sedimentation equilibrium, a particularly convenient method for molecules of this size. As before, these data can be combined to calculate the number of sites per T7 DNA.

The fraction of nuclease resistant DNA is more accurately measured by radioactivity and the molecular weight by sedimentation equilibrium. The combination of these data should give the best measurement of the number of initiation sites per T7 DNA.

Renaturation kinetics can be employed to calculate the complexity of the resistant DNA and, hence, to ascertain whether or not it has a unique sequence (10). 6  $\mu\text{g}/\text{ml}$  is  $A_{260} \simeq 0.1$ , which is sufficient for optical measurements. The kinetic complexity will closely agree with the molecular weight calculated from sedimentation equilibrium data if the DNA is unique.

We have, then, isolated the initiation sites relatively free of other DNA, so we can use conventional methods to determine the base composition of the sites (11, 12). By adding 2-3 mc of carrier-free phosphoric acid to a 1-1 culture growing in low phosphate medium, one can obtain DNA with a specific activity of about  $10^5$  cpm/ $\mu\text{g}$ , which is sufficient for our purpose. If the RNA polymerase initiation sites are as unusual as stretches of poly dG:dC as has been suggested (13), this can be easily detected. Even modest differences from the overall G+C content of T7 DNA (done as a control) are observable. The two previous attempts at this experiment (1, 2) have both indicated a relatively GC-rich region for the initiation site. If RNA polymerase recognizes nucleotide sequence, we shall have defined the G+C content of that sequence.

Assuming one unique initiation site per T7 DNA can be isolated, a fascinating experiment can be accomplished. The specificity of RNA polymerase apparently resides in its  $\sigma$  subunit (14). E. coli RNA polymerase will transcribe an early gene(s) of T7 DNA and two early genes of  $\lambda$  DNA (15) before phage-specific  $\sigma$  (polymerase) is produced.

Coli polymerase possesses the coli-specific  $\sigma$  factor and is probably recognizing the same sequence on different DNA's. This potentially informative hypothesis can be tested.

The conventional DNA-DNA hybridization is not adequate, for if denatured T7 DNA initiation sites are challenged with denatured  $\lambda$  DNA immobilized on a membrane, the sites will preferentially self-renature.

If the  $\lambda$  initiation site can be isolated analogously to the isolation of the T7 initiation site, mixed renaturation rates can be measured. The complexity of T7 sites alone and  $\lambda$  sites alone should be closely the same. The complexity of the mixture of T7 and  $\lambda$  sites will be equal to the complexity of one site alone, if the site sequences are identical.

That test presupposes the isolation of the  $\lambda$  initiation sites, which has not yet been attempted. A second test, which can be accomplished using current techniques, is therefore proposed.  $P^{32}$ -T7 sites are mixed with an excess of one of the separated strands of  $H^3$ - $\lambda$  DNA. Denaturation followed by extensive renaturation is allowed.  $\lambda$  DNA is separated from the much smaller T7 DNA by sucrose gradient centrifugation. The presence of  $P^{32}$ -T7 DNA with the  $H^3$ - $\lambda$  peak demonstrates a sequence homology. From the specific activities, the ratio of T7 sites per  $\lambda$  DNA may be roughly calculated.

Thus, two methods have been proposed to test the identicalness of coli RNA polymerase recognition sites on different coliphage DNA's.

## REFERENCES

1. Novack, R. L., Biochim. Biophys. Acta, 149, 593 (1967).
2. Matsukage, A., S. Murakami and T. Kameyama, Biochim. Biophys. Acta, 179, 145 (1969).
3. Cheong, L. and E. Chargaff, Nature, 221, 1144 (1969).
4. Jones, O. W. and P. Berg, J. Mol. Biol., 22, 199 (1966).
5. Anthony, D. D., E. Zeszotek and D. A. Goldthwait, Proc. Nat. Acad. Sci., Wash., 56, 1626 (1966).
6. This is a plausible hypothesis of mine.
7. Hyman, R. W. and N. Davidson, J. Mol. Biol., submitted.
8. Burgess, R. R., Ph.D. Thesis, Harvard University (1969).
9. Elson, E. and T. Jovin, Anal. Biochem., 27, 193 (1969).
10. Wetmur, J. G. and N. Davidson, J. Mol. Biol., 31, 349 (1968).
11. Ray, D. S. and P. C. Hanawalt, J. Mol. Biol., 9, 812 (1964).
12. Hurst, R. D., A. M. Marko and G. C. Butler, J. Biol. Chem., 204, 847 (1953).
13. Hradecna, Z. and W. Szybalski, Virology, 32, 633 (1967).
14. Burgess, R. R., A. A. Travers, J. J. Dunn and E. K. Bautz, Nature, 221, 43 (1969).
15. Hallick, L., R. Boyce and H. Echols, Nature, 223, 1239 (1969).

## PROPOSITION II

AN INTERPRETATION OF EXTANT DATA FOR  
O-ACETYL SERINE SULFHYDRASE

ABSTRACT

The extant data for the enzyme O-acetylserine sulfhydrase is found to be consistent with a mechanism essentially identical to that of Michaelis-Menten with  $k_3 \gg k_2$ .

Too many enzymologists automatically assume that the Michaelis constant,  $K_M$ , determined kinetically, is equal to the association constant of substrate and enzyme,  $K_{eq}$ . In the original Michaelis-Menten mechanism,  $K_{eq} = k_2/k_1$  and  $K_M = (k_2 + k_3)/k_1$ , so that  $K_{eq} = K_M$  only when  $k_3 \ll k_2$ , which is usually, but not always, the case. The confusion that results when the assumption that  $K_M = K_{eq}$  is made automatically is apparent in a recent paper (1).

The last step in the biosynthesis of L-cysteine in E. coli and S. typhimurium is (2)



This reaction is catalyzed by O-acetylserine sulphydrase. This enzyme has been isolated in essentially pure form from S. typhimurium by Becker, Kredich and Tomkins (1). They have measured the association constant,  $K_{eq}$ , of O-acetylserine and enzyme alone and the apparent Michaelis constant for the overall reaction. The two values do not agree. I now quote from their paper to demonstrate my point. (Space does not allow an extensive quotation, and I realize that editing to my service may be a disservice to the authors.)

"The kinetically determined Michaelis constant for O-acetylserine is  $J \times 10^{-3} \underline{M} \equiv 5 \times 10^{-3} \underline{M}$ , whereas the equilibrium constant for the substrate binding reaction, determined spectroscopically, is  $6 \times 10^{-7} \underline{M}$ . The large

"disparity between these values could signify that the kinetics method does not give a valid indication of substrate binding affinity. . . . Until the mechanisms of the reaction. . . have been worked out, the interpretation of this data must remain open to speculation."

However, there is enough data already available from those authors to make a valid interpretation of the disparity, if we remember the assumption that leads to the case  $K_M = K_{eq}$ .

The reaction rate is independent of the order of addition of the reactants and of sulfide concentration, when the sulfide concentration is relatively high. The enzyme requires pyridoxal-phosphate as a cofactor, which is consistent with the postulation of the formation of a complex between O-acetylserine and enzyme as the first step in the reaction. The simplest mechanism is closely related to that of Michaelis and Menten:



where

$S_1 \equiv$  O-acetylserine,

$S_2 \equiv$  sulfide, and

$E \equiv$  the intimate complex of enzyme and cofactor.

In practice, only  $(S_1)_0$  is varied, and  $(S_1)_0 \gg E_0$ . Making the usual steady-state approximation leads to this equation for the rate of reaction:

$$\frac{1}{V} = \frac{1}{k_3(S_2)_0 E_0} + \frac{k_2 + k_3(S_2)_0}{k_1} \frac{1}{k_3(S_2)_0 E_0 (S_1)_0} \quad (3)$$

When  $k_3(S_2)_0$  is much larger than  $k_2$ , three self-consistent consequences follow: (a) The spectral shift due to complex formation is not observed because of the very short lifetime of the complex. This consequence is experimentally true. (b) The rate of the reaction becomes independent of sulfide concentration at high sulfide concentration. From Equation (3) and with  $k_3(S_2)_0 \gg k_2$ ,

$$\frac{1}{V} = \frac{1}{k_3(S_2)_0 E_0} + \frac{1}{k_1(E_0)(S_1)_0} \quad (4)$$

when

$$(S_2)_0 > (S_1)_0$$

and probably

$$k_3 \geq k_1$$

$$k_3(S_2)_0 > k_1(S_1)_0$$

$$V = k_1 E_0 (S_1)_0 . \quad (5)$$

This consequence is also experimentally true. (c) The Michaelis constant,  $K_M$ , is not equal to the constant for complex formation,  $K_{eq}$ , which is the crux of the matter. Unlike (b), these measurements were

carried out with  $(S_2)_0 \approx (S_1)_0$ .

$$K_{eq} = k_2/k_1 \quad (6)$$

$$K_M = \frac{k_2 + k_3(S_2)_0}{k_1}$$

$$K_M = K_{eq} \left( 1 + \frac{k_3(S_2)_0}{k_2} \right) \quad (7)$$

If  $k_3(S_2)_0$  were much less than  $k_2$  (the usual situation),  $K_M$  would equal  $K_{eq}$ , which is not the case. But, when  $k_3(S_2)_0 \gg k_2$  (the unusual case),

$$K_M = K_{eq} \frac{k_3(S_2)_0}{k_2} \quad (8)$$

and  $K_M \neq K_{eq}$ . This also is experimentally true.

Further, we can demonstrate the consistency of the assumption that  $k_3(S_2)_0 \gg k_2$ , using the experimental data and the proposed mechanism:

$$K_{eq} = 6 \times 10^{-7} \underline{M}$$

$$K_M = 5 \times 10^{-3} \underline{M}$$

$$\frac{k_3(S_2)_0}{k_2} = K_M/K_{eq}$$

$$= 8 \times 10^3$$

$$k_3(S_2)_0 \approx 10^4 k_2$$

$$k_3(S_2)_0 \gg k_2 \quad (9)$$

Therefore, using a simple mechanism, all the data can be interpreted in an entirely reasonable and self-consistent way. Indeed, the kinetics method ( $K_M$ ) does not "give a valid indication of substrate binding affinity" ( $K_{eq}$ ). There was no trick involved; simply the knowledge that while usually  $k_3 \ll k_2$ , the latter is not always true, and, when  $k_3 \geq k_2$ ,  $K_M \neq K_{eq}$ , but  $K_M$  defines a steady-state condition.

## REFERENCES

1. Becker, M., N. Kredich and G. M. Tomkins, J. Biol. Chem., 244, 2418 (1969).
2. Kredich, N. M. and G. M. Tomkins, J. Biol. Chem., 241, 4955, (1966).

## PROPOSITION III

THE CONSTRUCTION OF Hfr STRAINS OF  
SEVERAL BACTERIAL SPECIES AND THEIR  
USE IN CROSS SPECIES MARKER RESCUE EXPERIMENTS

ABSTRACT

A simple method is proposed for the possible construction of Hfr strains of several bacterial species using a temperature-sensitive E. coli F' lac. The frequency of integration of the E. coli F'<sub>TS</sub> lac into the chromosome of various bacteria can be easily measured. It is proposed to use the Hfr strains so constructed for cross species marker rescue experiments to test which genes are recognized as the same in different bacterial species.

The E. coli sex factor episome, F, transfers from E. coli F<sup>+</sup> cells to the cells of several other bacterial species besides E. coli: Shigella, Salmonella, Proteus, Serratia, Pasteurella, and Vibrio (1, 2). An E. coli with the F factor integrated, Hfr, can transfer part or all of its genome to at least Shigella and Salmonella besides E. coli (3, 4). The existence of Hfr's provide a mechanism for transfer of genes not only within a species but between different species. The evolutionary consequences are considerable. I propose here (a) the measurement of the frequency of integration of E. coli F into the chromosome of E. coli, Shigella, Salmonella, Proteus, Serratia, Pasteurella, and Vibrio by a simple method, and (b) the measurement of the frequency of marker rescue among the bacterial species to test for possible evolutionary consequences. The integration process involves at least DNA-DNA recognition, DNA-DNA homology, and a recombination system, so a comparative measurement of the frequency of integration among species is a measure of the speciation of this process. That DNA-DNA homology is important is attested to by the fact that E. coli F' lac integrates into E. coli with a frequency of  $10^{-2}$ , but into E. coli with the lac region deleted at a frequency of  $10^{-4}$  (5).

A Salmonella Hfr with the E. coli F integrated, Salmonella Hfr, has been constructed by dosing the E. coli F<sup>+</sup> donor cells with UV radiation before mixing them with the Salmonella F<sup>-</sup> and then identifying the rare recipient Salmonella Hfr by replica plating (4, 6). The Salmonella Hfr so constructed transfers its chromosome to Salmonella F<sup>-</sup> and to E. coli F<sup>-</sup> (4, 6). However, UV irradiation kills or damages

all the donor cells and is, therefore, of little use for comparative evolutionary arguments. In such an experiment, the Salmonella Hfr's arise as a result of two processes, conjugation and integration, and therefore one measures the product of the frequency of integration and the frequency of transfer, not the frequency of integration alone, which is the more interesting number. Therefore, while this method does allow the laborious isolation of a single Salmonella Hfr strain, it is not useful for our purpose.

To measure the frequency of integration alone, we must first construct a bacterial strain harboring E. coli F as an episome. We allow the conjugation of coli  $y^- F'_{TS} lac$  and Bact  $y^+ lac^-$ , where y is any convenient metabolite, Bact is one of the bacterial species under consideration (Shigella, Salmonella, Proteus, Serratia, Pasteurella, Vibrio are all  $lac^-$ ), and  $F'_{TS} lac$  is an E. coli sex factor harboring the lac genes that is unable to replicate autonomously at high temperature (5). The frequency of conjugation between E. coli and Proteus mirabilis is about  $5 \times 10^{-6}$  (ref. 7). If we select for  $lac^+ y^+$  bacteria, we isolate Bact  $F'_{TS} lac$ ; the E. coli is selected against by the absence of y from the medium. A Proteus strain, P. mirabilis-1-F' lac, with the E. coli  $F' lac$  as a stable episome, has been constructed in this manner (7).

Starting with a single clone of each Bact  $F'_{TS} lac$ , where Bact is E. coli, Shigella, Salmonella, Serratia, Proteus, Pasteurella, and Vibrio, we grow each culture in nutrient medium at permissive temperature and then plate at restrictive temperature with lactose as the sole carbon source. Only those bacteria with  $F'_{TS} lac$  integrated can form

colonies. From the number of colonies we can calculate the frequency of integration per cell for the different bacteria and, hence, measure the speciation of the integration mechanism.

When we establish Hfr's of several different bacterial species (E. coli and Salmonella Hfr's are known), we can turn our attention to evolutionary considerations and do marker rescue experiments. In these experiments we attempt to rescue bacteria that are  $y^-$  by mating them with Hfr  $y^+$ . E. coli Hfr mates with E. coli, Salmonella, and Shigella, and Salmonella Hfr mates with Salmonella and E. coli (3, 4); therefore, at least these species can be tested. Marker rescue has been attempted by transduction (8). A very low frequency of rescue was observed ( $\sim 10^{-9}$ ) presumably because of the need for DNA-DNA homology for the recombination process and because, in transduction, there is only a limited amount of DNA transferred. Luria and Burrous (3) measured the frequency of recombination from E. coli Hfr  $\times$  Shigella mating to be about  $10^{-5}$  per donor cell. By zygotic induction, E. coli ( $\lambda$ ) Hfr  $\times$  E. coli; E. coli ( $\lambda$ ) Hfr  $\times$  Shigella, they measured the frequency of mating to be  $10^{-3}$  (in both cases). The reason for the frequency of recombination being less than the frequency of mating is again presumably because of less DNA-DNA homology between E. coli and Shigella than between E. coli and E. coli.

Therefore, for marker rescue experiments, we should start with genes that have characters in common, though this does not necessarily mean they are alleles. Each Bact Hfr possesses the E. coli lac genes and, hence, should rescue E. coli lac $^-$  to lac $^+$ :

for example, E. coli Hfr × E. coli lac<sup>-</sup> (control), Salmonella Hfr × E. coli lac<sup>-</sup>. The next obvious, similar characters are the abilities to metabolize sugars such as glucose and fructose, or to anabolize amino acids: for example, Salmonella Hfr glucose<sup>+</sup> × Salmonella glucose<sup>-</sup> (control), Salmonella Hfr glucose<sup>+</sup> × E. coli glucose<sup>-</sup>; E. coli Hfr leucine<sup>+</sup> × E. coli leu<sup>-</sup> (control), E. coli Hfr leu<sup>+</sup> × Shigella leu<sup>-</sup>. In such a series of experiments we can measure the frequency of marker rescue among bacterial species and define which genes are recognized as (approximately) the same and, hence, rescued, and which are different.

## REFERENCES

1. Campbell, A. M., Episomes, Chapter 3, Harper and Row, New York, 1969.
2. Hayes, W., The Genetics of Bacteria and Their Viruses, Chapter 24, John Wiley and Sons, Inc., New York, 1967.
3. Luria, S. E. and J. W. Burrous, J. Bact., 74, 461 (1957).
4. Zinder, N., Science, 131, 924 (1960).
5. Beckwith, J. R., E. R. Signer, and W. Epstein, Cold Spr. Harb. Symp. Quant. Biol., 31, 393 (1966).
6. Baron, L. S., W. F. Carey, and W. M. Spilman, Proc. Nat. Acad. Sci., Wash., 45, 1752 (1959).
7. Falkow, S., J. A. Wohlheiter, R. V. Citarella, and L. S. Baron, J. Bact., 87, 209 (1964).
8. Zinder, N., Science, 131, 813 (1960).

## PROPOSITION IV

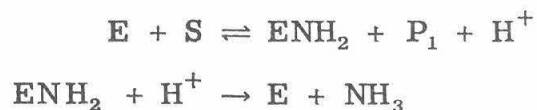
ON TWO ASPECTS OF HISTIDINE METABOLISMABSTRACT

Because of the confusion in the literature, it is proposed to reconsider the mechanism of bacterial histidase now that pure enzyme has been prepared.

In man, the hereditary lack of histidase is responsible for the disease histidinemia. The possibility that the clinical symptoms are due in part to the lack of urocanic acid, rather than solely to the high levels of histidine, is considered, and the administration of urocanic acid to patients with histidinemia is proposed.



Peterkofsky (2), working with an enzyme preparation that was at best 30% pure, proposed a mechanism for the reaction based on (a) data from an earlier paper (3) that he stated indicated the reaction was irreversible, and (b) his own exchange data wherein C<sup>14</sup>-urocanic acid and T<sub>2</sub>O exchanged into histidine in the presence of enzyme but N<sup>15</sup>H<sub>4</sub><sup>+</sup> did not.



where S represents histidine and P<sub>1</sub> urocanic acid. Peterkofsky proposes that the second step is "irreversible" based on his use of the earlier data of Mehler and Tabor (3) and on his own nonexchangeable N<sup>15</sup>H<sub>4</sub><sup>+</sup> data. However, the former argument is incorrect, because Mehler and Tabor used an enzyme preparation that was unfractionated homogenized guinea pig liver which contained significant amounts of urocanase (as they pointed out). Since urocanic acid was destroyed, there was no substrate for the back reaction. As to the latter argument, Williams and Hiroms (4), using an enzyme preparation 50-60% pure, found that histidase catalyzed the conversion of NH<sub>4</sub><sup>+</sup> and urocanic acid to histidine and measured the rate. Therefore, the most compelling adta for Peterkofsky's mechanism, the nonexchangeable N<sup>15</sup>H<sub>4</sub><sup>+</sup>, is directly contradicted by the data of Williams and Hiroms (4).

Now that pure enzyme has been prepared, we may sensibly

re-examine the problem. The postulation that the histidase-catalyzed reaction is (relatively) irreversible is disquieting, but not impossible. In a series of interconversions and syntheses, it is more efficient for the cell to conserve free energy by having little free energy change for a reaction;  $\Delta F \simeq 0$ ,  $K \simeq 1$ , or the reaction is reversible. The reaction catalyzed by histidase leads to the syntheses of pyrimidine and glutamate. It would, therefore, be surprising to find a relatively irreversible step, because the cell would be losing free energy in a synthetic pathway. I propose to remeasure with pure enzyme the histidase-catalyzed exchange of  $C^{14}$ -urocanic acid,  $T_2O$ , and  $N^{15}H_4^+$  with histidine and to measure the kinetics of the forward and back reactions. Since no enzyme-catalyzed reaction is irreversible, we can measure the equilibrium constant for the in vitro reaction, the relative equilibrium concentrations of histidine and urocanic acid, and compare the latter to the in vivo pool sizes.

The second aspect of histidine metabolism concerns the hereditary metabolic defect in man that results in the disease histidinemia: a lack of histidase. Histidinemia was discovered in 1961, and the number of laboratories working on the problem since then has been limited. Patients with the disease are generally mentally retarded, have speech defects, and show high levels of histidine in their blood and urine (5, 6, 7). Direct measurements failed to detect histidase in the epidermis of two patients (5) and in the liver of two others (7). These are the only two tissues that normally exhibit histidase activity in man. The postulation

has been that the high levels of histidine are the cause of the symptoms (5, 6, 7). However, since urocanic acid is produced solely from histidine in mammalian cells, one consequence of a lack of histidase is a lack of urocanic acid. Since urocanic acid is, at least, a normal component of human sweat, it may be that some of the clinical symptoms of histidinemia are caused by the lack of urocanic acid either within the tissue or on the skin, or both. It is, therefore, possible that these symptoms may be alleviated by administering urocanic acid in the diet and/or spraying it on the skin. Previously, all treatment of patients with histidinemia has centered on removing histidine from the diet, which is difficult because infants require histidine. Some success has been achieved; histidine concentrations in blood and urine have dropped to about normal (7). I propose to add urocanic acid to the diet of patients with histidinemia and/or to apply it to their skins in the hope that their symptoms can be further alleviated.

## REFERENCES

1. Rechler, M., J. Biol. Chem., 244, 551 (1969).
2. Peterkofsky, A., J. Biol. Chem., 237, 787 (1966).
3. Mehler, A. and H. Tabor, J. Biol. Chem., 201, 775 (1953).
4. Williams, V. and J. Hiroms, Biochim. Biophys. Acta, 139, 214 (1967).
5. La Du, B. N., in J. B. Stanbury, J. B. Wyngaarden and D. S. Fredrickson, The Metabolic Basis of Inherited Disease, Chapter 17, McGraw-Hill, New York, 1966.
6. Ghadimi, H. and R. Zischka, in W. L. Nyhan, Amino Acid Metabolism and Genetic Variation, Chapter 6, McGraw-Hill, New York, 1967.
7. Auerbach, V., A. M. Digeorge, and G. C. Carpenter, in W. L. Nyhan, Amino Acid Metabolism and Genetic Variation, Chapter 7, McGraw-Hill, New York, 1967.

## PROPOSITION V

THE IMPLICATIONS FROM  
COMPLEMENTARY SEQUENCES BETWEEN 5 S RNA AND tRNA

ABSTRACT

The standard model for the participation of the ribosome in protein synthesis is modified to include base pairing between 5 S rRNA and charged tRNA. An experiment is proposed to test whether or not E. coli 5 S RNA and E. coli Met tRNA<sub>M</sub> form a complex in solution.

The fourteen tRNA's that have been sequenced can all be envisioned in the "cloverleaf" model with three single-strand loops (1). One loop contains the anticodon; a second loop has the function of being the synthetase recognition region (2); the function of the third loop has not been assigned. Whether the tRNA is from rat liver, yeast, or E. coli, the third loop generally contains the sequence GT $\Psi$ CG. This is a remarkable conservation of structure, which indicates an important functional role for this loop.

The 5 S ribosomal RNA of E. coli and KB cells have both been sequenced (3, 4). Both 5 S RNA's contain the sequence complementary to the tRNA third loop and contain it twice. Since during protein synthesis charged tRNA binds to the ribosome, of which the 5 S RNA is part, the idea that these potential base pairs are part of the basis of the interaction was quickly recognized and published (3-9).

What has not been said is that there are two non-equivalent binding sites for tRNA on each ribosome as a necessary part of protein synthesis and that each ribosome contains one 5 S RNA which has two non-equivalent sequences complementary to the third loop of tRNA. A model is proposed here which assigns to the tRNA third loop the function of stabilizing the charged tRNA-ribosome interaction by base-pairing with 5 S RNA.

Of the five sequenced coli tRNA's, four contain GT $\Psi$ CG in the third loop (1, 10-12); the fifth, Met tRNA<sub>F</sub>, contains the sequence GT $\Psi$ CA (13). E. coli 5 S RNA contains the separate sequences

CGAAC and GAAC (3, 4), which are capable of 5 and 4 base pairs with tRNA, respectively, except for Met tRNA<sub>F</sub> which can form only 4 base pairs with either sequence. However, Met tRNA<sub>F</sub>, unlike all others, has only one binding site per ribosome, because it can only start a protein.

The proposed model for the participation of base pairs between tRNA and 5 S RNA as part of protein synthesis is drawn in Figure 1. It adds to the previous model (14) by placing the 5 S RNA with the 50 S subunit, which agrees with experimental evidence, and by including the base pairing between the tRNA and the 5 S RNA. If a complex, such as is drawn in Figure 1c, is disrupted gently, the peptidyl-tRNA remains with the 50 S subunit indicating a stability that exists without intact ribosomes (14), and which this model attributes in part to base pairing between peptidyl-tRNA and the 5 S RNA. The two non-equivalent binding sites for tRNA are labeled "B", the peptide binding site, and "A", the amino acid binding site. The specificity of the site resides in part in the codon-anticodon pairing and in the inferences that site B cannot contain a positive charge (which formylmethionine alone does not possess) and that site A requires a positive charge. The stability of the tRNA on each site is enhanced by the base pairing between the tRNA third loop and 5 S RNA. The four base pair interaction is placed at site A and the five base pair interaction at site B, so that after translocation the system gains a base pair: that is, goes to a more stable configuration.

Figure 1. A model for protein synthesis which adds to the previous model (14) by including the 5 S RNA and the stabilizing base pairs.

(a) tRNA binding

(b) peptide band formation

(c) translocation, and another tRNA binding.

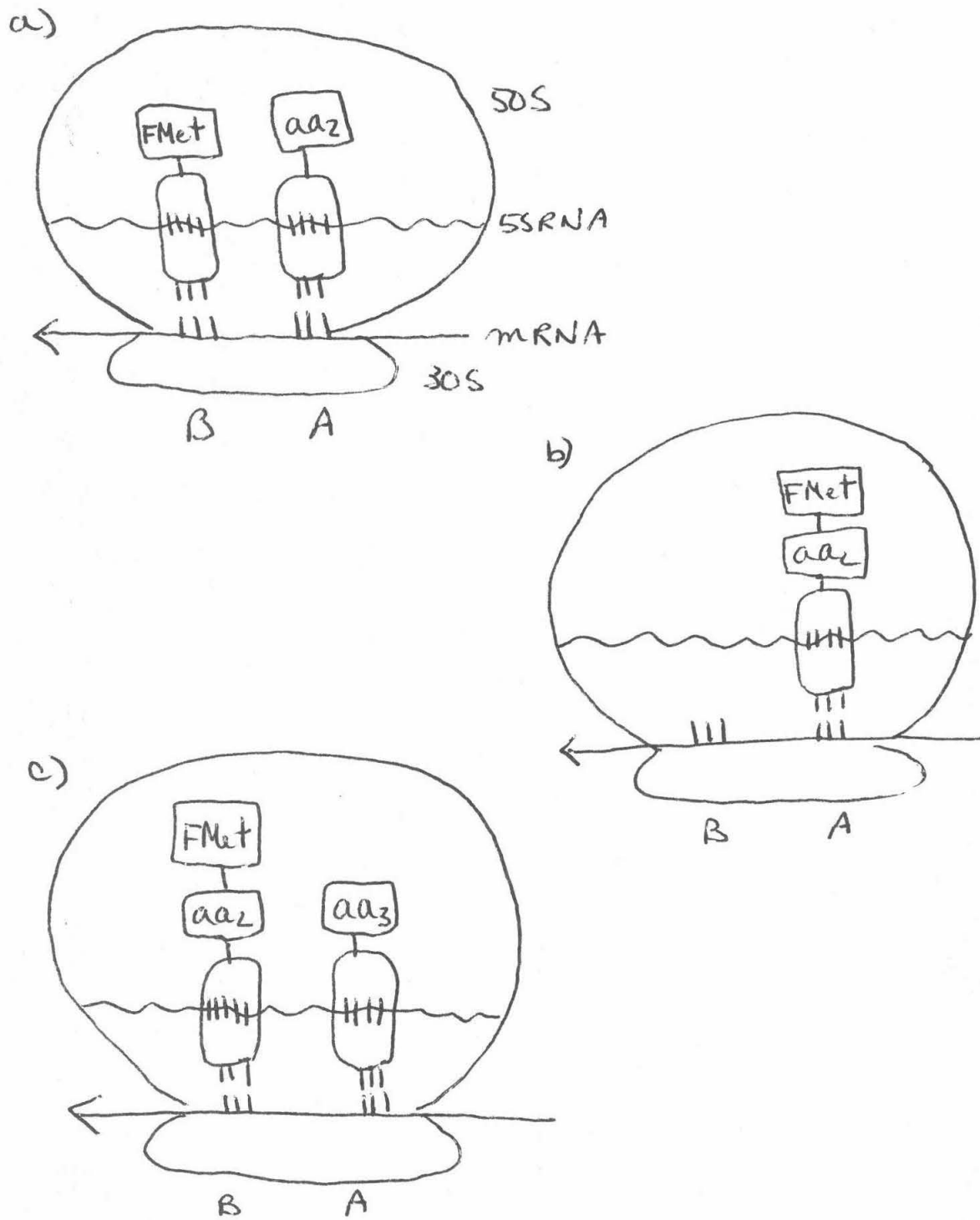
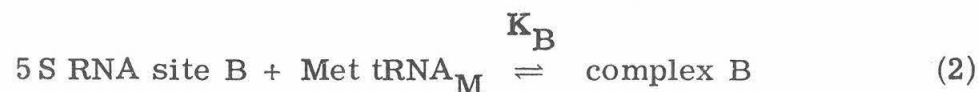
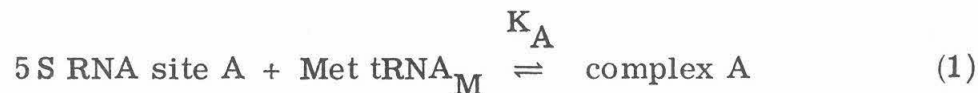


Figure 1

One way to present evidence favorable to the model for the tRNA third loop base pairing to 5 S RNA would be to demonstrate an in vitro complex between E. coli Met tRNA<sub>M</sub> and E. coli 5 S RNA. The reactions are:



These equations are written for independent sites; this assumption is not essential to the argument. We can estimate K following Wetmur and Davidson (15):

$$K = \sigma s_{AT}^a s_{GC}^b \quad (3)$$

where  $\sigma$  is the nucleation constant;  $s_{AT}$  ( $s_{GC}$ ) is the equilibrium constant for the formation of an AT (GC) base pair next to an existing base pair;  $a$  ( $b$ ) is the number of AT (GC) base pairs.

$$\sigma = 34 \exp(-7000/RT) \text{ l/mole}$$

$$s_{AT} = 1.04 \times 10^{-5} \exp(8000/RT) \quad (4)$$

$$s_{GC} = 1.04 \times 10^{-5} \exp(8935/RT)$$

For the case of four base pairs,  $K_A$ ,  $a = b = 2$ ; for the case of five base pairs,  $K_B$ ,  $a = 2$ ,  $b = 3$ . Values of K for different values of T are presented in Table 1.

TABLE 1

K as a Function of T

T (°C)	$K_B$ (1/mole)	$K_A$ (1/mole)
37	30	3
20	300	30
5	3000	300

While it would be better to work at an elevated temperature where nonspecific interactions would be less likely, the estimated values of  $K$  necessitate working at low temperature:  $5^{\circ}\text{C}$ . There is no simple way to measure  $K_A$  and  $K_B$ . The best method would be sedimentation equilibrium, but, unfortunately, the theory and practice of two different interacting macromolecules have not been published. While we cannot measure  $K_A$  and  $K_B$ , we can use sedimentation equilibrium to establish that a complex is formed, because we can tell the difference between the presence of two interacting and two non-interacting macromolecules. A necessary control is to measure the molecular weights of both 5S RNA and Met tRNA<sub>M</sub> separately to determine that no self-aggregation occurs.

A convenient RPM can be calculated from the basic relationship

$$\text{RPM} = \frac{30}{\pi} \left[ \frac{2RT \ln(C_b/C_m)}{M(1 - \bar{\nu}\rho)(r_b^2 - r_m^2)} \right]^{\frac{1}{2}} \quad (5)$$

where  $\underline{b}$  and  $\underline{m}$  refer to the bottom and the meniscus of the column, respectively:  $r_m = 6.9$  cm and  $r_b = 7.2$  cm. For a good experiment,  $C_b/C_m \approx 3$ . Therefore, for RNA of molecular weight  $3.5 \times 10^4$ ,  $\text{RPM} \approx 10^4$ , an easily attainable, stable speed. The time for reaching equilibrium can be approximated if we assume it is proportional to the column height and, hence, is diffusion-controlled (16),

$$\begin{aligned} t(\text{hr}) &= \frac{(r_b - r_m)^2}{3600 D_{20, w}} \\ &\approx 40 \text{ hr} . \end{aligned} \quad (6)$$

Therefore, it takes about two days to do an experiment.

For a noninteracting system of two ideal macromolecules with the same  $\bar{\nu}$

$$\frac{2RT}{\omega^2(1 - \bar{\nu}\rho)} \left( \frac{C_{2b} - C_{2m}}{C_2^0} \right) = \bar{M}_w^0 (r_b^2 - r_m^2) \quad (7)$$

where  $C_2 = \sum_{i=1}^2 C_i$ , and  $\underline{b}$  and  $\underline{m}$  can be any two reference points (17). At reasonable salt concentrations it is experimental fact that RNA may be treated as if it were ideal. Thus, for a noninteracting system, a plot of  $(C_{2b} - C_{2m})/C_2^0$  against  $(r_b^2 - r_m^2)$  will yield a straight line with the slope a function of the weight-average molecular weight:  $[\omega^2(1 - \bar{\nu}\rho)/2RT] \bar{M}_w^0$ . We test the formation of a complex between Met tRNA<sub>M</sub> and 5 S RNA by sedimenting a mixture to equilibrium and constructing the appropriate plot. If there is a complex formed, that plot will be convex, rather than a straight line. For  $T = 5^\circ\text{C}$ ,  $K_B = 3000$  l/mole and  $K_A = 300$  l/mole (Table 1), and as a first assumption, we take  $K$  to be independent of pressure. If 5 S RNA and Met tRNA<sub>M</sub> are initially both  $10^{-3}$  M, the B complex concentration will be about  $0.9 \times 10^{-3}$  M, and the A complex about  $10^{-4}$  M at equilibrium. The  $\bar{M}_w$  will be about 70,000 as compared to  $\bar{M}_w = 34,000$  for a noninteracting system. If the initial concentrations of Met tRNA<sub>M</sub> and 5 S RNA are  $2 \times 10^{-2}$  M and  $10^{-2}$  M, respectively, both equilibria A and B are essentially completely to the right (Eqs. 1 and 2):  $\bar{M}_w = 93,500$ .

Because of the complexity of the system, there is no way at present to achieve good quantitative measurements of  $K_A$  and  $K_B$ . However, we should be able to demonstrate the formation of a complex and that complex of about the correct  $\overline{M}_w$ , and this will provide encouragement for the model for protein synthesis which assigns to the third loop of tRNA the function of stabilizing the ribosome-bound complex by base pairing with the 5 S RNA of the 50 S ribosomal subunit.

## REFERENCES

1. Madison, J. T., *Ann. Rev. Biochem.*, 37, 131 (1968).
2. Yaniv, M. and F. Gros, *J. Mol. Biol.* 44, 17 (1969).
3. Brownlee, G. G., F. Sanger, and B. G. Barrell, *Nature*, 215, 735 (1967).
4. Brownlee, G. G., F. Sanger, and B. G. Barrell, *J. Mol. Biol.*, 34, 379 (1968).
5. Forget, B. G. and S. M. Weissman, *J. Biol. Chem.*, 244, 3148 (1969).
6. Forget, B. G. and S. M. Weissman, *Science*, 158, 1695 (1967).
7. Boedtker, H. and D. G. Kelling, *Biochem. Biophys. Res. Commun.*, 29, 758 (1967).
8. Raacke, I. D., *Biochem. Biophys. Res. Commun.*, 31, 528 (1968).
9. Möller, W., *Nature*, 222, 979 (1969).
10.  $Su^+$  III tRNA and  $Su^-$  III tRNA  
Goodman, H. M., J. Abelson, A. Landy, S. Brenner, and J. D. Smith, *Nature*, 217, 1019 (1968).
11. Val I tRNA  
Yaniv, M. and B. G. Barrell, *Nature*, 222, 278 (1969).
12. Met tRNA<sub>M</sub>  
Cory, S., K. A. Marcker, S. K. Dube, B. F. C. Clark, *Nature*, 220, 1039 (1968).
13. Met tRNA<sub>F</sub>  
Dube, S. K., K. A. Marcker, B. F. C. Clark, and S. Cory, *Nature*, 218, 232 (1968).

14. Watson, J. D., Molecular Biology of the Gene, Benjamin, 1965, Chapter 11.
15. Wetmur, J. G. and N. Davidson, J. Mol. Biol., 31, 349 (1968).
16. Van Holde, K. E. and R. Baldwin, J. Phys. Chem., 62, 734 (1958).
17. Tanford, C., Physical Chemistry of Macromolecules, John Wiley and Sons, Inc., New York, 1966, Section 16e.